An analysis on the technical capabilities of a PV/t based energy system installed in primary schools

Master Thesis
45 EC

Ruben van der Veen
r.vanderveen4@students.uu.nl
4696794
Systems Analysis Track

28 June 2024

1st supervisor: Dr. Sara Mirbagheri Golroodbari
2nd supervisor: Prof. dr. Wilfried van Sark

Copernicus Institute of Sustainable Development
Faculty of Geosciences

Universiteit Utrecht

Abstract

The Netherlands is, in line with the Paris agreement, transitioning from fossil fuels towards more sustainable forms of energy. This impacts all sectors, also the built environment. In the future the electricity and heat used in this sector must be generated without CO^2 emissions. This research focuses on Photovoltaic/thermal (PV/t) panels to generated both. The generated thermal energy is stored in a seasonal thermal energy storage, which doubles as an energy source for the cold side of the heat pump. The technical feasibility of this system is studied in a Mediterranean climate. However, because the climate in Central Europe is much different, the technical capabilities can not be extrapolated to other regions. Therefore, the optimal design and operational parameters for a PV/t system, combined with an energy storage and heat pump installed are analyzed. In addition to this, the year-round technical performance to effectively meet the heating and electricity demands of a near net-zero energy primary school in a Central European climate are researched. Firstly, the current energy integration of 115 primary schools in the region of Utrecht are determined. This leads to an energy demand and distribution over 2022 and 2023 for 115 primary schools in the region of Utrecht. The PV/t based energy systems is modelled in Excel and linear programming is used to determine the optimal storage size to reach net-zero from a thermal perspective. In the model different amounts of PV/t panels on the roofs are modelled. According to the simulations of the model, 61 of the 115 primary schools are able to reach net zero from a thermal perspective with 100% of the available roof area filled with PV/t panels. In addition to this, 19 of these 61 schools reached net-zero from an electrical standpoint. Reaching fully net-zero is highly dependent on the ratio between available roof space for solar panels and energy demand. Primary schools with a large available roof space and low energy demand are more often able to reach fully net-zero. Additionally, primary schools with an unfavourable ratio require larger storage capacities, have lower storage temperatures and their heat pump's COP is worst, compared to primary schools with a more favourable ratio. Despite this, installing more PV/t panels does not always result in a more yearly energy generation. More research is needed on this cross over point to help when making design choices.

Contents

1 Acronyms

ATES Aquifer Thermal Energy Storage

BAG Basisregistratie Adressen en Gebouwen

BTES Borehole Thermal Energy Storage

CBS Centraal Bureau voor de Statistiek

CHP Combined Heating and Power

COP Coefficient Of Performance

DHW Domestic Hot Water

ECN Energieonderzoeks Centrum Nederland

HDD Heating Degree Days

HRV Heat-Recovery Ventilator

HVAC Heating Ventilation and Air Conditioning

FPC Flat Plate Collector

IEA International Energy Agency

KNMI Koninklijk Nederlands Metreologisch Instituut

PTES Pit Thermal Energy Storage

PV Photovoltaic

PV/t Photovoltaic/thermal

RVO Rijksdienst voor Ondernemend Nederland

STES Seasonal Thermal Energy Storage

TTES Tank Thermal Energy Storage

2 Introduction

With the signing of the Paris Agreement, the Netherlands committed itself to holding "the increase in the global average temperature to well below 2°C above pre-industrial levels and pursuing efforts to limit the temperature increase to 1.5°C above pre-industrial levels" [1]. The Dutch government translated these goals into a target of reducing CO_2 emissions by 49% in 2030 compared to 1990, and 95% in 2050 [2]. To put this in perspective, the Netherlands emitted 165 megatons of CO_2-equivalent in 2022, which is 24% less than in 1990 [3].

In 2022 the built environment emitted 13% of the total emitted CO_2-equivalent in that year. This was 22 megatons of CO_2-equivalent. Parallel to this, the built environment emitted 27% of the final energy use in 2022 [3]. It is important to note that these numbers don't include the CO_2 emissions and final energy use related to the electricity used in the built environment. Even tough 30% of the energy used in the built environment is electricity. Therefore, the actual CO_2 emissions and final energy of the built environment is higher as portrait by these numbers.

While 30% of the final energy use is electricity, the other 70% of the energy used in the built environment is heat [4]. The heat is for a large part generated with natural gas boilers, as 82% of the built environment uses a natural gas boiler as their main heat source [5]. Approximately, 60% of this natural gas is used in the residential sector, while the other 40% is used to heat utility buildings [6]. It can be established that both residential and utility buildings rely heavily on the burning of natural gas for heating. However, in 2050 in both sectors, must have a net-zero emissions alternative to the natural gas boiler, to achieve the CO_2 emission reduction goals. While, net-zero is the ultimate goal, at this time near net-zero is also a step in the right direction.

A popular near net-zero alternative of a natural gas boiler is a heat pump [7]. A heat pump extracts energy from one source and uses electricity to increase that thermal energy, to provide heat to the inside of the building. Usually this source is the outside air or ground. The efficiency, or Coefficient Of Performance (COP) of the heat pump is dependent on the temperature difference between the source and inside [8]. To ensure a high COP, the output temperature of a heat pump is typically low, between 35 °C and 45 °C. A higher output temperature would decrease the COP of the heat pump considerably. Contrary to the low output temperature of a heat pump, the output temperature of a natural gas boiler is relatively high, around 75°C [9]. Because of the difference in output temperature, switching to a heat pump without decent insulation is often not sufficient to keep the building warm on cold days. While newer buildings are often well insulated and therefore able to make the switch to a heat pump without any further insulation. This is not always the case when it comes to older buildings. In these instances, additional insulation is a necessity to keep the building warm on cold days. The downside of insulating older buildings is that it often comes at a substantial cost and may not always be practical [10]. A near net-zero alternative with an output temperature similar to that of a natural gas boiler, eliminates the need for further insulation and could therefore be solution.

In addition to the generation of energy with natural gas, 30% of the energy used in the built environment in 2021 was electricity [4]. This is partially offset by the on site generation of electricity through solar panels. The installed capacity of solar panels in the Netherlands increased from 149 MW in 2012 to 19.143 MW in 2022 [11]. This makes the Netherlands the country with the highest installed capacity of solar power per capita in Europe [12]. Moreover, in 2022 32% of all residential buildings the Netherlands had solar panels [13]. Despite the popularity of solar panels in the Netherlands, almost all the installed solar capacity is regular Photovoltaic (PV) [11]. These panels produce only electricity and therefore only provides in the electricity demand of the building. Solar panels that produce heat are less common, but are commercially available [14].

An example of heat producing solar panels are Photovoltaic/thermal (PV/t) panels. These panels convert solar radiation into both electricity and heat. The electricity is generated similar to a regular PV panel. In addition to this, the radiation hitting the solar panel, heats up the cells. PV/t panels make use of this heat, utilizing energy that goes to waste with a regular PV panel [15]. Because of this, PV/t panels typically have a higher overall efficiency, compared to a PV panel. However, according to Tian and Zhao, this is not the only reason why PV/t panels have a higher efficiency compared to their PV counterparts. The PV module in the PV/t panel has a higher performance because of the transportation of heat. The heat removal plate transports the heat away from the panel, simultaneously cooling the PV/t panel down to a more suitable operational temperature for electrical performance [16]. The increase in performance from this effect is dependent on the mass flow rate through the panel. Therefore, increasing the mass flow rate, also increases the performance of the PV unit of the PV/t panel [17].

Even tough there are advantages to the use of PV/t panels, installing them is more complex compared to their PV counterpart. PV panels can often be installed with only minor adjustments to the roof and some changes to the fuse-box. This is the case because, the electricity of PV panels is used on site or distributed to the electricity grid. This isn't the case with the thermal energy generated by the PV/t panels. The produced heat that isn't used immediately needs to be stored. Therefore, systems that utilize PV/t panels, typically need more installations compared to regular PV panels.

Examples systems that utilize PV/t panels on utility buildings are more common around the Mediterranean, compared the Netherlands. For example, Del Amo et al. proposed a PV/t based heating system for the University of Zaragoza. The system included a 196 m^2 PV/t solar array, facing south on the top of the Zaragoza University. The heat produced by this solar array fed a 300 m^3 Seasonal Thermal Energy Storage (STES). A heat pump used the storage as an energy source to provide energy at the required temperature. The thermal energy from the seasonal storage enhances the performance of the heat pump, since the increase in temperature of the cold side of the heat pump results in a higher COP. The temperature in of the storage fluctuated between 5 °C in February to 72 °in August. The study showed the system to be technically feasible. However, the location was an important factor in this, as the solar radiation was 1.794 kWh/m^2/yr [18]. A similar system was studied for a social housing project on the campus of the university of Zaragoza. This was also technically

feasible, partly due to the local climate conditions [19], [20]. Lastly, a system based on heat form PV/t panels was studied for a university sport complex in Bari, Italy. In this case, the PV/t panels and storage weren't enough the provide the complex with heat the entire year. While during the summer, the 70 °C required for the radiators was reached. During the winter auxiliary heating was needed because the temperature in the storage wasn't high enough. The PV/t panels were able to cover 51.3% of the yearly thermal energy needed [21].

The PV/t panel, STES and heat pump heating systems proposed for the utility buildings and large residential complexes in Zaragoza and Bari were able to provide heat at temperatures around 70 °C. However, these studies only showed the capabilities of this system in Mediterranean climates. It is uncertain if the capabilities are the same in colder climates, with less yearly solar radiation. The yearly solar radiation per m^2 in Central Europe is 700 kWh lower compared to Southern Europe [22]. Therefore, it is not unreasonable to suspect that the technical potential of such an energy system is lower when placed in Central Europe. However, it is unclear how much lower this potential is, and if such a system on a utility building is technically feasible in a Central European country like the Netherlands.

3 Research objective and research question

This research focuses on primary schools, instead of including all types of utility building. The reason for this, are the large variations between utility buildings when it comes to energy demand, daily load curves and construction characteristics. Comparing local community centre and a public swimming pool, is comparing apples with oranges. Therefore, this research focuses on primary schools as an utility building. Primary schools yield certain advantages from a energy demand and construction stand point. The PV/t panels produce most energy during the day and especially in the early afternoon [23]. Generally, the energy demand of a primary school increases during that time [24]. This is in contrast to the demand curve of a residential building. In that case the energy demand is highest in the morning and evening. Apart from the demand curve, primary schools yield certain practical advantages compared to other buildings. For example, most primary schools have flat roofs [25]. This makes applying solar panels easier, and generally more panels can be placed [26]. Additionally, most of the times there is a playground somewhere around the school. Here the STES could be placed.

Because of these reason, the main objective of this research is to present a technical analysis of a heating and electricity system bases on energy generated by PV/t panels, in combination with an seasonal thermal energy storage and heat pump. The technical analysis is conducted within the context of a primary school in a Central European climate. It is the aim to make the system as small as possible, to find the technical limitations of the system. This means that the PV/t array, storage size and other installations are scaled to the demand and other practical limitations of the primary school e.g. roof size and already installed PV panels. Moreover, the system is to be at least net-zero energy from a thermal perspective. In addition to this, if possible net-zero from an electrical stand point must also be achieved. Lastly, the heat from the system has to be 75 °C to present a direct net-zero alternative to the natural gas boiler.

The technical analysis of the system is to be conducted along the lines of the following main research question:

Main research question:

What are the optimal design and operational parameters for a Photovoltaic Thermal system combined with energy storage and heat pump to effectively meet the heating and electricity demands of a near net-zero energy primary school in the Netherlands and what is the year-round technical performance of such a system?

To help answer the main research question, the following sub-questions are formulated:

Sub questions:

- What limitations and potentials do primary schools face in transitioning towards near net-zero energy buildings?
- What is the current state of electrical energy integration and electrical energy demand in primary schools?
- What is the current state of thermal energy integration and thermal energy demand in primary schools?
- What are the possible installation setups that make up an optimized Photovoltaic Thermal powered electricity and heating system?
- How can Photovoltaic Thermal systems and energy storage contribute to this transition with minimal installation components?

3.1 Scientific and societal relevance

The scientific and societal relevance of this research, in the most general sense, is to present a net-zero heating and power system based on PV/t panels that could contribute to a more sustainable built environment and to that extent a more sustainable Netherlands. This research will provide relevant insights into the technical capabilities of a net-zero PV/t panel based electricity and heating system in a Central European climate. Scientifically, this research addresses the lack of research on the technical capabilities of a PV/t panel based electricity and heating system in colder climates, such as in the Netherlands.

From a societal perspective, this research offers insights into an electricity and heating system that is net-zero or near net-zero energy. This means that the building generates as much energy as the building requires over a specific period of time. No or limited, additional electricity, natural gas or heat has to be imported from their respective grids. Therefore, the PV/t system analysed in this research, contributes to the societal goal of reducing CO_2 emissions, thought the reduction of central energy generation. In addition to this, according to the International Energy Agency (IEA), PV/t technologies lack visibility in the building community despite the successes of several PV/t industries in France and Spain making breakthroughs since 2015 [27]. It is the aim of this research to shown the capabilities of these technologies anno 2024. Consequently, technologies get consideration when there is data to back it up and positive progression over the years is observed [27]. Therefore, research is relevant from an societal perspective, as it makes PV/t technologies more visible. For these reasons this research is scientifically and socially relevant.

4 Theory

4.1 Scope and boundaries

This research is conducted within the scope of the Netherlands and focused on the technical capabilities of a PV/t powered electricity and heating system for primary schools. 115 primary schools in the region of Utrecht are used as references. This region includes the municipality of Utrecht, De Meern, Vleuten and Haarzuilens. The 115 schools within the region of Utrecht differentiate in size, year of construction and shape. Therefore, robust results are obtained from researching these schools. A list of these schools shown in Appendix A.

Figure 1 shows the schematic overview of the PV/t powered system.

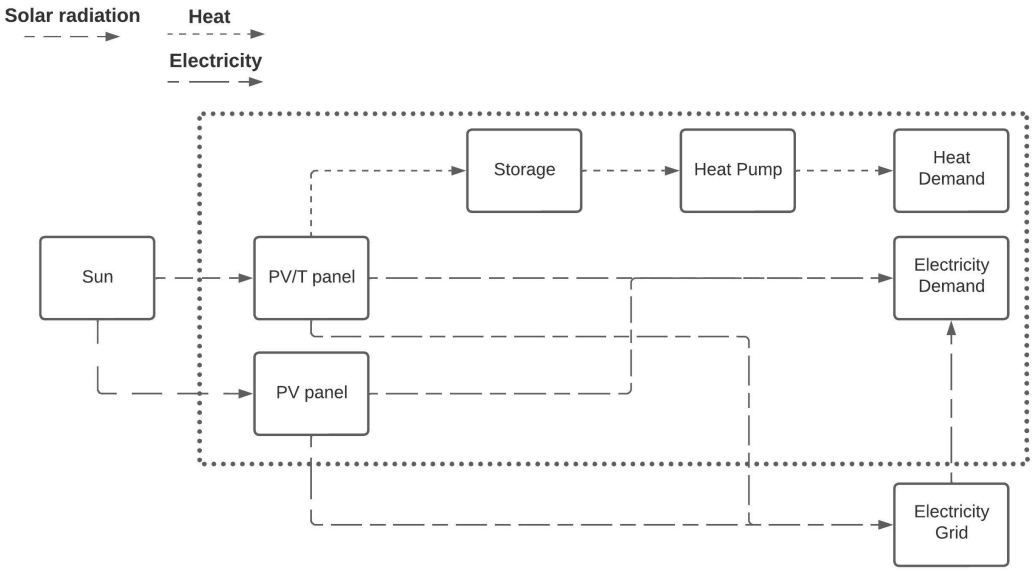

Figure 1. *Schematic overview of the PV/t panel powered electricity and heating system.*

The system scheme starts with the radiation from the sun and ends with the energy demand. The research boundary is presented by the dotted square in Figure 1. The system functions as follows: The PV/t panels generate heat during summer. This energy is stored in the STES. A heat pump extracts energy from the storage, increasing the temperature and supplying it to the primary school. Electricity is supplied from and to the grid whenever the PV/t and PV panels generate too much or too little electricity. In a situation where the panels don't produce enough electricity to meet the demand. Additional electricity must be supplied by the grid. In this case, the system is not fully net-zero energy. It is also important to note that the electricity from the grid is generated with CO_2 emissions [28]. Therefore, when importing electricity from the grid CO_2 is emitted.

Batteries to storage the excess energy are not included in this research. However, in a future scenario it might possible to make use of a micro-grid to store electricity. In this case, electricity is stored in a small local grid and used if there is not enough electricity from the PV/t and PV panels. As of now, micro-grids were still in the testing phase in the Netherlands, however this technology is considered to be the important piece in the future energy distribution system [13], [29].

Figure 2 shows a visualization of the PV/t panel powered electricity and heating system.

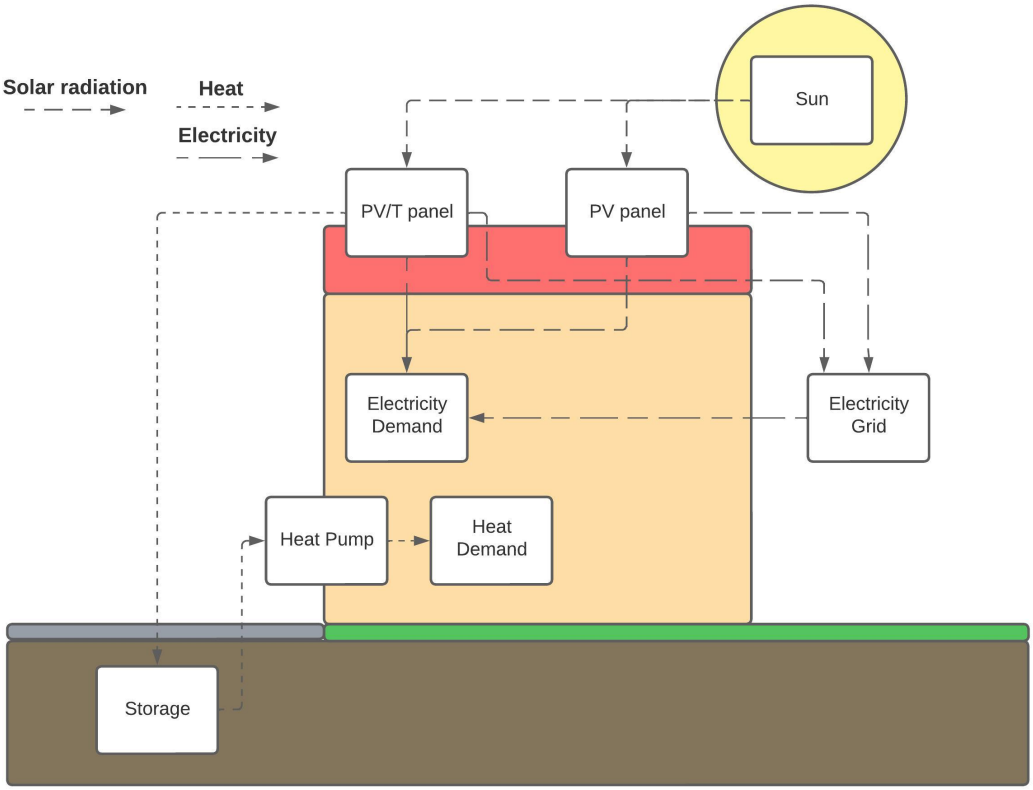

Figure 2. *Visualization of the PV/t panel powered electricity and heating system.*

Figure 2 is essentially the same schematic as Figure 1, however it shows where the different installations are with respect to the building.

4.2 Key concepts

In this Section the most important key concepts used in this research are elaborated upon. Many key concepts form the basis of the methodology used to answer the main and sub questions.

4.2.1 PV panels

To provide the primary school with the necessary electricity, PV/t and PV panels can be placed on the roof. The electricity generated by the PV panels is calculated with the following equation:

$$P_{electrical} = \eta_{electrical} \cdot A \cdot G \tag{1}$$

In equation 1, $P_{electrical}$ represents the electrical power generated by the PV panel. The electrical efficiency of the PV panel is shown as $\eta_{electrical}$. The area of the solar panels is represented as A in m^2 and solar radiation is shown as G in Watt/m^2. The electrical efficiency $\eta_{electrical}$ is dependent on certain environmental and structural factors [30]. These are encompassed in the following equation:

$$\eta_{electrical} = \eta_{0,electrical}(1 - \beta(T_c - T_{ref})) \tag{2}$$

$\eta_{0,electrical}$ represents the electrical efficiency of the PV panel at a temperature of 25°C. The coefficient of temperature is shown as β in °C^{-}1. T_{ref} is 25°C and T_c is the PV cell temperature in °C [30].

In this research the cell temperature is calculated with a simple empirical model used by Koehl et al. and proposed by Faimann [31], [32].

$$T_c = T_0 + \frac{G}{U_0 + U_1 \cdot V_w} \tag{3}$$

T_0 represents the ambient temperature in °C in equation 3. The coefficient U_0 describes the effect of the radiation on the module temperature in the Faiman model, in W/m^2K. U_1 is a coefficient describing the cooling by the wind in the Faiman model, in Ws/m^3K. Both, U_0 and U_1 are coefficients specified for different types of PV panels by Koehl et al [31]. The coefficients for Monocrystalline and Polycrystalline PV panels are shown in Appendix B. V_w is local wind speed near the modules in m/s.

4.2.2 PV/t panels

PV/t panels consist of a PV module, used to produce electricity and tubes underneath the module to extract the heat from the panel. Even though all PV/t panels are based on this, there are different types of PV/t panels, built with different intended purposes. Figure 3 shows an overview of the different types of PV/t panels, their intended purposes and operating temperature.

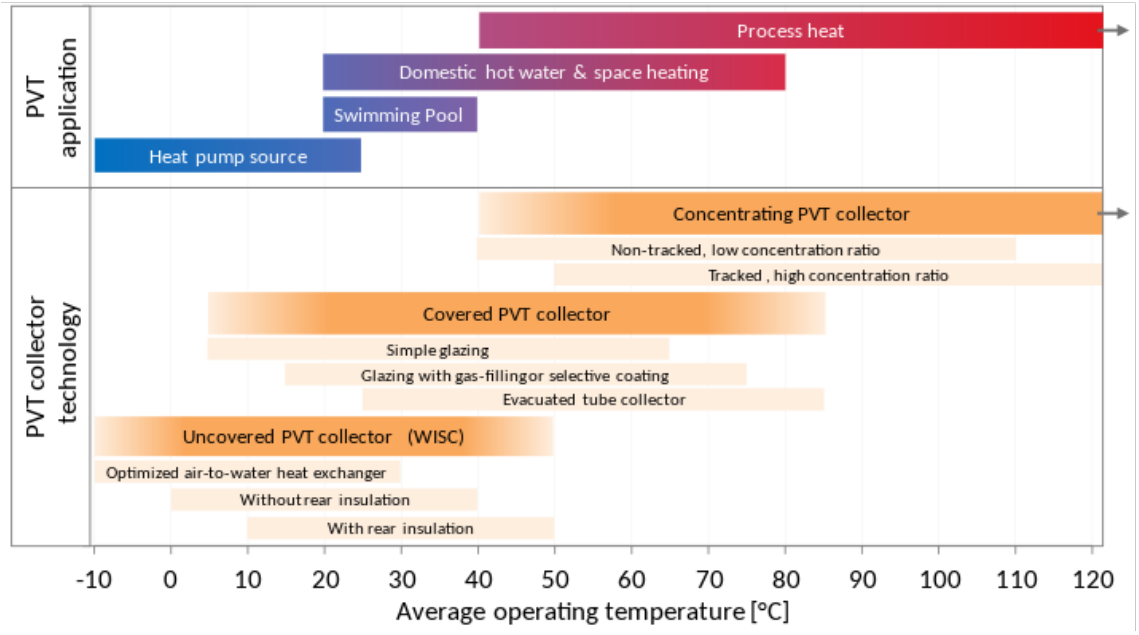

Figure 3. *Different types of PV/t panel technologies with their use and average operating temperature [33].*

PV/t panels with an operating temperature, able to provide domestic hot water and space heating, are often found around the Mediterranean. While, uncovered PV/t collectors used as a source for a heat pump, are more common in Central Europe [34]. Because this research focuses on the technical capabilities of a PV/t powered electricity and heating system, in combination with an STES, PV/t panels able to provide electricity and heat for domestic hot water and space heating are relevant to this research. According to Figure 3, covered PV/t collectors are suitable for this.

Figure 4 shows a schematic cross Section of a covered PV/t panel, considered in this research.

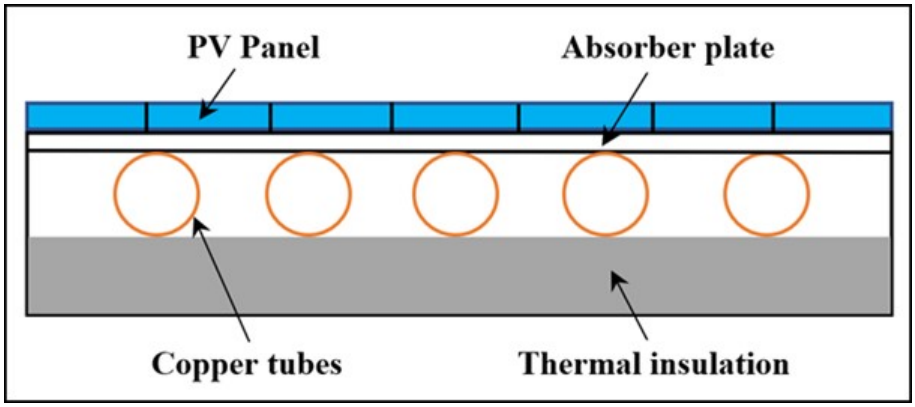

Figure 4. *Cross Section of a flat plate PV/t panel [35].*

On top of the PV/t panel a glass pane is place to protect the cells from damage. Behind this glass pane the PV module is situated. This component is responsible for the generation of electrical energy. The heat from the cells is transferred via conduction to the absorber plat, directly behind the PV panel. From there, the heat is transferred through the absorber plat to the water in the tubes. This is mixture of conductive and convective heat transfer. The thermal resistance of the absorber plate and tubes are low to maximize the transfer of energy from the cells to the fluid [36]. Behind the absorber and pipes thermal insulation is placed. Because of this insulation, heat lost through the back of the panel can be neglected.

The electricity generated by the PV/t panels is calculated similarly to the PV panels, using equations 1 and 2. The only difference being the method cell temperature is calculated. The method used for the PV panels only dependents on the temperature increase by ambient temperature, radiation and wind. However, the temperature of the cell is cold because of the fluid that runs at the back of the PV/t panel [18], [37]. Therefore, the method to calculate cell temperature proposed by Koehl is not used for the PV/t panels. Terashima et al. proposes the following equation to determine the mean temperature of the module of a PV/t panel:

$$T_m = (T_{out} + T_{in})/2 \tag{4}$$

The equation proposed by Terashima et al. takes the mean temperature of the panel, T_m, as the cell temperature. T_{out} and T_{in} represent the temperature at the inlet and outlet of the PV/t panel [37]. Via this equations the cooling related to the fluid in the PV/t panel is taken into account. Additionally, ambient temperature, radiation and wind are taken into account. This is further elaborated upon next.

As the sun shines on the black surface of the panel, the cell temperature increases. The heat from these cells flow through the panel to the fluid module. The heat flow through the PV/t panel is calculated with Fourier's law [38], [39]:

$$q = K \cdot T_c - T_m \tag{5}$$

Where q is the heat flux through the panel, from the cell to the fluid module in W/m^2. K is the thermal resistance between the heated cell and fluid in W/m^{2}K. This resistance is a mixture between conductive and convective heat transfer. The temperature of the cell and mean temperature of the module are presented as T_c and T_m respectively. The cell temperature is determined by the method proposed by Koehl, shown in equation 3. In this equation the effect of wind, on the temperature of the cell is 0 for a PV/t panel. This is the case because no wind flows behind the cell's, as the absorber and fluid module are placed there [30], [40]. The mean module temperature, Tm is calculated with equation 4.

To calculate the heat flux through the entire surface of the panel, the following addition to Fourier's law is needed:

$$\dot{Q}_{pvt} = q \cdot A \tag{6}$$

From this, $\dot{Q}_{pvt}$ presents the heat flow, through an area presented as A [38], [39]. The consequent increase in temperature of the fluid due to the heat flow is calculated with equation 7:

$$T_{out} = \frac{\dot{Q}_{pvt}}{\dot{m} \cdot cp} + T_{in} \tag{7}$$

The temperature at the outlet of the PV/t panels is heated due to the heat flow $\dot{Q}_{pvt}$, calculated in equation 6. $\dot{m}$ is the nominal flow of the fluid in the panel in kg/s and cp is the specific heat of the fluid in J/kgK or kwh/kgK. Lastly, T_{in} represents the temperature at the inlet of the PV/t panel.

In the end, the heat generated by the PV/tpanel and consequent temperature increase of the fluid, is dependent on the ambient temperature and radiation, via equations 3, 5, 6 and 7 (not wind speed as this is 0 for PV/t panels). In addition to this, the characteristics of the PV/tpanel, e.g. the conductive and convective thermal resistance of the absorber and fluid also affect heat flow and consequent temperature increase.

4.2.3 Thermal energy storage

The thermal energy storage makes it possible to store the heat produced in the summer by the PV/tpanels. This heat can then be used in the winter, when the PV/t panels generate less energy. Seasonal energy storage's can be divided into three main categories: Sensible, latent and chemical STES. With sensible STES the energy is stored in a selected materials and retrieved when heat is required. Compared to latent and chemical storage, sensible STES is the most mature technology. It is therefore, also the most common type of storage. Latent energy storage's use the phase change of a material to store energy. This is more space-efficient compared to sensible storage, however latent energy storage is relatively new and therefore not extensively used. Moreover, it is more expensive compared to sensible STES. Lastly, the storing of energy in chemical components is the most novel technology of the three. Currently, the studies on chemical storage are at the theoretical and laboratory testing stages [41]. Because latent STES is rare and chemical STES is still only used in laboratories, this research focuses on sensible STES.

Sensible STES can be roughly categorized into four categories. Borehole Thermal Energy Storage (BTES), Aquifer Thermal Energy Storage (ATES), Tank Thermal Energy Storage (TTES) and Pit Thermal Energy Storage (PTES). BTES and ATES go deep into the ground, where the energy is stored and retrieved when necessary. These storage's are expensive technologies, typically used for large scale energy storage's. Because of the depth, special geological conditions are needed to install BTES or ATES. This means that applying these technologies is limited to certain locations. TTES and PTES consist of tanks or containers filled water or water and gravel. These tanks or containers are used for smaller storage's and go to a depth of 5 to 15 meters under ground. Because of this, they are cheaper compared to BTES or ATES [42]. Of the four types of STES, TTES is the most mature technology and fits best to the scope of a primary school. Additionally, there are no geographical or geological limitations to TTES, which makes it applicable to all locations. Therefore, this research focuses on TTES as seasonal storage.

The energy in the storage slowly disappears over time, whenever the ground surrounding the storage is colder than the inside of the storage. This flux can be calculated with Fouriers's law as shown in equation 5. In this case the heat flows from the inside of the storage, to the outside, as the storage is dug into the ground. The thermal resistance is typically high, resulting in a low K. This is achieved due to the extensive insulation surrounding the storage to limit the energy lost through the walls. The addition to Fourier's law, equation 6 is also applicable to the conduction loss trough the storage. In this equation the walls of the storage are the area A. These two equations are the theoretic principals behind the STES. Because the storage is dug into the ground, conductive heat loss can be neglected.

4.2.4 Heat pump

A heat pump is used to provide heat to the heat distribution system of the primary school. This is done by extracting the heat from the air, water or ground. The heat is transferred to a refrigerant and compressed. As a result of the compression, the temperature and pressure of the refrigerant is increased. Thereafter, the refrigerant flows through a condenser, where the heat is supplied to the connected heat distribution system. The heat pump is essential in the PV/t powered electricity and heating system, as a means to increase the temperature before it is supplied to the heat distribution system. Without the heat pump the temperature supplied to the heat distribution system would be high enough in the winter. Within the scope of this research, the storage is used as the source for the water-water heat pump. This increases the COP of the heat pump compared to a standard air source heat pump [8]. Because the temperature of the storage, the source of the heat pump, is higher than the ambient temperature during the largest part of the year. This effect of the difference between source temperature and output temperature is shown by equation 8:

$$COP_{hp} = \frac{|\dot{Q}_h|}{|\dot{W}|} = \frac{|\dot{Q}_h|}{|\dot{Q}_h| - \dot{Q}_l} = \frac{\dot{m}(h_3 - h_2)}{\dot{m}(h_2 - h_1)} \tag{8}$$

In equation 8 $|Q_h|$ presents the heat generated by the condenser, used to heat the primary school. $|Q_l|$ represents the heat extracted from the source. $|W|$ is the work in the form of electricity needed by the compressor to compress the refrigerant. The mass flow rate is shown as $\dot{m}$ in kg/s and is the same at every stage of the system because a heat pump is a closed cycle. Enthalpy is shown as h in kj/kg in equation 8 [43]. The different enthalpy stages, numbered from 1 to 4 are shown in Figure 5.

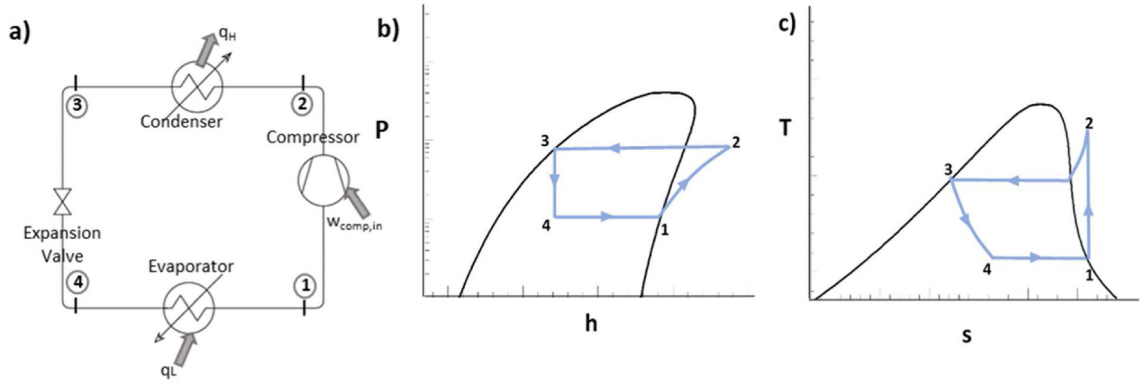

Figure 5. *(a) Reverse Rankine vapour compression cycle schematic illustrated using (b) P-h and (c) T-s diagrams [44].*

The heat pump cycles shown in Figure 5 assume isobaric exchange of heat in the evaporator and condenser and adiabatic expansion valve. Additionally, for further calculations regarding the heat pump steady state is assumed.

The enthalpy levels, needed to calculate the COP, $|W|$, $|Q_h|$ and $|Q_l|$, are obtained as follows. Because stages 1 and 3 are on the saturation line, it is possible to obtain the enthalpy levels and associated pressure from saturation tables [45]. The

enthalpy of stages 3 and 4 are the same, as is shown in Figure 5 (b). The enthalpy of point 2 can be obtained via the vertical line from stage 1 to 2 in Figure 5 (c), indicating a constant entropy shown as: s. Therefore, stage 2 can be obtained with the saturation tables. Finding this by matching the entropy at stage 2 and the operating pressure at stage 3. The obtained enthalpy in stage 2 is correct when a 100% isentropic compressor is assumed. However, this is not the case in reality. Therefore, the line from stage 1 to 2 is not fully vertical, in reality the line tilts to the right, as shown in Figure 6.

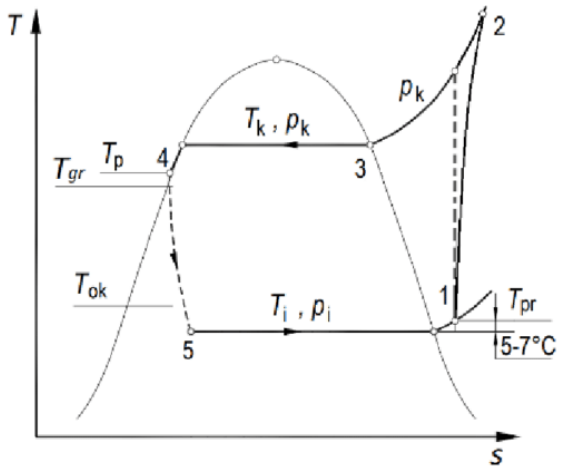

Figure 6. *Representation of a real heat pump cycle in a T-s diagram [46].*

The impact of the tilt on the enthalpy level can be calculated with 9:

$$h_2\text{"} = \frac{(h_2 - h_1)}{\eta^{isen}_{compressor}} + h_1 \tag{9}$$

The enthalpy at the top of the tilted line is presented as h_2". With the operating pressure, the enthalpy of this stage can be obtained. $\eta^{isen}_{compressor}$ is the isentropic efficiency, this is a characteristic of the compressor [47], [48].

The theoretical principals shown in equations 8 and 9 in combination with figures 5 and 6, make it possible to calculate the COP of the heat pump. Additionally, it is possible to calculate the thermal energy extracted from the source, thermal energy generated by the condenser and work required by the heat pump.

5 Methodology

5.1 Research strategy

The research strategy consists of four main methods. Using these methods with the associated sub-question will provide an answer to the sub-question. Each sub-question contributes to the results and ultimately answers the main research question. The research strategy and methods used for each sub-question are shown in Figure 7.

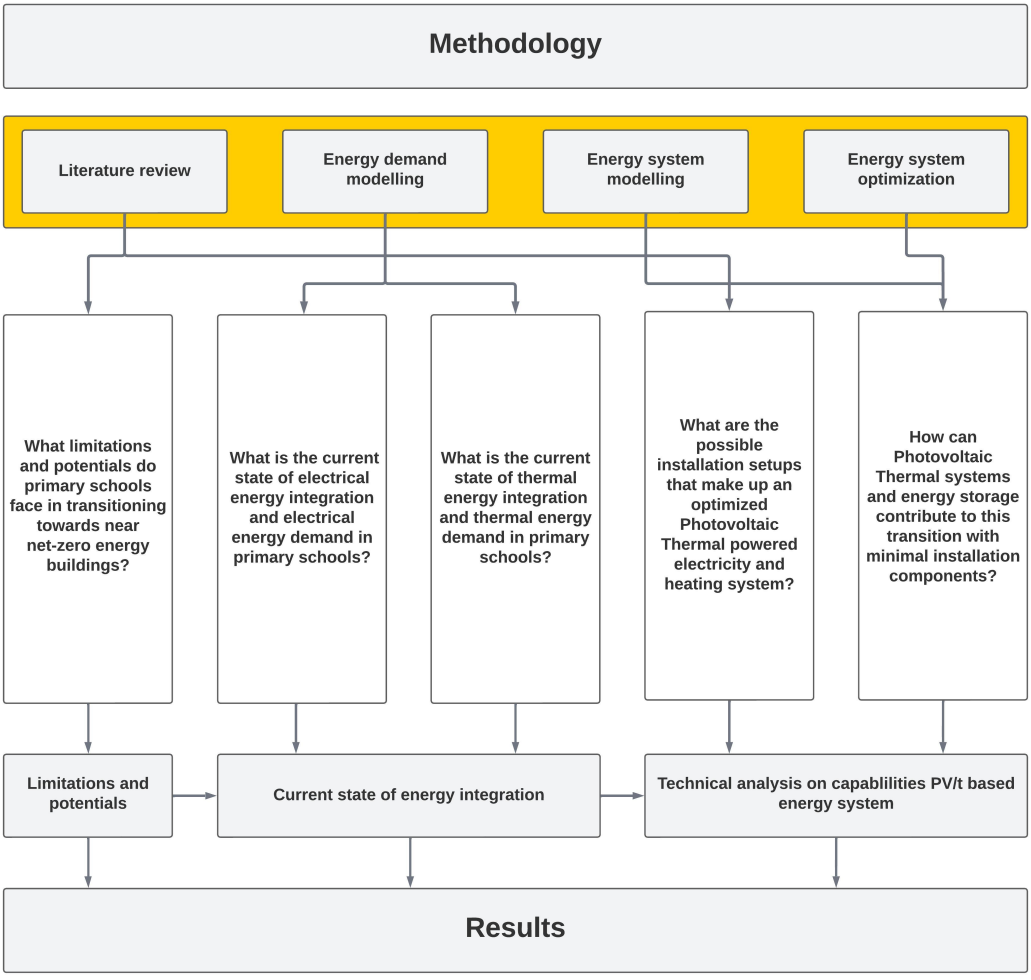

Figure 7. *Overview of the methodology with the methods used for each sub-question.*

Methods:

- Literature review
- Energy demand modelling
- Energy system modelling
- Energy system optimization

5.2 Literature review near net-zero primary schools

The first step in answering the main research question is to understand what limitations and potentials primary schools face in transitioning towards near net-zero energy buildings. This is researched trough a literature review on the topic: The limitations and potential concerning primary schools in transitioning towards becoming near net-zero. In this literature review, papers on this topic are elaborated upon. Papers concerning other types of utility buildings are also included to provide a broader perspective on this topic. Relevant papers are obtained from Google Scholar and Scopus. The limitations and potentials found by the literature review are take into account when determining the energy demand and energy distribution curve of the primary schools in the region of Utrecht. The insights gained from the literature review are also used to put the results, shown in Section 6.1, in perspective in the discussion, Section 7.

5.3 Energy integration

The energy integration of primary schools in the region of Utrecht is divided into energy generation and energy supply. It is the goal of this section to provide insight into the energy generation, supply and distribution of the primary schools in the region of Utrecht during 2022 and 2023. In addition to this, the current state of the energy integration and energy demand of primary schools form the basis of further modelling of the PV/t-panel powered electricity and heating system.

5.3.1 Energy generation

The energy generation of primary schools in the region of Utrecht can be divided further into the generation of electricity and thermal energy. Electricity is generated by solar panels on the roofs of the primary schools. Of the 115 primary schools in the region of Utrecht, 46 have a solar array installed on the roof. The exact type of these panels are unknown, as it is not possible to distinguish regular PV panels from solar collectors or PV/t-panels with only satellite images. Other sources than satellite images are not available. Because other panels than regular PV panels are less common in The Netherlands [14]. This research assumes that all solar panels on the roofs of the primary schools in the region of Utrecht are regular PV panels. The yearly yield of each PV panel installations is calculated with SolarGIS. This website and database is used by many organisations and companies, such as The World Bank, EDF and Fraunhofer, to view prospects, forecast yields and monitoring of PV installation. The area of the PV installation on top of the roofs of the primary schools is determined with equation 10:

$$A_{solararray} = N_{solarpanel} \cdot A_{solarpanel} \tag{10}$$

$A_{solararray}$ represents the area of the solar array in m^2. The number of PV-panels installed is shown as $N_{solarpanel}$, this is derived from satellite images and shown for each

primary school in Appendix C. The size of the individual PV panel is $A_{solarpanel}$ in m^2. The commercial size of the solar panel is between 1.6 and 1.7 m^2. This research considers a solar panel of 1.7 m^2.

The azimuth and tilt of the panels are variables required to determine the yearly yield in SolarGIS. The azimuth of the PV installation of each primary school is determined with Google maps. The tilt of the installation is distinguished into two options. Installations on a flat roof typically have a tilt between 10 and 15 ° [49]. Therefore, all array's on a flat roof are assumed to have an 12 °tilt. This includes East-West and South orientated installations. Installations on a tilted roof are assumed to have the same tilt as the roof. The azimuth and tilt for each primary school is shown in Appendix C.

Apart from the size of the solar installation, azimuth, and PV array tilt, all values in SolarGIS are kept at default.

This research assumes on-site thermal energy generation no to be present at any of the primary schools. On-site thermal energy generation might be present in the form of solar collectors or PV/t panels. However, as mentioned before, this research only assumes the installation of regular PV panels on the roofs of primary schools. Therefore, no thermal energy generation occurs on the roofs. Thermal energy generation with a natural gas boiler or heat pump, need a form of energy supply to function. Therefore, these forms of thermal energy generation are mentioned in the next section.

5.3.2 Energy demand

To determine the supply of electrical and thermal energy to the primary schools a dataset from the Centraal Bureau voor de Statistiek (CBS) is used. This dataset shows the yearly supplied electricity in kWh per m^2 floor area and natural gas in m^3 per m^2 floor area. Additionally, the report categorizes the results in size and construction year of the primary school. These characteristics are selected by the CBS because there is a correlation between them and the energy demand [50]. Smaller schools with the same insulation levels as larger school use more energy for heating, because of the less favourable ratio between the floor area and heat transmission area i.e., facade, roof and floor. Therefore, smaller schools use per m^2 of floor area more energy for heating compared to larger primary schools. The construction year tells something about the insulation level of the building. Insulation has increased over the years. Consequently, newer primary schools use less energy for heating per m^2 floor area. It might be possible that over the years older schools are renovated, however this research assumes this not to be the case. It is not possible to know when renovation has taken place for each individual school. Additionally, the CBS datasets takes renovations into account because it is based on the real energy demand of primary schools in the Netherlands. The CBS data for natural gas supply is presented in Table 1 and the CBS data for electricity supply is presented in Table 2.

Table 1. *Yearly natural gas supply to primary schools per m^2 of floor area, with construction year on the horizontal axis and size of the primary school on the vertical axis [50].*

	<=1946	**1947-1978**	**1979-1992**	**1993-2015**	**>=2016**
<500	13.7	14.8	14.0	11.6	6.2
501-1000	12.8	12.2	11.1	10.3	5.5
1001-2500	10.9	10.4	10.0	7.5	5.1
2501-5000	7.7	7.4	7.0	6.0	4.5
5001-10000	4.1	3.9	4.4	3.9	2.9

The Energieonderzoeks Centrum Nederland (ECN) and school umbrella organization, SPO Utrecht, present similar results in their reports when it comes to natural gas usage [25], [51].

Table 2 shows an increase in electricity usage per m^2 as the construction year increases. The CBS relates this increase to the increase in electrical appliances in newer schools e.g., more computers, larger Heating Ventilation and Air Conditioning (HVAC) systems, ect.

Table 2. *Yearly electricity supply to primary schools per m^2 of floor area, with construction year on the horizontal axis and size of the primary school on the vertical axis [50].*

	<=1946	**1947-1978**	**1979-1992**	**1993-2015**	**>=2016**
<500	27.2	23.0	25.2	28.1	35.7
501-1000	24.8	12.2	22.1	27.4	34.8
1001-2500	22.2	21.0	22.2	27.4	37.3
2501-5000	19.2	18.0	18.6	31.9	42.8
5001-10000	9.0	8.4	14.3	34.0	45.6

To obtain the correct yearly electricity and natural gas demand from tables 2 and 1, the construction year and floor area for each primary schools is determined with the Basisregistratie Adressen en Gebouwen (BAG). The BAG is a database maintained by the Dutch government containing information of all buildings in the Netherlands. This includes: Addresses, construction year and building size. As the BAG is a 2D database, size of the building shown by the BAG is the size of the roof. The floor area can not directly be obtained from the BAG, as some buildings have multiple stories. The amount of stories are manually obtained from Google Maps. This is done for all 115 primary schools in the region of Utrecht. Thereafter, the number of stories are multiplied by the roof area obtained from the BAG. This results in the floor area. For each primary schools the year of construction and floor area is shown in Appendix D. This makes it possible to track down what values in tables 1 and 2 are used for which primary school.

The electricity demand is calculated with the floor area and correct value from Table 2 for each primary school. When it comes to electrical energy, the energy supply and demand are the same. This seems unnecessary to note, however the supply and demand of heat is not the same. This will be elaborated upon later. The electricity demand of the primary schools is calculated with equation 11.

$$E_{electricity} = A_{floorspace} \cdot B_{elecfloor} \tag{11}$$

In equation 11 $E_{electricity}$ represents the yearly electricity demand of a primary school. $A_{floorspace}$ is the amount of floor area of a primary school in m^2. As mentioned before, this is obtained from multiplying the roof area, obtained from the BAG, by the number of stories. Lastly, $B_{elecfloor}$ represents the values in Table 2. This value changes from school to school depending on the size and construction year.

The heat demand is calculated with the floor area and correct value from Table 1 for each primary school. Because natural gas is supplied and converted to heat the supply of energy supply is not the same as the demand of thermal energy. After all, the conversion from natural gas to heat is not 100% efficient. Therefore, the equation used to calculate yearly thermal energy demand is similar to equation 11, with an addition to take the efficiency of the natural gas boiler into account.

$$Q_{heatdemand} = A_{floorspace} \cdot B_{naturalgasfloor} \cdot \eta_{naturalgasboiler} \cdot 9.769 \tag{12}$$

In equation 12 $Q_{heatdemand}$ represents the yearly heat demand of a primary school. $A_{floorspace}$ is the amount of floor area of a primary school in m^2. The values for $B_{naturalgasfloor}$ in equation 12 refer to the corresponding values in Table 1. This value changes from school to school depending on the size and construction year. The $\eta_{naturalgasboiler}$ is 94% [38]. Lastly, the amount of natural gas is multiplied by 9.769 to convert from m^3 of natural gas to kWh. According to the GasUnie, the energy contend of Dutch natural gas is 9.769 kWh/m^3 (35.17 MJ/m^3) [52].

5.3.3 Energy distribution

To determine if a PV/t powered electricity and heating system is technically capable of providing a primary schools with energy all year long. Only the energy demand doesn't provide the full picture. For example, the demand for heat is not the same for the summer and winter, also the need for electricity during school hours is higher compared to the electricity demand at midnight. Therefore, the demand for heat and electricity needs to be distributed over at least one year. Because the year starts and ends in the middle of winter it is difficult to asses the technical capabilities of the PV/t system when only looking at one year. It is expected that during the winter the PV/t powered electricity and heating system produces the least amount of energy. At the same time the system must supply the most of energy. This makes the winter an important time in determining the net-zero capabilities of the system. Not including a full winter will not result in a representative view on the capabilities of the PV/t system. The same is true for not including a full summer. The summer is

the time when the PV/t-panels charge the STES to prepare for the winter. For these reasons, this research includes an energy distribution for 2 years.

The electricity and thermal energy demand distribution is determined on an hourly bases over the years 2022 and 2023. The electricity demand distribution over 2022 and 2023 is split into two parts: Workdays and weekend/holidays. During workdays the electricity is distributed according to Table 3.

Table 3. *Hourly electricity demand distribution of a primary school during a workday [24].*

Hour	1	2	3	4	5	6	7	8	9	10	11	12
kWh/m^2	0.09	0.09	0.09	0.09	0.09	0.09	0.09	0.09	2.79	3.21	2.61	2.42

Hour	13	14	15	16	17	18	19	20	21	22	23	24
kWh/m^2	2.32	1.76	2.07	1.80	0.35	0.40	0.49	0.27	0.09	0.09	0.09	0.09

The values from Table 3 are obtained from a study conducted by Ouf et al. [24]. In this study, the values represent the hourly electricity demand of a primary school in kWh/m^2. For this research they are considered relative values without a unit, because only the proportional distribution over the day is relevant when distributing the electricity over the day.

During work days the electricity demand follows the proportional distribution shown in Table 3. However, during the weekend and holidays nobody is present at the primary school. Therefore, assuming a proportional distribution as a workday would be incorrect. Table 3 shows a low stable electricity demand during the night. Therefore, this is recognized to be the base-load of the primary school. During weekends and holidays a proportional base-load is assumed. A Table with school holidays during 2022 and 2023 are include in Appendix E.

For each hour of 2022 and 2023 the electricity demand is determined. During weekends and holidays the proportional demand is set to base-load, 0.09. During work days the proportional electricity demand is similar to the proportional distribution shown in Table 3. To allocate the electricity demand properly, all hourly proportional distribution values are summed up, weekends and holidays are 0.09 and workdays are similar to Table 3. Thereafter, the hourly proportional demand is divided by the total sum and multiplied by the total electricity demand of the primary school. This results in the an hourly electricity demand for the years 2022 and 2023 for each school.

The heat demand distribution is based on Heating Degree Days (HDD). HDD are the differences between ambient and indoor temperature. Consequently, the difference between the ambient and indoor temperature affects the amount of thermal energy that has to be allocated to heating the primary school. A large difference between ambient temperature and indoor temperature, in winter for example, results in a larger thermal energy demand. The HDD are only calculated when the outdoor temperature falls below the required indoor temperature [38], [53]. The hourly ambient temperature during 2022 and 2023 is obtained from the Koninklijk Nederlands Metreologisch Instituut (KNMI) station at the Bilt [54]. The Bilt is a few kilometers

from Utrecht, therefore they are relevant for the primary schools included in this research. The indoor temperature during school hours is set at 18.5 °C. School hours are defined as the time between 7 o'clock in the morning till 17 o'clock in the afternoon. Primary schools in the Netherlands typically end earlier than 17 o'clock. However, it is possible teachers have some activities in the building after school ends for the kids. Between 17 o'clock in the afternoon and 7 o'clock in the morning the required indoor temperature is set at 14 °C. This is also the case during the weekends and holidays because there is nobody in the school. The difference between the indoor and ambient temperature is calculated for every hour in 2022 and 2023. Through this, the heat demand is allocated hourly over 2022 and 2023. All HDD's during 2022 and 2023 are summed up. Thereafter, the hourly HDD's are divided by the total sum and multiplied by the total heat demand of the primary school. This results in the an hourly electricity demand for the years 2022 and 2023 for each school.

The results of the energy generation, demand and distribution of the primary schools in the region of Utrecht are shown in Section 6.2.

5.4 Installation setups and system

To determine the technical capabilities of a PV/t based heating and electricity system. A model based on the energy demand and distribution curves is build. However, before this model is built a literature review is conducted on the setup of the different components of the system. The goal of this literature review is to provide insights in the way these components interact with each other. Additionally, the literature review aims to evaluate the different types of PV/t panel based energy systems setups. Based on this evaluation the setup that will be modelled to determine the technical capabilities of the PV/t based energy systems further, is selected. The different setups are obtained from relevant papers obtained from Google Scholar and Scopus. The literature review is shown in the Results Section 6.3.

5.5 Model of the PV/t electricity and heating system

An Excel model is built do determine the technical capabilities of a PV/t system, with STES and a heat pump in a Central European climate. The model is built according to the suggested setup in Section 6.3 as a result of Section 5.4. Additionally, the energy distribution curves, generated in accordance with Section 5.3.3, are used to determine whether the system is able reach (near) net-zero energy. To asses this, the model simulates the energy flow trough the system of all hours during 2022 and 2023.

In this Section an explanation is given on how the Excel model is built. The text tries to follow the same order as the model calculates. A schematic overview of the the heating part of the system is shown in Figure 8.

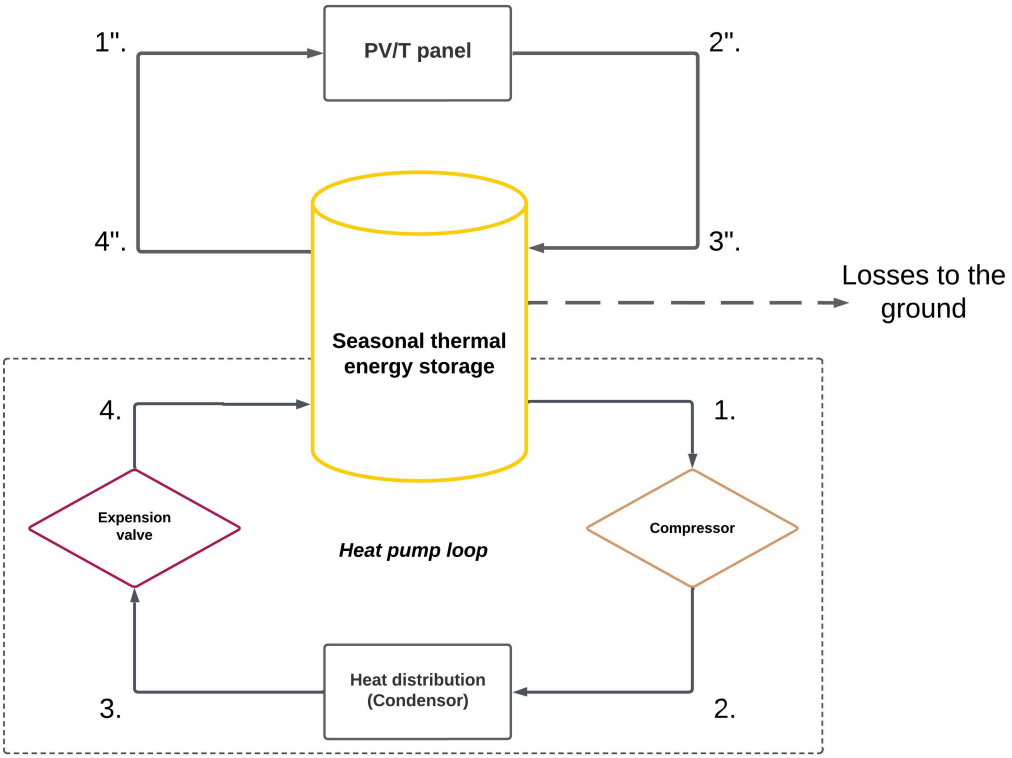

Figure 8. *Schematic overview of the heating system based on PV/t panels, thermal storage and heat pump*

Figure 8 shows two loops connected by the storage. The top loop extracts the thermal energy from the PV/t panels and transports this energy to the storage. The thermal energy losses between the PV/t panel and storage are neglected. This is assumed because the pipes are well insulated and are relatively short (only on site). Therefore, the thermal energy loss through the pipes is small. Also, the length of the pipes can not be estimated accurately as this depends on specific building characteristics and installation requirements. Researching this is outside the scope of this research. The bottom loop is a standard heat pump reversed Rankine cycle. In the cycle, the storage functions as the energy source of the heat pump. How this system functions is explained more in dept in Section 4.2.4.

The model simulates the energy flow trough both loops every hour. This time interval is selected because it is frequent enough to model accurately, while limiting the computation time. Additionally, this time interval pair well with already determined values. The ambient temperature, radiation, wind speed and the demand curve of all 115 primary schools is determined hourly. Therefore, the model is constructed on an hourly cycle. This means that the calculations shown in the next subsections are repeated for every hour of 2022 and 2023.

5.5.1 Radiation and array

The solar radiation during 2022 and 2023 is obtained hourly from the KNMI station the Bilt [54]. Because the KNMI measures the radiation, the values of the KNMI include direct and diffuse solar radiation. The KNMI measures the radiation on horizontal collector [55]. According to the ISSO, a horizontal panel yields 87% of the maximum amount of solar radiation, while a solar panel facing South at a 34°angle yields 100% of the maximum amount. Based on a latitude of North/Western Europe. Therefore, the Excel model adjusts the amount radiation for the azimuth and tilt of the modelled solar array. The relative percentages for all azimuth and tilt percentages are obtained from the ISSO and shown in appendix F [56].

The correct amount of PV/t and PV panels for the simulation are determined manually for each primary school. The maximum number of solar panels is dependent on the available roof area. This roof area is could be limited due to on roof installations or already installed solar array's. Satellite images from Google Maps are used to determine the available roof area. From there equation 13 is used to calculate the maximum amount of solar panels on the available roof area:

$$N_{max} = \frac{A_{available}}{(L_{width} + L_{row}) \cdot L_{length}} \cdot 90\% \tag{13}$$

A row space of 0.8 meter is taken into account for flat roof array's, to service the panels and limit self shading. Panels in an East-West array are assumed to have a row spacing of 0 meters. Because there is not self shading. All panels on a flat roof are modelled on a tilt of 12 °. Panels on a gable roof have the same tilt as the roof. For the dimensions, this research assumes 1 meter wide and 1.7 meters long for both PV/t panel and PV panel. In equation 13, only 90% of the solar panels that fit are actually taken as the max. This margin is taken into account, because the panels won't fit perfectly into the available space, as the size of the panels are fixed. Additionally, an empty space between the available roof area and the edge of the roofs is taken into account. Equation 13 is used for all available roof areas on the roofs of the primary schools. As an example, the maximum available roof area of primary school De Binnentuin is shown in Figure 9.

Figure 9. *Top view of primary school De Binnentuin, with available space for solar panels, obtained from Google Map.*

The maximum available roof area as shown in Figure 9. The empty space between the availabe roof area and the edge of the roof can be observed. The result of equation 13 in relation to Figure 9 are shown in Table 4.

roof area [m^2]	**Tilt [°]**	**Azimuth [°]**	**Row Space [m]**	**Max panels**
172	12	195	0.8	51
264	12	195	0.8	78

Table 4. *Available space for solar panels with appropriate tilt and azimuth for primary school De Binnentuin.*

Table 4 shows the maximum number of solar panels that fit in the available roof area on De Binnentuin calculated with equation 13. The array's, shown in Table 4 are divided into PV/t and PV panels. This is done on the basis of 3 scenario's. In the first scenario 100% of the available roof area is filled with PV/t and 0% with PV. In the second scenario it is 50% to 50% and in the third scenario it is 25% PV/t and 75% PV panels. An example of the scenario's of De Binnentuin, as a result of Table 4, is shown in Table 5.

Array	Tilt	Azimuth	100%	50%	25%
1 PV/t	12	195	129	64	32
1 PV	12	195	0	64	96

Table 5. *Number of PV/t and PV panels installed in different scenario's for primary school De Binnentuin.*

Because of the decrease in PV/t panels per scenario, it is possible to see the affect of lower thermal energy generation on the storage size, COP and storage temperature. Additionally, the thermal and electrical net-zero capabilities for different amounts of PV/t panels become clear.

5.5.2 PV panel modelling

The hourly yield of the PV panels is calculated by the model, in line with the theory in Section 4.2.1. Every hour, equations 1, 2 and 3 are used by the model to calculate the yield. The area A in equation 1 is obtained by multiplying the number of panels of the array by the size of the PV panel, 1.7 m^2. The hourly radiation, obtained from the KNMI is adjusted to the orientation and tilt, as described in Section 5.5.1. The model assumes Polycrystalline PV panels as they are cheaper compared to monocrystalline panels [57]. However, polycrystalline PV panels have a slightly lower efficiency. The model uses the polycrystalline characteristics shown in Appendix B.

5.5.3 PV/t panel modelling

The PV/t panels supply the storage with heat. This can be observed from Figure 8. The hourly amount of thermal energy generated by the PV/t panels is calculated by the model according to the theory in Section 4.2.2. The hourly radiation, obtained from the KNMI is adjusted to the orientation and tilt, as described in Section 5.5.1. Table 6 shows the parameters of the PV/t panels used in the model. The parameters are based on Koehl, and a report on PV/t panels from the Rijksdienst voor Ondernemend Nederland (RVO) [31], [36]. The nominal flow is obtained from PV/t panel manufacturer Abora [58]. An overview of the PV/t panel characteristics, considered in this research is shown in Table 6.

Table 6. *Parameters PV/t panel [31], [36], [58].*

Parameter	Data
Type	Monocrystalline
β	0.0038
η_{Elec}	18.4%
U_0	30.02 W/m^{2}K
U_1	6.28 Ws/m^{3}K
Size	1.7 m^2
Nominal flow	60 L/h
$K_{cell-absorber}$	250 W/m^{2}K
$K_{absorber-water(fluid)}$	100 W/m^{2}K

The PV/t panel produced by Abora is a monocrystalline panel. Therefore, the monocrystilline data obtained from Koehl are adopted in Table 6. The full characteristics of the monocrystalline and polycrystalline panels presented by Koehl, are shown in Appendix B.

Based on the theory presented in Section 4.2.2, the model uses equations 3, 4, 5 and 6 to calculate the thermal energy yield from the PV/t array. Firstly, the heat flux is calculated by the model with equation 5. The K values used for Fourier's law are obtained from the RVO and shown in Table 6. The 2 thermal resistances are combined according to equation 14 [38]:

$$K_{tot} = \left(\frac{1}{K_{cell-absorber}} + \frac{1}{K_{absorber-water}} \right)^{-1} \tag{14}$$

This yields an K_{tot} of 71.42 W/m^{2}K for the mentioned PV/t panel in Table 6.

The module temperature used in equation 5 is calculated with equation 4. The outcome of this equation is dependent on the fluid temperature at the inlet and outlet of the PV/t panel. However, the fluid temperature at the outlet of the PV/t panels is dependent on the heat transferred trough the panel. This creates a loop where the module temperature is dependent on the heat transferred trough the module and the heat transferred through module is dependent on the mean module temperature. To solve this, the outlet temperature of the previous hour is used. The change in temperature because of this is small because the calculations happen hourly. Therefore, no major differences occur.

At the start of the model there is no value for the previous hour. Therefore a start temperature of 10 °C is used. This temperature is adopted because it is in line with the temperature in the system at the first hour of 1-1-2023. Despite changes in the PV/t array and storage, the temperature at that time remains close to 10 °C. In addition to this, changing the starting temperature from 1 to 75 °C, doesn't change the system temperature at the first hour of 1-1-2023. For these reasons, the temperature of the system at the start of 2023 seems a robust starting point for the starting temperature in 2022.

The model calculates the energy flow $\dot{Q}_{pvt}$ with equation 6. The heat flux needed for this equation is a obtained from equation 5. The area A in equation 6 is obtained by multiplying the number of panels by the size of the panel, 1.7 m^2. The result of equation 6 is negative for some hours. During the night there is no radiation to increase the cell temperature. The temperature of the cell cools down to the ambient temperature. Whenever the temperature of the fluid that flows through the panels is warmer than the ambient, $\dot{Q}_{pvt}$ becomes negative. In this case the flow is set to 0, assuming the system stops pumping fluid through the panels as there is no energy to gain.

The temperature increase of the fluid (point 2" in Figure 7) due to the heat from the PV/t panels is calculated with equation 7. As previously mentioned, $\dot{Q}_{pvt}$ is calculated hourly with equation 6. The nominal flow used in equation 7 is shown in Table 6 and multiplied by the amount of panels simulated. The fluid in the panels is water with a Cp of 0.00116 kWh/kg·K (4186 J/kg·K). T_{in} is the inlet temperature of the PV/t unit (point 1" in Figure 7) and is the same as the storage temperature of the previous hour. This is the case, because the energy loss between point 4" and 1" in Figure 8 is neglected. For the first hour a temperature of 10 °C is used for reasons already mentioned earlier in this section.

The energy generated by the PV/t panels and the consequent increase in temperature of the fluid is transported to the STES (point 3" in Figure 8). Equation 7 is used to calculate the amount of energy transferred to the storage. In this instance, not T_2, but Q is the unknown variable. Because, the heat transfer to the storage and from the PV/t panels are in the same cycle, with the same fluid. The mass flow rate and specific heat are the same as mentioned before. T_1 represents the temperature at the outlet of the heat exchanger (point 4" in Figure 8). This value is obtained from the calculations made in the previous hour. The energy transferred to the storage will be used to calculate the temperature of the storage at the end of the hour in Section 5.5.5.

Now, the temperature at point 2" in Figure 8 is calculated as a result of the energy input by the PV/t panels. The temperature at point 3" is the same as point 2". This is the case because energy loss between the points is neglected. The temperature at point 4", the end of the heat exchanger, is assumed to be the same as the temperature of the storage. This is assumed because the temperature at point 4, can not be lower than the temperature of the storage. This is true because the heat exchanger is assumed to be 100% efficient. In reality this might not be the case, which would result in a slightly higher return temperature to the PV/t panel. However, this energy is not lost. It is transferred through the system to the next hour. Thereafter, the energy can then be exchanged with the storage the next hour, therefore not changing the outcome significantly.

Lastly, the electricity generated by the PV/t panels is calculated according to theory in Section 4.2.2.

5.5.4 Heat pump

While the PV/t panels transfer heat into the storage, the water-water heat pump extracts heat from the storage to heat the primary school. The refrigerant R134a is implemented into the model because this fluid is widely used for refrigerators, airco's and heat pumps [59]. Because of it's wide use, saturation tables are available for this refrigerant. The function of the water-water heat pump is to increase the temperature of the fluid from the level of the storage to a usable 75 °C. The heat at 75 °C is then transferred to the heat distribution system of the primary school, e.g. radiators and underfloor heating. A temperature of 75 °C is selected because most building in the Netherlands are heated by a natural gas boiler [5] and typical natural gas boiler provides heat at a temperature of 75 °C [9]. Changing heating system but maintaining the same temperature output eliminates the necessity for additional insulation [10].

To determine the amount of energy extracted from the storage, the enthalpy levels and mass flow rate need to be determined. The hourly amount of thermal energy that has to be transferred to the distribution system is known. This is equal to the hourly heat demand determined in Section 5.3.3. Because the temperature of the heat transferred to the distribution system is fixed. The mass flow rate is the only variable that can increase or decrease the heat transfer to the distribution system. However, because the heat pump is a closed system, an increase or decrease in mass flow rate affect the whole system. Therefore, when the mass flow rate is increased more energy is transferred to the distribution system and at the same time more energy is extracted from the storage. To determine the mass flow rate needed to full fill the energy demand to the distribution system, the model calculates the enthalpy at all 4 points every hour. The 4 point of the heat pump cycle are shown in Section 4.2.4 and Figure 8. The model calculates the enthalpy levels at the 4 point according to the theory in Section 4.2.4.

Points 1 and 3 are on the saturation line. Therefore, they can be determined with saturation tables and temperature. Because the energy transfers to the distribution system is 75 °C and the refrigerant is R134a, point 3 in the heat pump loop has an enthalpy of 164.98 kJ/kg [45]. Additionally, enthalpy at point 4 is the same as point 3. The temperature of enthalpy at point 1 is dependent on the temperature of the storage. Appendix G shows the different levels of enthalpy at point 1 related to the temperature of the storage. Interpolation is used to determine the enthalpy levels whenever the temperature of the storage doesn't exactly match the known levels from the saturation tables. For the first hour a temperature of 10 °C is used for reasons mentioned in Section 5.5.3

Lastly, the model calculates point 2 on the basis of the entropy level at point 1. The entropy level at point 1 is found from the saturation tables as shown in Appendix G. Interpolation is used whenever the temperature of the storage doesn't exactly match the known entropy levels from the saturation tables. Because the process between points 2 and 3 is assumed to be adiabatic, the pressure at point 2 is the same as in point 3, which is 2365.8 kPa at 75 °C [45]. Combined with the entropy level at point 1, as the compressor is assumed to be isentropic, the enthalpy is obtained from the saturation tables in Appendix G.

Because the compressor is in reality not isentropic, an isentropic efficiency of 85% is used to determine a more accurate enthalpy at point 2 [45]. The model uses equation 9 to calculate the real enthalpy at point 2.

When the enthalpy at all 4 point of the heat pump loop are known the following equation is used to calculate the mass flow rate, needed to full fill the hourly heat demand of the primary school.

$$\dot{m}_{heatpump} = \frac{\dot{Q}_{heatdemand}}{(h_2 - h_3)} \tag{15}$$

In equation 15 $\dot{Q}_{heatdemand}$ is the hourly heat demand in kWh. This value is determined according to Section 5.3.3. h_2 and h_3 are the ethalpy levels in point 2 and 3, respectively. $\dot{m}_{heatpump}$ represents the mass flow rate of the fluid in the heat pump cycle in kg/s.

With the mass flow rate, the hourly amount of energy extracted from the storage is calculated with equation 16.

$$\dot{Q}_{heatpump} = \dot{m}_{heatpump} \cdot (h_1 - h_4) \tag{16}$$

$\dot{Q}_{heatpump}$ is the energy extracted from the storage. $\dot{m}_{heatpump}$ represents the mass flow rate in kg/s of the heat pump. h_1 and h_4 are the enthalpy levels of point 1 and 4, respectively. $\dot{Q}_{heatpump}$ will later be used to calculate the temperature of the storage at the end of the hour in Section 5.5.5.

The work in the form of electricity supplied to the heat pump to produce the required thermal energy is calculated with equation 17:

$$\dot{W}_{heatpump} = \dot{m}_{heatpump} \cdot (h_2 - h_1) = \dot{Q}_{heatdemand} - \dot{Q}_{heatpump} \tag{17}$$

$\dot{W}_{heatpump}$ is the power supplied to the heat pump. Calculating the work over enthalpy points 1 and 2 yields the same result as subtracting the energy supplied to the heat pump from the storage from the energy demand of the primary school.

Lastly, because the enthalpy of all stages and mass flow rate are known, the model calculates the COP of the heat pump every hour with equation 8.

5.5.5 Seasonal thermal energy storage

The storage is modelled after a real STES build by HoCoSto. The walls of a HoCoSto storage are insulated with 16 cm of PIR, therefore this is adopted in the model. The λ for PIR is 0.023 W/mK [60]. The length and width of the storage has no limitation, however the height is set at 3.6 meters. The storage as is the maximum capacity is 4,000m^3, this is in line with the reference storage from HoCoSto. The inside of the storage is filled with water. Water is selected, due to its high specific heat and high availability. Water is also used in the reference storage from HoCoSto.

Equations 5 and 6, in combination with the storage characteristics are used to calculate the hourly energy losses thought the walls. This is shown as Q_{losses} in equation 18. The ground temperature used by the model is set at 10 °C [61]. The amount of energy lost through the walls is dependent on the temperature of the storage. However, the temperature of the storage is dependent on the amount of energy lost through the walls. To prevent this from being in a loop $T_{storage}$ is taken from the previous hour, resulting in $T_{storage_t-1}$. For the first hour a temperature of 10 °C is used for reasons already mentioned in Section 5.5.3.

The thermal energy produced by the PV/t panels is transferred to the storage, while the heat pump extracts the energy from the storage when the primary school needs to be heated. Moreover, every hour a certain amount of energy is lost or gained through the walls of the STES. When these three energy flows are taken into account, the model calculates the final temperature at the end of the hour with the following equation, also proposed by Bellos and Tzivanidis [62]:

$$T_{storage} = \frac{(Q_{pvt} - Q_{heatpump} - Q_{losses})}{m \cdot cp} + T_{storage_t-1} \tag{18}$$

The energy in Q are notated without a dot, even though they were calculated as energy flows. However, the mass from the storage is not a flow, therefore they are left out. This change from energy flow to energy is not a problem as the model calculates all values hourly, therefore Watt and Watt hour can be used interchangeably. The mass of the storage is determined by the capacity of the storage filled with water. A conversion of 1 m^3 is 1000 kg is used.

5.6 Linear programming and optimization

Linear programming is used to optimize the size of the installation of the PV/t based energy system. The linear programming tool 'Solver' in Excel is used for this. Within this tool, Non-Linear GRG is adopted.

5.6.1 Thermal optimization.

The linear programming and optimization of the components is based on the following principle: It is the aim of this research to present a (near) net-zero energy PV/t electricity and heating system. In practice this means that the energy generation is the same or nearly the same as the energy required by the primary school over a period of time. When it comes to thermal energy, the STES makes it possible to store the energy when it is not required. This increases the possibility of reaching net-zero energy from a thermal perspective. Therefore, it is the aim to reach net-zero from a thermal perspective first. The thermal energy flows of the system can be described as follows:

$$\dot{Q}_{heatdemand} - \dot{Q}_{pvt} + \dot{Q}_{losses} + \dot{W}_{heatpump} = 0 \tag{19}$$

In equation 19 the energy balance of the system is shown. $\dot{Q}_{heatdemand}$ is the heat demand of the primary school. $\dot{Q}_{pvt}$ presents the thermal energy generated by the PV/t panels. $\dot{Q}_{losses}$ is the energy lost or gained via conduction between the storage and the ground. $\dot{W}_{heatpump}$ is the electrical energy needed to compress the fluid in the heat pump to the required enthalpy level. The system is thermally net-zero when the energy balance of the variables in equation 19 is zero, over 2 years of simulation (with the footnote that the electricity for the heat pump has to be generated).

The changing variables that impact the thermal energy balance are, the amount of PV/t panels and storage capacity. The number of PV/t panels impacts $\dot{Q}_{pvt}$ and storage capacity impacts $\dot{Q}_{losses}$. The power of the heat pump, $\dot{W}_{heatpump}$ is largely dependent on the mass flow rate. And the mass flow rate is dependent on the thermal energy demand, $\dot{Q}_{heatdemand}$ which is a fixed value obtained in Section 5.3.3. The energy required by the heat pump is also dependent on the storage temperature. However, this temperature can not be changed directly. The storage temperature can only be changes by the amount of PV/t panels and storage capacity. Therefore, no variables directly impact the power of the heat pump, only indirectly.

Thus, there are two variables that affect the outcome of equation 19, amount of PV/t and storage capacity. Because they both affect the outcome of equation 19, it is not possible to calculate an optimum with the Solver when both are changing variables. Therefore, one of them has to be determined manually, while the other one is optimized by the Solver. Because of this, the amount PV/t panels installed on the roof, are determined manually based on Section 5.5.1. The length and width of the storage are kept as changing variables. Ultimately resulting in the storage capacity. The result of the solver in relation to equation 19 is and optimal storage size that yields a exactly thermally net-zero if possible.

Lastly, two additional constrains are added to the solver. The size of the storage is limited to a maximum of 4000 m^3. This is in line with the reference STES manufactured by HoCoSto [60]. And the storage temperature must be above 0 and smaller than 75 °C at all time. This is to prevent the storage from freezing and to prevent the heat pump from cooling instead of providing heat.

5.6.2 Electrical optimization

Because it is the goal of this research to analyze a near net-zero energy PV/t based electricity and heating system. It is the aim to generate as much electricity on site as required by the primary school yearly. The PV/t and PV panels are determined for each scenario in line with Section 5.5.1. Because of the grid connection, on-site electrical storage is not necessary for reaching net-zero.

The electricity produced by already installed PV panels on the roofs of primary schools are taken into account when making the electricity balance over 2 years. The yearly electricity yield of the already installed PV panels is shown in Appendix F.

6 Results

In this section, the various results are presented. The results are structured in the same order as the methodology section.

6.1 Potentials and limitations near net-zero primary schools

To determine the limitations and potential concerning primary schools in transitioning towards becoming near net-zero energy, a literature review on this topic is conducted.

A net-zero energy building generates as much energy as the building requires over a specific period of time, typically a year [63]. To make a start with this, the European Union past the Energy Performance of Buildings Directive. In this directive the European Union has directed its member states to ensure that by 2020, all new buildings shall be nearly zero energy buildings [64]. It is relevant to note that this directive is about net-zero energy, not net-zero emissions. The focus of this directive is therefore, not primarily reducing emissions, but generating more energy onsite and reducing energy demand. While both of these measures generally help reduce CO_2 emissions, there is no direct causality.

According to Zeiler et al., in the Netherlands the ambitious targets for a new net-zero energy built environment are currently rarely met. To reach this target for a new net-zero energy built environment buildings must be nearly zero energy and should reach this goal by implementing cost-effective (passive-) measures for a high energy performance and application of sustainable energy source(s) for the remaining demand. This target is especially ambitious when it comes to renovating excising buildings. [65], [66].

The biggest challenge for net-zero projects is the best fit of energy saving design and primary onsite renewable energy utilization, according to Musall et al. [67]. This is especially true for renovation projects with the aim of being net-zero. Musall et al. concludes that a large actor in selecting the best fit of energy saving and renewable generation, is climatic and topological peculiarities. For small residential buildings most of the time the best fit is a low energy house concepts are combined with solar thermal systems, heat pumps and PV panels. For larger residential buildings energy efficient HVAC technology combined with Combined Heating and Power (CHP) and PV systems are most common. When it comes to non-residential building e.g., primary schools, the net-zero solutions are more expensive compared to residential buildings. In most cases reduce in energy demand and the use of mechanical ventilation are used in heating dominated countries. Additionally, utility buildings are limited due to their higher electricity loads and the mostly unfavourable relation of solar suitable surfaces on the roof or facade and floor area of the building. Because of this, most common is a on site CHP to provide heat and power. To summarize the relevant findings from Musall et al., high investment cost and the unfavourable relation between high electricity demand and suitable surfaces for solar panels.

These are not the only limitations to taken into account when transitioning towards net-zero. According to Wei and Harrison, when designing a near net-zero building available infrastructure connections must be considered as this could be a limitation. A necessary reinforcing of the electricity connection is an example of this. Other limiting factors are: Available energy sources, climate conditions and economic factors, some already mentioned by Musall et al. [67]. Lastly, Wei and Harrison mention that achieving a net-zero building requires a high energy efficiency to reduce loads and the implementation of renewable energy sources to balance the energy use [68], [69].

Kneifel et al. used simulations to determine the potential of measures that lead to the requirements mentioned by Wei and Harrison [68], [69], [70]. The following measures to transition towards a net-zero building were included in the simulation: Insulation thicknesses, window specifications, air tightness, heat pump efficiency, water heating, and PV panel array size. The potential of these options and combinations of options where simulated to find the set of measures with the most potential. According to Kneifel et al. the following set of measures has the potential of transitioning towards net-zero energy. Increasing energy generation by placing PV panels (61%), reduced air leakage (21%), more-efficient HVAC equipment including both heat pump and a Heat-Recovery Ventilator (HRV) (15%), and more-efficient domestic hot water Domestic Hot Water (DHW) equipment (9%). From these results a high potential for PV panels can be concluded. The results of the simulations made by Kniefel et al. are not 100% applicable to all buildings. However, these percentages give an indication on what the effect would be for an average building.

In 2013, Aelenei et al. wrote a study about design strategies for non-residential buildings transitioning towards net-zero energy. This was based on 8 net-zero school projects selected from IEA Task 40/Appendix 52 - "Towards net-zero Energy Solar Buildings" in Central and Southern Europe. The study mentions the following potentials in transitioning towards becoming near net-zero: Reducing energy demand and more efficient HVAC installations when designing a net-zero school. Additionally, buildings that are dealing with heating challenges should adopt passive strategies which are oriented towards solar heating maximization and prevention of heat loss strategies [71]. These findings are in line with the findings from Musall et al. and Kneifel et al [67], [70].

Musall et al. and Kneifel et al. also mentioned the potential of PV panels for buildings transition towards net-zero [67], [72]. While regular PV panels are common in the Netherlands [11], [14]. PV/t panels are more rare, however, they have the potential to aid in transitioning to net-zero buildings. PV/t generate heat and electricity simultaneously an are therefore an interesting technology for building applications, which can potentially lead to a higher total efficiency and lower use of space [73]. Additionally, according to Kazanci et al., PV/t panels enable the house to be self sufficient and even produce more energy than it consumes on the electrical side and PV/t panels also contribute significantly to the heat demand [74].

Aelenei et al. proposes an order in which different measures that aid in transitioning towards net-zero should be applied to a building. The first step is to reduce the building energy demand, and second, generate electricity or other energy carriers, to achieve the desired energy balance. The combination of energy demand reduction and use of solar energy has the potential to use a building's site, climate, and materials, when transitioning towards net-zero energy [75]. Effectively Aelenei et al. proposes the same order as the Trias Energetica suggests [76].

Lastly, Attia et al. build a database with the most important energy performance indicators for primary schools. These indicators provide several insights on the reference schools building and systems characteristics. Included indicators are: Occupant density, heating and cooling energy use, energy use intensity and cost. Through these indicators Attia et al. describes the major energy and occupancy performance criteria. With the database of energy performance indicators Attia et al. created two building performance models to set a benchmark for a net-zero primary school. They concludes from the model that the dominant energy use of electricity in Belgian net-zero school is mainly related to the intensive use of mechanical ventilation and electric installations [77]. This electricity use needs to be offset with electricity generation. As mentioned before by Musall et al., the ration between roof area suitable for solar panels and floor size is unfavourable for utility buildings, making transitioning towards net-zero complex.

To summarize, the limitations in transitioning towards becoming near net-zero are related to the local climate and topological peculiarities. When it comes to utility buildings, the relation between available and suitable surface for solar panels and floor area is a limitation. A large floor area in this case is linked to a large energy demand, this is taken into account for the following sub-question. Additionally, energy connections and economic factors are limitations for buildings transitioning towards net-zero. The potential most papers mention is energy reduction. Ultimately, energy that isn't used doesn't need to be generated. In addition to this, more efficient installations and PV panels have the potential to help a building transition towards net-zero.

6.2 The current state of electrical and thermal energy integration

In this Section the current state of electrical and thermal energy integration of the primary schools in the Region of Utrecht is presented. Because of clarity and conciseness, the current state of energy integration is not shown for all 115 primary schools in the region of Utrecht. The energy generation, demand and distribution of the following schools are further elaborated upon: De Kleine Prins, De Olijfboom, De Weide Vleuten Utrecht, De Binnentuin, Montessori Buiten Wittevrouwen, Luc Steve School and Prof. Kohnstammschool. These 7 schools are selected because they differentiate in roof area, stories and construction year. This different building characteristics makes it possible to give insight into what building characteristics enhance or hamper the capabilities of PV/t panels energy systems. Table 7 shows why these 7 primary schools stand out.

Table 7. *Primary schools that stand out because of their building characteristics.*

	roof area	Stories	Construction year
High	De Binnentuin	De Weide Vleuten	De Olijfboom Utrecht
Low	Montessori Buiten Wittevrouwen	Luc Stevenschool	Prof. Kohnstammschool

Table 7 shows which school has a high or low building characteristic. Primary school De Kleine Prins is missing from Table 7. De Kleine Prins mentioned separately, because of the expected high net-zero potential. This is expected because of its low energy demand and large available roof area suitable for solar panels. Therefore, primary school De Kleine Prins is focused on in this research.

In the following sections, energy integration is divided into generation of energy and demand of energy.

6.2.1 Generated energy

Firstly the current generation of electricity is discussed. Electricity is generated with PV panels on the roof of 46 of the 115 primary schools in the region of Utrecht. The yield of De Olijfboom Utrecht, De Binnentuin, Luc Stevenschool and Prof. Kohnstammschool are shown in Figure 10 and 11. The other 3 primary schools from Table 7 don't have PV panels on the roof.

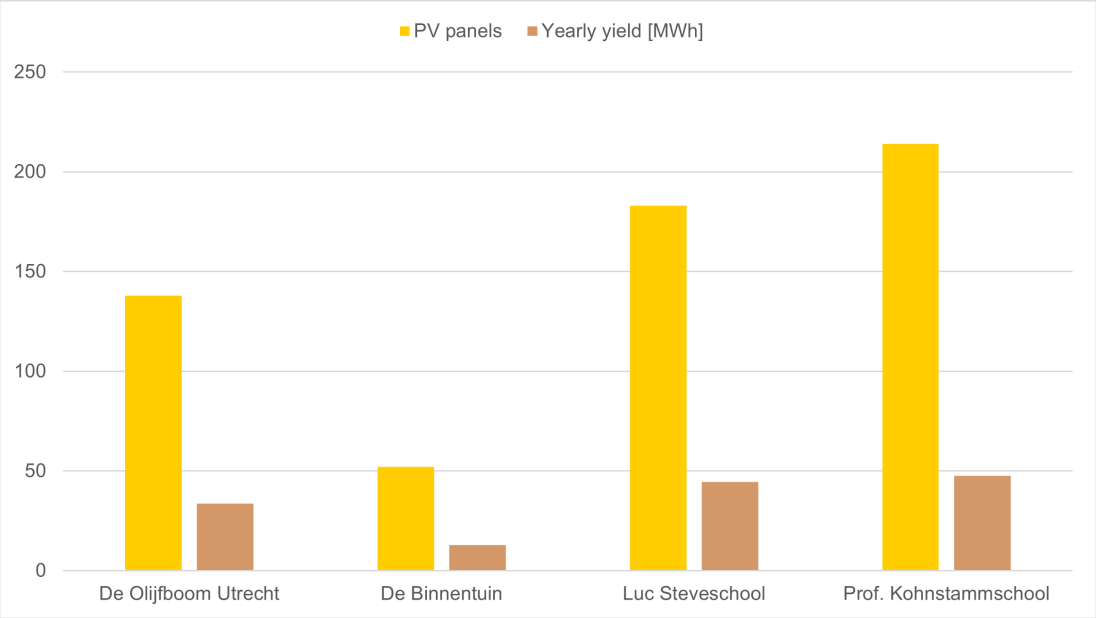

Figure 10. *Number of solar panels and yearly yield in MWh for De Olijfboom Utrecht, De Binnentuin, Luc Steve School and Prof. Kohnstammschool. Data is obtained from SolarGis [22].*

De Olijfboom Utrecht, De Binnentuin and Luc Steve School all have South facing solar array's. The array on De Binnentuin has an azimuth of 195 °while the array's on the other two schools have an azimuth of 145 °. The Prof. Kohnstammschool as an East-West array.

The specific yield of the already installed solar array's are shown in Figure 11.

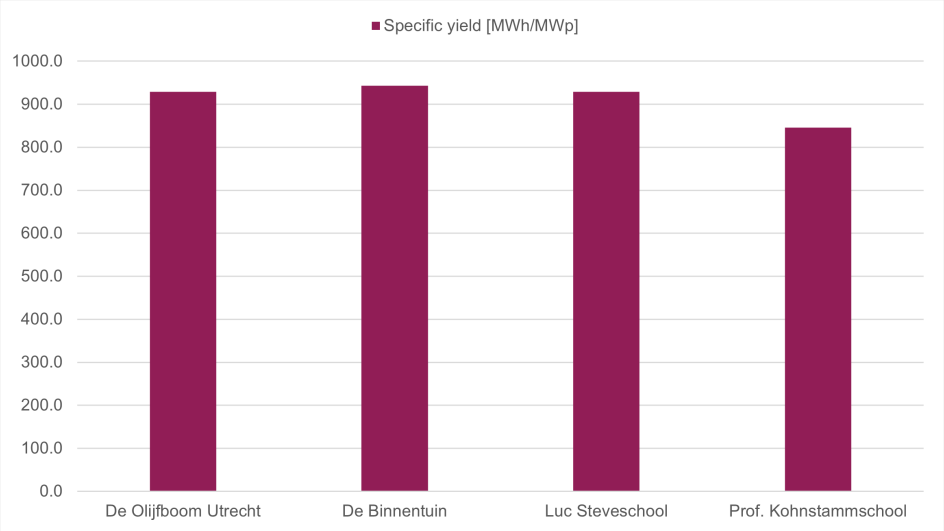

Figure 11. *Specific yield in MWh/MWp for De Olijfboom Utrecht, De Binnentuin, Luc Steve School and Prof. Kohnstammschool. Data is obtained from SolarGis [22].*

Figure 11 shows the specific yield of the panels on the roofs of the primary schools. The specific yield panel of De Binnentuin is slightly higher compared to the other three schools. The reason for this, is the South facing array at an azimuth of 195°. The other schools with a South facing array have an azimuth of 145 °. Therefore, the specific yield is slightly lower. The Prof. Kohnstammschool has an East-West array on the roof. This results in a specific yield of 845 MWh/MWp. This is slightly lower compared to the other array's. This doesn't mean that a South setup is always the best. Because, the panels in an East-West array are placed at a 12 °angle, self shading limited. Therefore, no row spacing is needed between the panel rows. It is therefore possible to place more panels per square meter in an East-West array and consequently generate more electricity. Because of this, the specific yield doesn't show the whole picture.

As mentioned before, 46 of the 115 primary schools in the region of Utrecht have some amount of PV panels on the roof. While these PV panels make the primary school more net-zero, they limit the space for PV/t panels. Therefore, a roof full of PV panels limits the technical possibilities of heat production with PV/t panels.

The yearly yield form the solar array of the other primary schools is shown in Appendix C.

6.2.2 Demand energy

The energy demand is split into heat and electricity. Both are calculated in accordance with the methodology shown in Section 5.3.2. The yearly energy demands of the 7 primary schools are shown Figure 12.

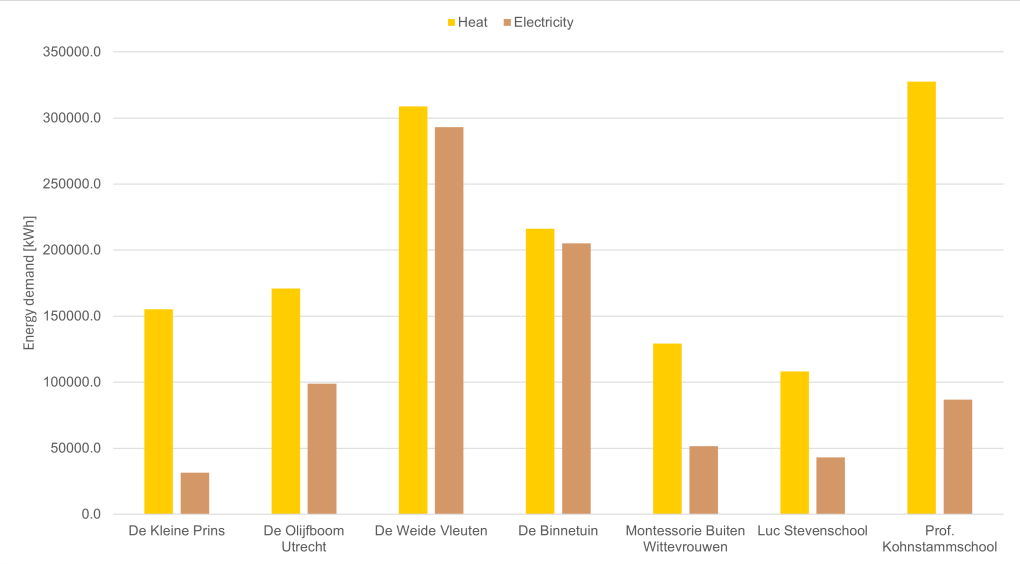

Figure 12. *Yearly heat demand in kWh and electricity demand in kWh for 7 schools in the region of Utrecht.*

Primary school De Weide Vleuten has the highest electricity and second highest heat demand of the 7 primary schools presented in Figure 12. This is due to the size of De Weide Vleuten. This primary schools has 3 stories. These stories in combination with an average roof area, result in a floor area of 8622 m^2. Additionally, De Weide Vleuten is built in 2004 and the CBS dataset, used to estimate the electricity and natural gas demand per square meter, gives newer buildings a higher electricity demand. Consequently, this results in a yearly electricity demand of 293,148 kWh. This electricity demand is exceptionally high. As it is significantly above the average of 96,216 kWh. When it comes to heat, the CBS dataset estimates a lower natural gas use per square meter for newer primary schools, to account for better insulation.

The Prof. Kohnstammschool has yearly heat demand of 327,670 kWh. This is third highest yearly heat demand of all 115 primary schools and the higest of the 7 school in Figure 12. The reason for this, is the age of the primary school. The Prof. Kohnstammschool was build in 1955. The CBS dataset gives a high natural gas use per square meter to account for poor insulation.

The Montessorie Buiten Wittevrouwen and Luc Stevenschool both have a low heat and electricity demand. This is due to the small size of the schools. The same is true for De Kleine Prins. However, de kleine Prins has a slightly lower electricity demand and an slightly higher heat demand. The reason for this, is the slightly older age of the building.

The yearly heat and electricity demand for all 115 primary schools is shown in Appendix H.

6.2.3 Energy distribution

The energy distribution in this Section is a direct result of the methodology in Section 5.3.3. The distribution of electricity demand over 2022 and 2023 for the Luc Stevenschool (top) and De Weide Vleuten (bottem) is shown in Figure 13. The distribution of electricity for the other 5 primary schools mentioned in Table 7 are shown in appendix I. The shape of the distribution is the same for all schools, with the only difference being the maximum and minimum loads.

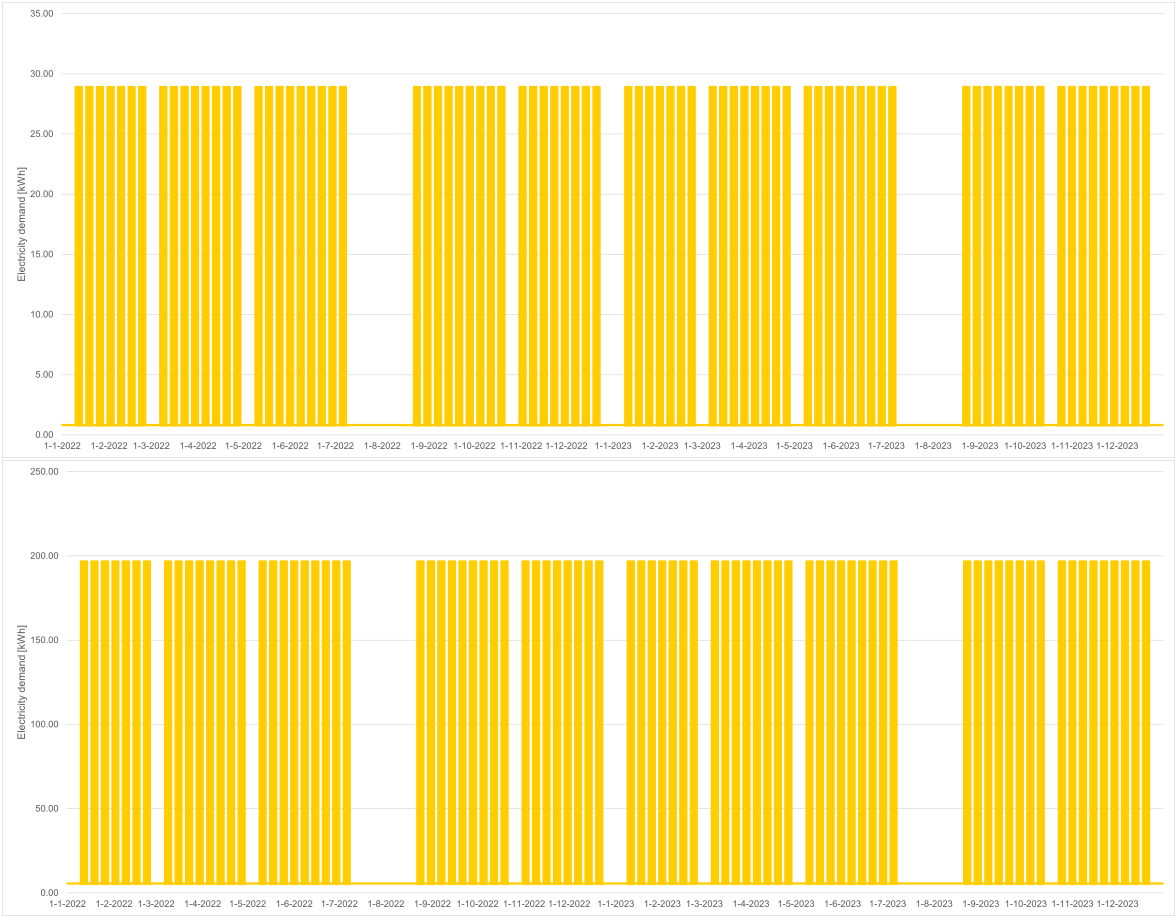

Figure 13. *Electricity demand distribution in kWh over the years 2022 and 2023. The top graph is the Luc Stevenschool and bottom graph is De Weide Vleuten.*

The electricity demand rises during the day and falls during the night, however because the data points are closely together the curve looks like small blocks. The small spaces between the blocks are the weekends, when the electricity goes to base load. The larger spaces between the blocks are school holidays. The Luc Stevenschool uses 43,072 kWh yearly and has an estimated hourly max demand of 29 kWh. In contrast, De Weide Vleuten has an yearly electricity demand of 293,148 kWh and an estimated hourly max demand of 196 kWh. This is also shown in Figure 14.

Figure 14. *Electricity demand distribution in kWh over 1 day (11-1-2022). The top graph is the Luc Stevenschool and bottom graph is De Weide Vleuten.*

Figure 14 shown the daily electricity load for de Luc Stevenschool (top) and De Weide Vleuten (bottom). This is a direct result of Table 3, shown in the methodology Section 5.3.3. Figure 14 shown more clearly how the electricity demand is distributed during a typical school day. Instead of the blocks shown by Figure 13. Again, the shape of the electricity demand for both schools in Figure 14 is the same. However, the maximum and base load is different due to the different electricity demands.

Figure 15 shows the distribution of thermal heat, over the years 2022 and 2023 for the Luc Stevenschool (top) and De Weide Vleuten (bottom). The shape of the distribution is the same fore both primary school. The only difference between the schools is the height of the maximum loads.

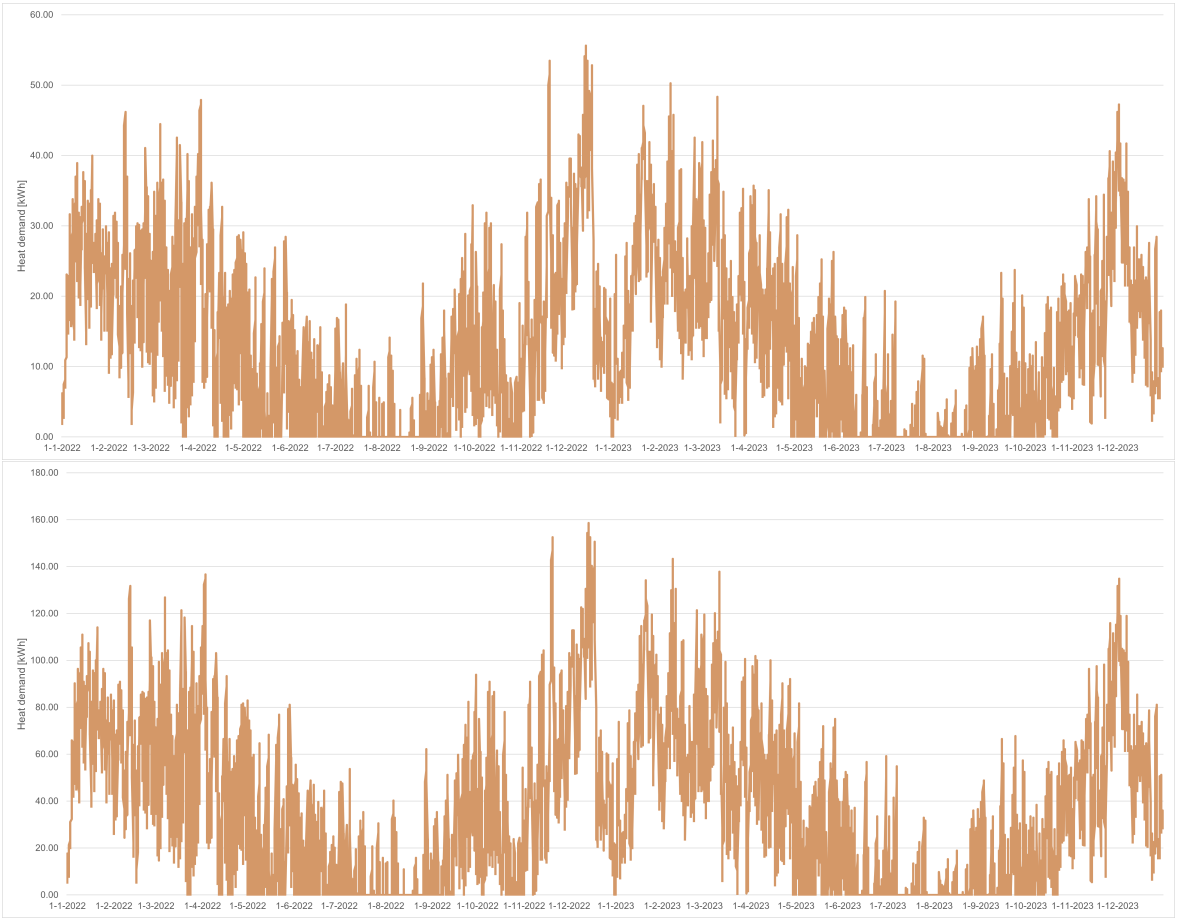

Figure 15. *Heat demand distribution in kWh over the years 2022 and 2023. The top graph is the Luc Stevenschool and bottom graph is De Weide Vleuten.*

The heat demand in Figure 15 seems less consistent compared to the electricity demand. This is the case because the heat demand is closely related to the ambient temperature and this fluctuates during the year. Even though the heat demand seems to be rather inconsistent, the distribution curve is not as inconsistent as it appears in Figure 15. It looks that way, because the data points in Figure 15 are closely packed together. Moreover, it seems that the heat demand rarely goes to 0 kWh in the summer. However, this is not the case, as the heat demand is 0 kWh for 26.6% of the hours over 2 years. This is the case for all primary schools, as the shape of the distribution curve is the same. The small Luc Stevenschool has a maximum hourly heat demand of 55 kWh, while the large De Weide Vleuten has a maximum hourly heat demand of almost 160 kWh. This again, shows the effect school size has on the distribution of energy.

The heat demand distribution over the years 2022 and 2023 for the other 5 primary schools are presented in Appendix J.

6.3 Setup of essential installation components

The energy demand of the primary schools, shown in the previous section, is to be provided by PV/t and PV panels. To provide an insight into the setup of the PV/t panels and other essential components, a literature review is conducted. Additionally, the literature review aims to evaluate the different types of PV/t panel based energy systems setups. Based on this evaluation the setup that will be modelled to determine the technical capabilities of the PV/t based energy systems further, is selected.

The required components in a PV/t powered electricity and heating system, depends on the setup. According to Mojanraj et al. and Chu et al., PV/t systems with the intend of space heating are characterized by there integration of PV/t and heat pump [78], [79]. This integration of PV/t and heat pump can be direct or indirect, as shown in Figure 16.

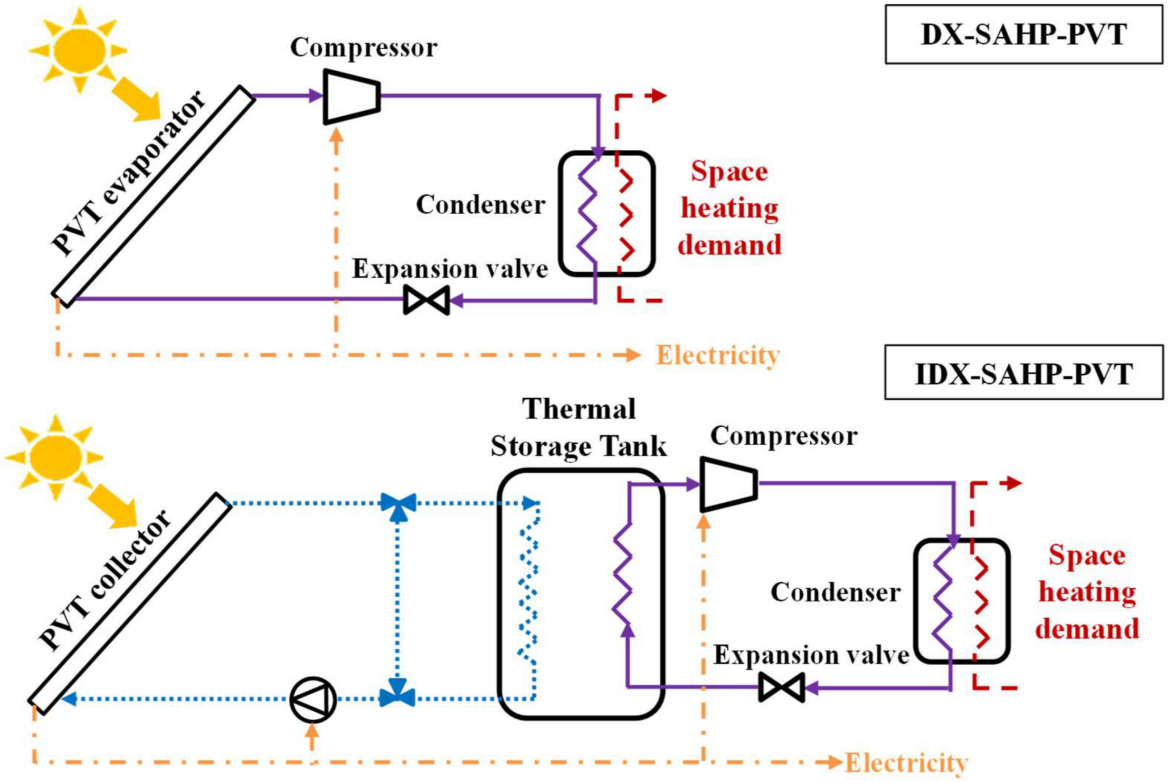

Figure 16. *Schematic diagram of a direct-expansion solar-assisted heat pump system and an indirect-expansion solar-assisted heat pump system [78].*

When directly integrated the PV/t panels the heat produced by the PVT collectors is used as the source for a heat pump to provide space heating [80]. In this case, the fluid is usually a refrigerant. While an aluminium tube functions as the absorber of a refrigerant-based PV/t collector. This functions as the evaporator of the heat pump, and the storage tank as the condenser. This system reached yearly average COP's of 3.4 and 5.2 in two different climates in China [81]. Direct PV/t panels in the direct systems typically don't generate energy at high temperatures. Therefore, mostly uncovered PV/t panels are used for these types of systems [33].

Alternatively, an indirect, more conventional system is shown Figure 16. In this case an energy storage is an intermediate between the PV/t panel and the heat pump. These systems are more expensive and thus usually have a longer payback times than the direct systems. Therefore, they are recommended in larger applications such as commercial, or industrial applications [78]. Bellos and Tzivanidis studied this indirect PV/t system, based on a case study in Greece. They found that the system works most optimal in April, while December is the month with the lowest energy production [62].

Bellos et al. compared this indirect PV/t setup with three other system: PV panels coupled with an air-water heat pump, water-water heat pump with a Flat Plate Collector (FPC), that only produce heat and a water-water heat pump with PV modules and a FPC [82]. The results of this comparison showed that the most suitable alternative is strongly dependent on the electricity price, with the PV panels coupled with an air-water heat pump being the most sustainable option for electricity prices up to 0.23 €/kWh, while for higher electricity prices PV/t panel setup integrated with a water-water heat pump seems the most potent system.

Indirect PV/t system are also proposed in various other case studies. Del Amo et al. proposed this for the university of Zaragoza [18]. Additionally, Pintanel et al. and Martínez-Gracia et al. proposed an indirect system for a social housing project in Zaragoza [19] [20]. Lastly, Wang et al. proposed an indirect PV/t panel system as one of the options for a sport complex in Bari, Italy [21]. All studies proposed small variations on the standard indirect PV/t system in Figure 16.

There are 3 types of indirect PV/t systems: series, parallel and dual [83]. Figure 17 shows the 3 variants of the indirect PV/t configuration setups.

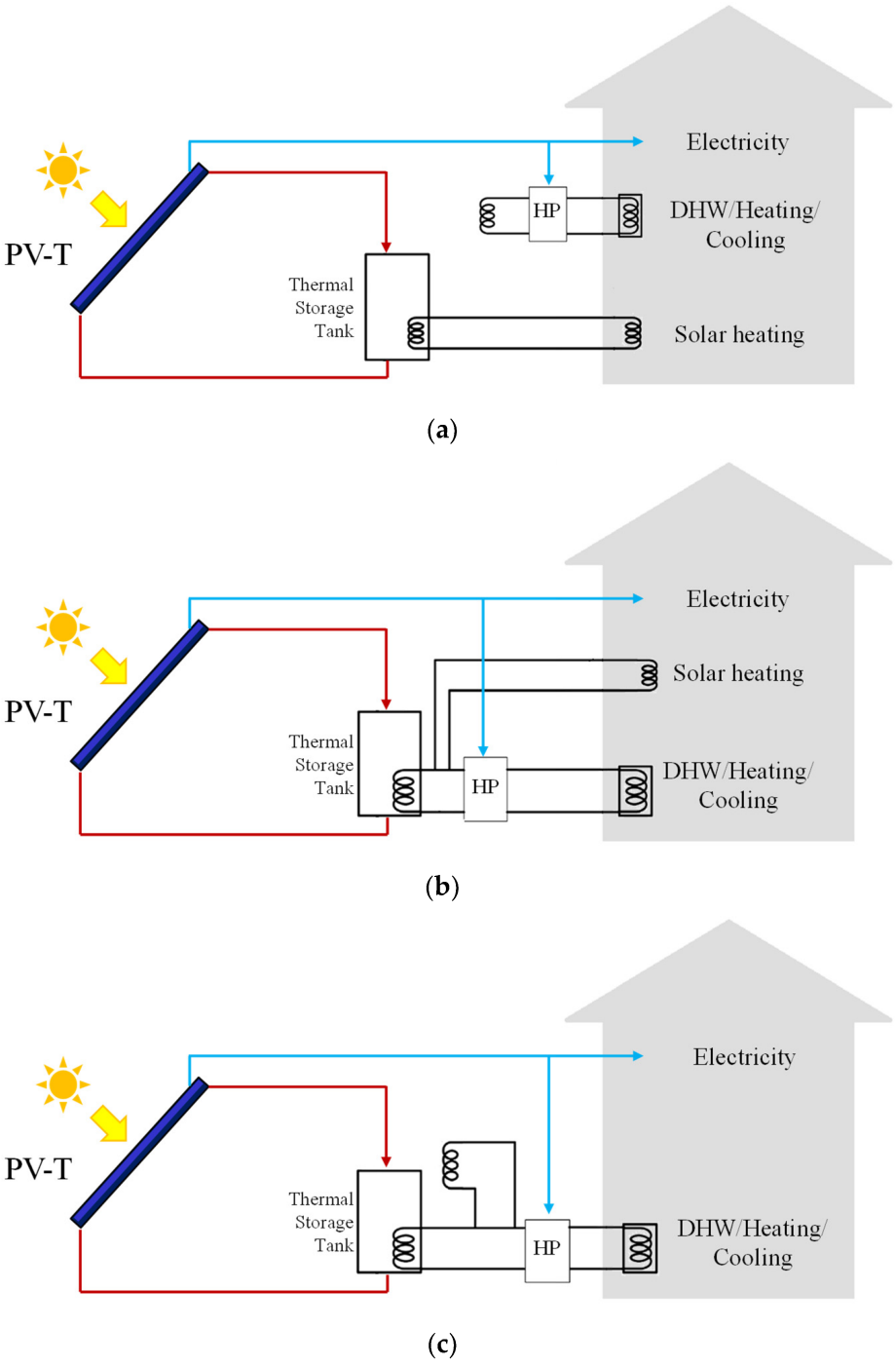

Figure 17. *Schematic diagram of (a) a parallel air-to-water HP system, (b) a series water-to-water HP and system (c) a dual-source air-to-water HP system, all based on PV-T collectors [83].*

In Figure 17 3 types of an indirect PV/t setup are shown: Parallel, series and dual. These setups consist of the same components in a different configuration. Figure 17 (a) shows a parallel configuration, consisting of a heat pump that receives electricity from the PV/t panels for DHW and cooling, depending on the heat pump operation mode. The thermal storage is connected to the solar heating of the building [84], [85].

In Figure 17 (b) a configuration in series is shown. In this case, the thermal output of the water-based PV/t panel is integrated with a water-to-water heat pump [86], [87]. This increases the COP of the heat pump, maintaining the source of the heat pump at a fairly constant temperature [88], [89]. Experimental results of this setup on a clear day show an average solar efficiency of 45% and a whole system average COP of 4.9 [90]. Obalanlege et al. developed a mathematical model able to analyse the influence of solar radiation, water storage tank size and water flow rate through the PV/t panels on the performance of the system. Their results show that increasing the flow rate enhances the total PV/t panel efficiency. Additionally, increasing the size of the storage tank increases the total efficiency of the PV/t panels. This is the case because for large storage volumes, the temperature decreases more slowly, compared to a smaller storage. A minimum COP of 4.2 was obtained [91].

Lastly, setup configuration (c) shows a water-based PV/t panel that is coupled with a dual-source air-to-water heat pump [92]. Therefore, this is a dual configuration. In this configuration, the energy source of the heat pump is the energy storage connected to the PV/t panel and outdoor fan unit. Therefore, the heat pump functions a water-water unit for the energy storage and air-water heat pump for the fan unit. This means that on cold days, the energy storage can act as the source for the heat pump. Increasing COP as the thermal storage is warmer than the outside. While on warm days the air-to-water heat pump can be used as the source, allowing the thermal storage to be refilled. It is even possible to run both units in parallel to provide more heat to the building. [87], [93], [94].

All setups have advantages and disadvantages. However, for this research the standard indirect setup is modelled. This setup is shown at the bottom in Figure 16. The direct setup is not modelled because it uses "uncovered" PV/t panels. These panels are outside the scope of this research, as mentioned in Section 4.2.2. Variants of the indirect PV/t setup, shown in Figure 17, differ only slightly from each other and the standard indirect PV/t setup. While the difference between the indirect systems is marginal. The three variants from Figure 16 are more complex to model as the heat is extracted from multiple sources or diverted to multiple users. While modelling, this would lead to the question: When does the system use which energy source? And how much energy is diverted to which user? Because the differences between the indirect variants are only minimal and the standard indirect setup is less complex, the standard indirect PV/t setup is selected for the model.

6.4 Technical analysis of the PV/t based energy system

In this section a technical analysis on the capabilities of a PV/t based electricity and heating system, in combination with a STES and heat pump for a primary school is presented. The PV/t system is modelled in Excel for each primary school and all scenario's. The theory and method behind the model are shown in sections 4 and 5. The technical analysis focuses on the 7 primary schools, already mentioned in Section 6.2, Table 7. However, the available roof area, array's and net-zero capabilities of all 115 primary schools in the region of Utrecht are shown in Appendices L and M.

6.4.1 Technical scenario analysis De Kleine Prins

The scenario analysis starts with primary school, De Kleine Prins. This primary school has a lower energy demand relative to the available roof area. The available roof area for solar panels is shown in 8. Additionally, a top view of the school, with the available roof area is presented in Appendix K.

Roof Area [m^2]	**Tilt [°]**	**Azimuth [°]**	**Row Space [m]**	**Max panels**
116	12	120	0.8	34
80	12	120	0.8	24
90	20	210	0	48
90	20	210	0	48
187	20	210	0	99

Table 8. *Available space for solar panels with appropriate tilt and azimuth for primary school De Kleine Prins.*

As shown in Table 8, there are 5 area's where panels can be placed. 2 of these area's are on a flat roof. Therefore a tilt of 12 °, with row size of 0.8 is selected. The array is modelled along the building, facing South. The 3 other area's aren't flat. Therefore, a tilt equal to the slope of the roof is selected. Again, the azimuth along the building is used. In the last column, the maximum number of solar panel for the specific area's are shown. This is calculated with equation 13, mentioned in Section 5.5.1. The 5 available roof area's can be brought back to 2 array's, one on the flat part of the roof and one on the sloped part of the roof.

The different scenario's for these 2 array's, with corresponding azimuth and tilt are shown in Table 9. The array's used in the scenario's for all 115 primary schools is shown in Appendix L.

Array	Tilt	Azimuth	100%	50%	25%
1 PV/t	12	120	58	28	14
1 PV	12	120	0	28	43
2 PV/t	20	210	194	97	48
2 PV	20	210	0	97	145

Table 9. *Number of PV/t and PV panels installed in different scenario's for primary school De Kleine Prins.*

The number of panels in the scenario's are used in model and the storage capacity is optimized with linear programming. This leads to the thermal energy generation and losses for various components during the simulated years, 2022 and 2023. The total thermal energy demand, production and losses are shown in Figure 18.

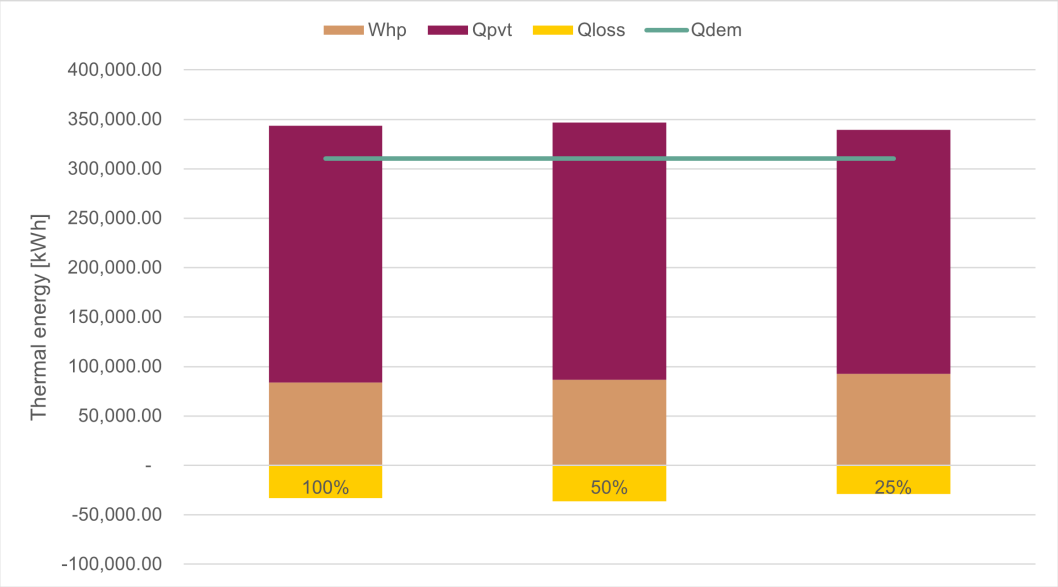

Figure 18. *Thermal energy demand (Qdem), production (Qpvt and Whp) and storage losses (Qloss) for the scenario's, 100%, 50% and 25% of available roof area filled in with PV/t. Presented for the simulation over the years 2022 and 2023 for primary school De Kleine Prins.*

The red line in Figure 18 shows the demand of thermal energy over 2022 and 2023. The energy demand is fulfilled by the PV/t panels and storage in all 3 scenario's. Therefore, from a thermal energy perspective, primary school De Kleine Prins is net-zero energy. With 100% of the available roof area covered by PV/t panels, about 25% of the thermal energy demand is provided by the heat pump. In this scenario, the other 75% is produced by the PV/t panels. More energy is provided by the heat pump when only 25% of the available roof area is cover with PV/t. The reason for this, is the reduction in thermal energy generation by the PV/t panels and consequent lower storage temperature. This increases the thermal energy demand that the heat pump has to provide.

The thermal energy generated by the PV/t panels is lower when 100% of the available roof area is filled with PV/t compared to 50% of the roof area. In the 100% scenario during the summer the temperature of the fluid in the panels and storage is almost the same as the cell temperature. The temperature of the fluid and temperature of the storage cannot go above the cell temperature. This is the stagnation temperature. Because the storage in the 100% scenario is smaller compared to the 75% scenario the stagnation point is reached earlier. Resulting in less energy transfer from the panel to the fluid as they have the same temperature.

The temperature of the storage in the 3 scenario's for De Kleine Prins are shown in Figure 19.

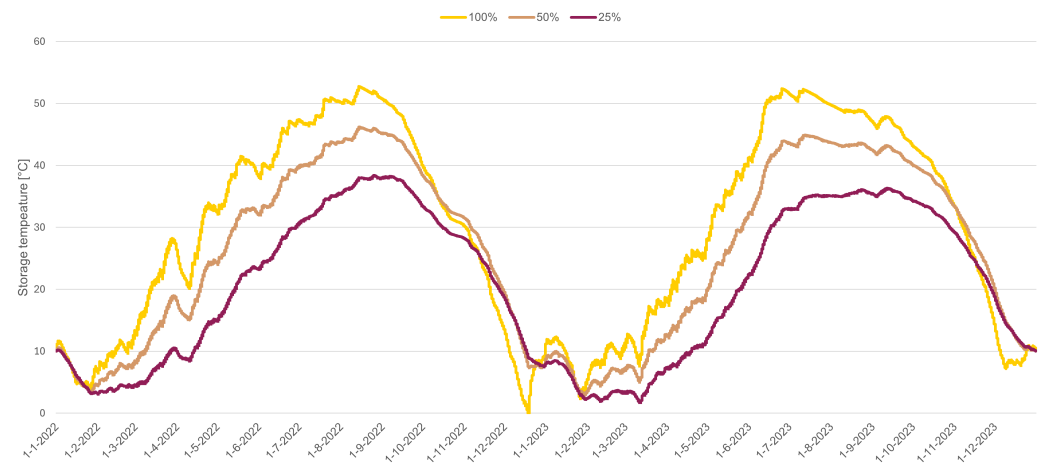

Figure 19. *The temperature in the storage of primary school De Kleine Prins in the years 2022 and 2023. The scenario's are discribed as the percentage of PV/t placed on the available roof area.*

Figure 19 shows the temperature of the storage in the 100% PV/t scenario is less stable compared to the 25% PV/t scenario. The reason for this, is the smaller storage. Because of the smaller storage and large PV/t array, the stagnation point is reached in the 100% scenario. Consequently, no additional energy is transferred to the storage, as it is all the same temperature. In this instance, it makes more sense to down scale the PV/t array or increasing the storage capacity.

The storage capacity for De Kleine Prins in all 3 scenario's is shown in Table 10.

	100%	**50%**	**25%**	Unit
Storage Cap	744.84	1,142.05	1,425.07	m^3
AveCOP	4.69	4.26	3.77	

Table 10. *Storage capacity and average COP of the heat pump over years 2022 and 2023 in different scenario's for primary school De Kleine Prins.*

As shown in Table 10, the storage gets larger when less PV/t is installed, resulting in a smaller energy loss according to Figure 18. This sounds counter intuitive, however during the winter the temperature of the storage goes below the ground temperature. Therefore, energy from the ground is transferred into the storage. During these periods, a larger storage is beneficial. While this pattern holds for all other schools and all other scenarios. The energy loss in the 100% scenario is smaller compared to the 50% scenario. Despite the smaller storage in this scenario. Due to the smaller storage and its consequent unstable temperature. The temperature of the storage is longer below the ground temperature, compared to the other scenario's. Therefore, more energy is transferred into the storage from the ground, which resuls in a lower thermal energy low trough the ground.

The electricity demand and production by the PV/t and PV panels for primary school De kleine Prins is shown in Figure 20.

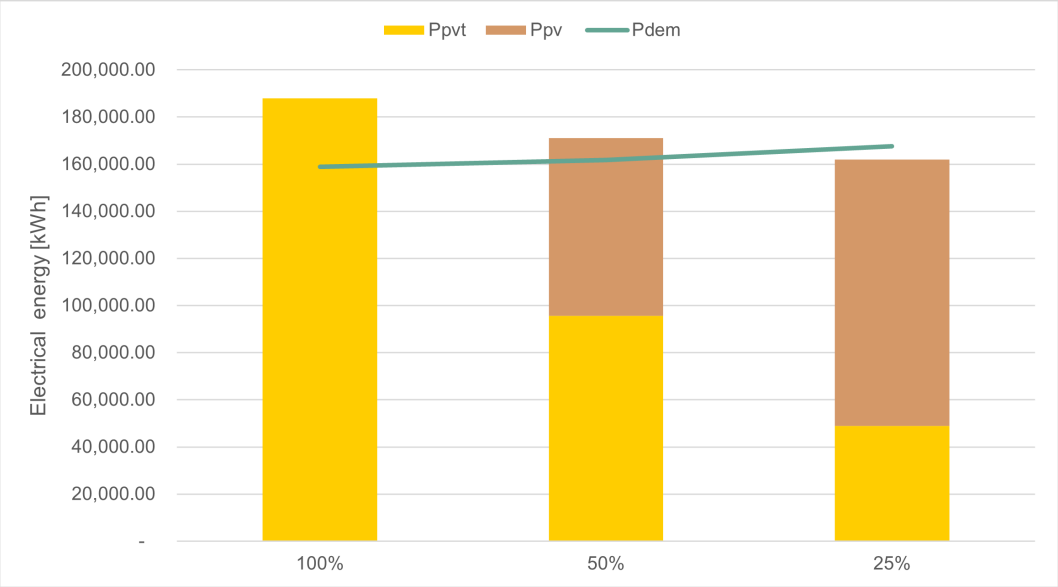

Figure 20. *Electrical energy demand (Pdem) and production (Ppvt and Ppv) for the scenario's, 100%, 50% and 25% of available roof area filled in with PV/t. Presented for the simulation over the years 2022 and 2023 for primary school De Kleine Prins.*

Figure 20 shown that the electrical energy demand is met in the 100% and 50% scenario's. This is achieved due to the large number of PV/t panels installed on the roof. It is important note that the connection to the electricity grid remains needed in all scenario's. Even tough the PV/t and PV panels generate in the 100% and 50% scenario's enough electricity to be net-zero. The reason for this, is the mismatch between the generation and demand of electricity, as an electricity storage is not considered in this research. Figure 20 an increas in electricity demand when less PV/t panels are installed. The reason for this, is the lower storage temperature when less PV/t panels are installed. This increases electrical load required by the heat pump. Also the electricity generation decreases when less PV/t panels are installed. This is the case because more PV panels are installed instead of PV/t panels. The PV panels produce less electricity than their PV/t counterparts because the efficiency of the polycrystalline PV panels is lower compared to the monocrystalline PV/t panels. However, even if the panels had the same efficiency, the PV/t panels would generate more electricity yearly, because they have a lower average cell temperature compared to their PV counterpart, due to the fluid that cools the cells.

6.4.2 Technical scenario analysis De Olijfboom

Primary school De Olijfboom is a relatively new building compared to the other school. The school was built in 2015 and has 2 stories. On the roof there are 3 area's available for solar panels, apart from the already exciting array of PV panels. A top view of De Olijfboom and 3 area's available for solar panels is presented in Appendix K. In Table 11 size of the area's and corresponding tilt, azimuth, row spacing and number of panels are shown.

Roof Area [m^2]	**Tilt [°]**	**Azimuth [°]**	**Row Space [m]**	**Max panels**
30	12	145	0.8	9
50	12	145	0.8	15
230	12	145	0.8	68

Table 11. *Available space for solar panels with appropriate tilt and azimuth for primary school De Olijfboom.*

The azimuth of the area's is in line with the already existing PV array, as is the tilt. The area's shown in Table 11 are translated to the scenario's shown in Table 12.

Array	**Tilt**	**Azimuth**	**100%**	**50%**	**25%**
1 PV/t	12	145	91	46	23
1 PV	12	145	0	46	68

Table 12. *Number of PV/t and PV panels installed in different scenario's for primary school De Olijfboom.*

Only one array of PV/t or PV is includes as there is only 1 orientation, tilt and row spacing used.

The thermal capabilities of the scenario's are shown in Figure 21.

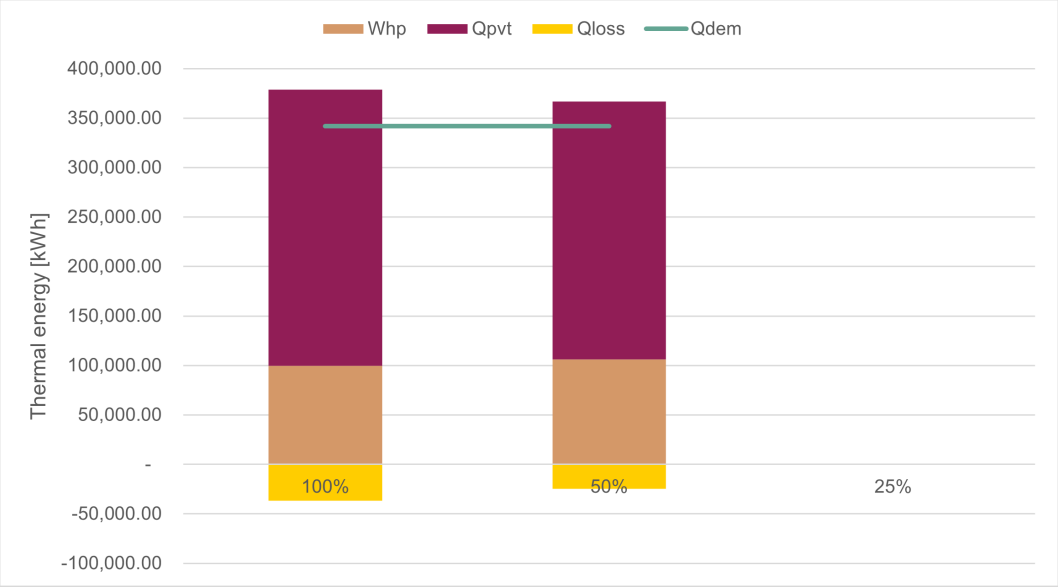

Figure 21. *Thermal energy demand (Qdem), production (Qpvt and Whp) and storage losses (Qloss) for the scenario's, 100%, 50% and 25% of available roof area filled in with PV/t. Presented for the simulation over the years 2022 and 2023 for primary school De Olijfboom.*

In scenario's in which 100% and 50% of the available roof area is filled with PV/t panels, net-zero energy from a thermal perspective is reached. The 25% scenario is left out in Table21. This is the case because it was not possible to make the thermal energy balance zero. All solutions left the storage emptier. Therefore, it is not possible to solely rely on PV/t panels, STES and a heat pump for the production and storage of thermal energy. Approximately the same ratio as between PV/t generation and heat pump can be observed, as was the case for De Kleine Prins. The PV/t panels and heat pump combined produce almost the same amount of thermal energy compared to De Kleine Prins. This similarity is not the case for the storage capacity. The storage capacity and average COP over the years 2022 and 2023 are shown in Table13.

	100%	**50%**	**25%**	Unit
Storage Cap	1,444.41	1,993.88	-	m^3
AveCOP	3.95	3.49	-	

Table 13. *Storage capacity and average COP of the heat pump over years 2022 and 2023 in different scenario's for primary school De Olijfboom.*

Because the maximum number of panels for De Olijfboom is lower than De Kleine Prins, a larger storage capacity is needed to reach net-zero from a thermal perspective. For the same reason, the COP is lower in both scenario's of De Olijfboom compared to De Kleine Prins.

The electricity production and demand is shown in Figure 22.

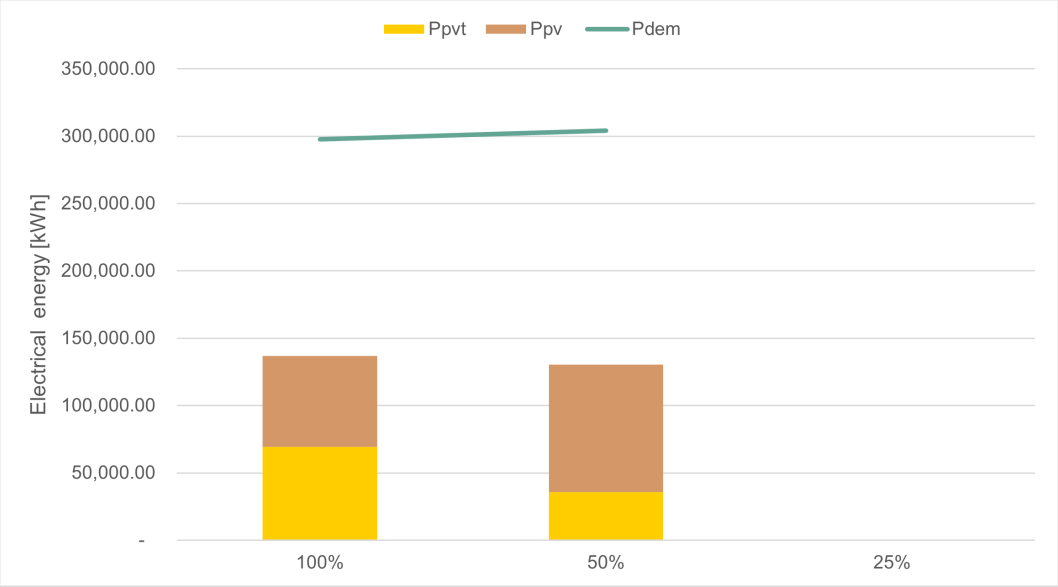

Figure 22. *Electrical energy demand (Pdem) and production (Ppvt and Ppv) for the scenario's, 100%, 50% and 25% of available roof area filled in with PV/t. Presented for the simulation over the years 2022 and 2023 for primary school De Olijfboom.*

The net-zero requirements for electricity are not reached in either of the scenario's for De Olijfboom. About 47% of the electricity demand can be generated on site in the 100% PV/t scenario. This decreases to 44% for the 50% PV/t scenario. Because, a PV array is already installed on the roof of De Olijfboom, in the 100% PV/t scenario, there is additional electricity generated with PV panels.

6.4.3 Technical scenario analysis De Weide Vleuten

De Weide Vleuten is a 3 stories high primary school, built in 2004. Because of the amount of stories and consequently, above average floor area, the energy demand of De Weide Vleuten is relatively high compared to other schools. This can be observed in Appendix H. A top view of De Weide Vleuten, with corresponding area's available for solar panels is presented in Appendix K. The size of the area's, tilt, azimuth, row spacing and maximum number of panels shown in 14.

Roof Area [m^2]	**Tilt [°]**	**Azimuth [°]**	**Row Space [m]**	**Max panels**
109	45	120	0	58
82	45	300	0	43

Table 14. *Available space for solar panels with appropriate tilt and azimuth for primary school De Weide Vleuten.*

Only two area's on the roof of De Weide Vleuten are available for solar panels. The tilt of the solar panels is adjusted to the tilt of the roof. De Weide Vleuten has a gable roof, therefore the tilt is 45 °. No row spacing is assumed, as the panels are installed on a tilted roof. The scenario's for De Weide Vleuten are shown in Table 15.

Array	**Tilt**	**Azimuth**	**100%**	**50%**	**25%**
1 PV/t	45	120	58	29	14
1 PV	45	120	0	29	43
2 PV/t	45	300	43	22	11
2 PV	45	300	0	22	33

Table 15. *Number of PV/t and PV panels installed in different scenario's for primary school De Weide Vleuten.*

The scenario's consist of 2 array's, 1 on each side of the roof.

The demand, production and loss of thermal energy in relation to the scenario's described in Table15, are presented in Figure 23.

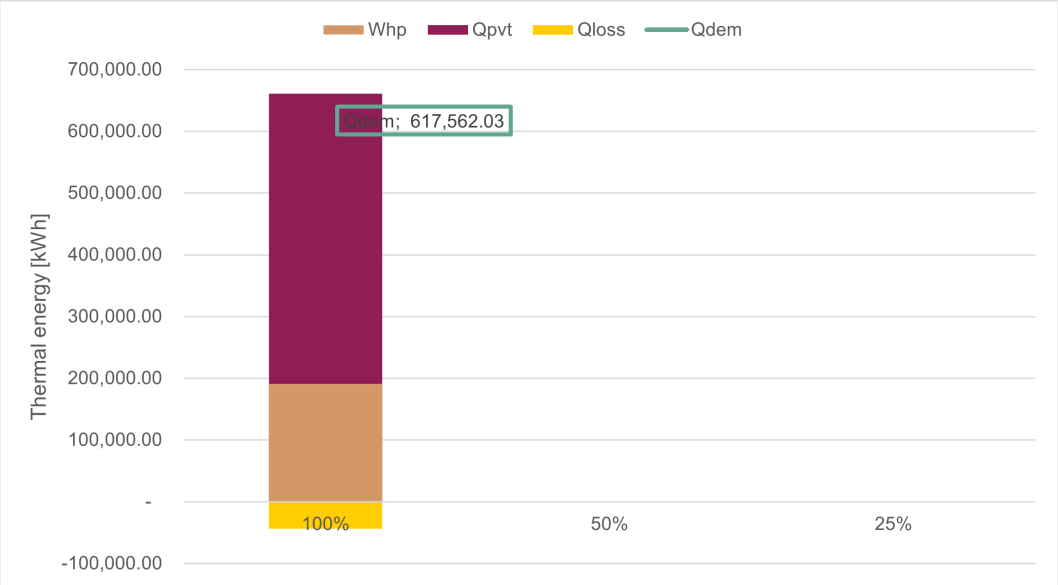

Figure 23. *Thermal energy demand (Qdem), production (Qpvt and Whp) and storage losses (Qloss) for the scenario's, 100%, 50% and 25% of available roof area filled in with PV/t. Presented for the simulation over the years 2022 and 2023 for primary school De Weide Vleuten.*

The thermal energy balance of primary school De Weide Vleuten is only 0 with 100% PV/t panels installed on the available roof area. It was not able to make a net-zero thermal energy balance with the other two scenario's. The reason for this, is the low amount of available roof area for solar panels, in relation to the high floor area and consequent, high heat demand. The number of stories is The reason for this, unfavourable ratio between the available roof area and energy demand. This also results in the need for a storage capacity twice as large as the STES's of De Kleine Prins and De Olijfboom.

The storage capacity and COP of the scenario's for De Weide Vleuten are shown in Table16.

	100%	**50%**	**25%**	Unit
Storage Cap	3,490.91	-	-	m^3
AveCOP	3.52	-	-	

Table 16. *Storage capacity and average COP of the heat pump over years 2022 and 2023 in different scenario's for primary school De Weide Vleuten.*

In addition to the high required storage capacity, the 100% scenario of De Weide Vleuten also results in a low COP. This is the case because of the high temperature difference between the energy source of the heat pump, the storage, and the distribution system. The temperature of the distribution system for all schools is set at 75 °C. However, the storage temperature in this scenario is lower compared to the other schools. This is the case because of the low thermal energy generation of the

PV/t panels, while a lot of energy is extracted from the storage to provide heat to the primary school. Because of this, the COP of the heat pump is low.

The electricity production by PV/t and PV and electricity demand is presented in Figure 24.

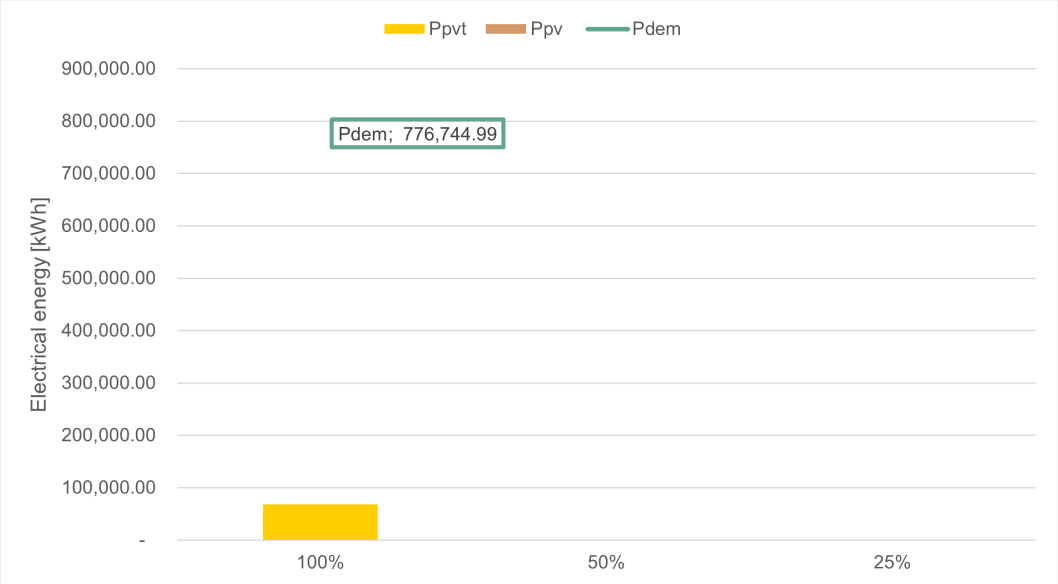

Figure 24. *Electrical energy demand (Pdem) and production (Ppvt and Ppv) for the scenario's, 100%, 50% and 25% of available roof area filled in with PV/t. Presented for the simulation over the years 2022 and 2023 for primary school De Weide Vleuten.*

Because of the unfavourable relation between energy demand and available roof area for solar panels, De Weide Vleuten is far from net-zero energy when it comes to electricity. There are no already installed PV panels and the installed PV/t panels in the 100% scenario are only able to generate 9% of the electricity demand. The remaining electricity has the be imported from the grid. The reason for this, is the high electricity demand due to the size of the primary school. De Weide Vleuten has a floor area of 8622 m^2. Additionally, the electricity required by the heat pump is relatively high due to the low COP.

6.4.4 Technical scenario analysis De Binnentuin

Primary school De Binnentuin has a floor area of around 6.000 m^2. Consequently, the primary school has an above average energy demand. Additionally, the school has a large roof with an already installed PV array of 54 panels. The large roof of the primary school makes placing large PV/t array's possible. The available area's for these panels on the roof are shown in the top view in Appendix K. The size of the area, orientation, tilt, row spacing and maximum panels is shown in Table17.

Roof Area [m^2]	**Tilt [°]**	**Azimuth [°]**	**Row Space [m]**	**Max panels**
172	12	195	0.8	51
264	12	195	0.8	78

Table 17. *Available space for solar panels with appropriate tilt and azimuth for primary school De Binnentuin.*

Despite the large installation on the roof and already installed PV array, there is still room for 129 solar panels. The orientation and tilt is in line with the already installed PV array. The scenario's for De Binnentuin are shown in Table18.

Array	**Tilt**	**Azimuth**	**100%**	**50%**	**25%**
1 PV/t	12	195	129	64	32
1 PV	12	195	0	64	96

Table 18. *Number of PV/t and PV panels installed in different scenario's for primary school De Binnentuin.*

No second array is used in the scenario, as both area's have the same orientation and tilt.

The results of the thermal energy production, losses and demand are shown in Figure 25.

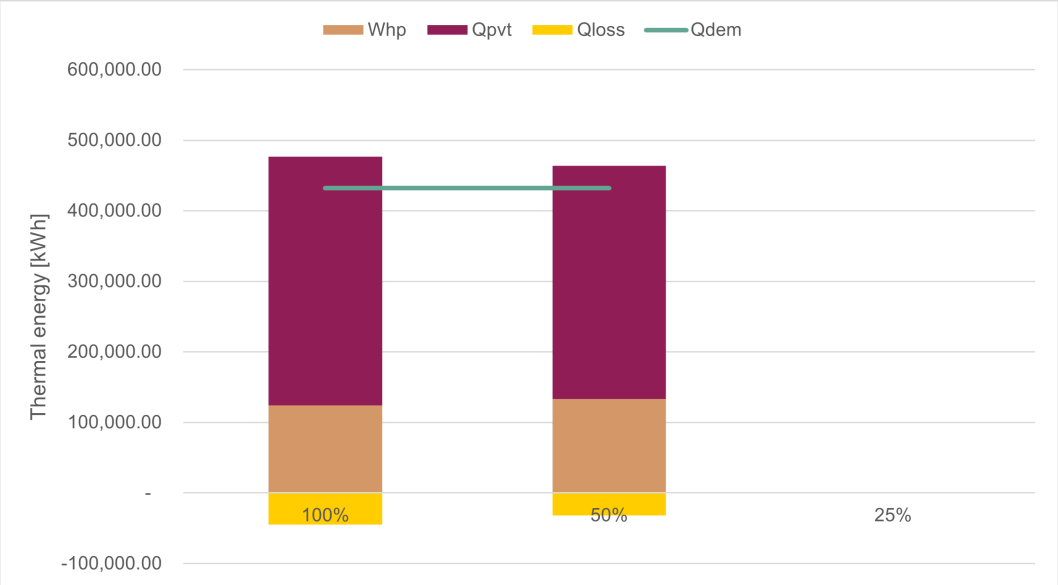

Figure 25. *Thermal energy demand (Qdem), production (Qpvt and Whp) and storage losses (Qloss) for the scenario's, 100%, 50% and 25% of available roof area filled in with PV/t. Presented for the simulation over the years 2022 and 2023 for primary school De Binnentuin.*

De Binnentuin is in both the 100% and 50% scenario net-zero from a thermal perspective. It was not possible to full fill the thermal energy demand net-zero when 25% of the available roof area was filled with PV/t panels. The thermal energy generation from the PV/t panels is the high relative to the other schools. This is due to the high number of PV/t panels installed and almost optimal orientation. Despite this, a large storage capacity is needed to reach net-zero thermal energy, as can be observed in Table19. This is due to the high thermal energy demand.

	100%	**50%**	**25%**	Unit
Storage Cap	1,729.10	2,306.24	-	m^3
AveCOP	4.04	3.56	-	

Table 19. *Storage capacity and average COP of the heat pump over years 2022 and 2023 in different scenario's for primary school De Binnentuin.*

The storage capacity for De Binnentuin, in both scenario's, is slightly larger than average. However, much smaller compared to primary school De Weide Vleuten. The ratio between energy from the PV/t and heat pump is similar to the previous schools. This can be observed from the similar COP of the previous schools.

The electricity generation and demand for the different scenario's of De Binnetuin are presented in Figure 26

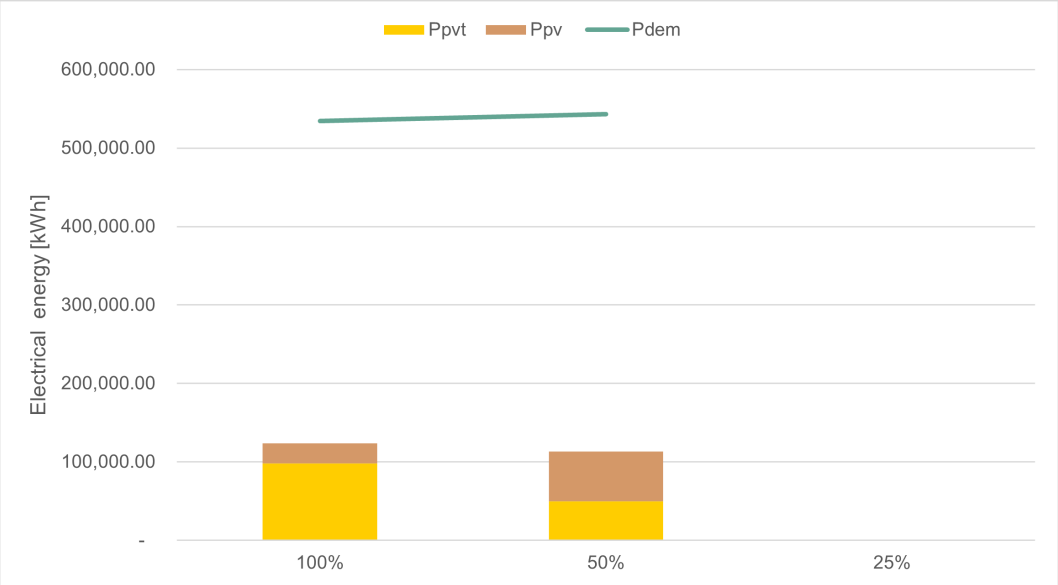

Figure 26. *Electrical energy demand (Pdem) and production (Ppvt and Ppv) for the scenario's, 100%, 50% and 25% of available roof area filled in with PV/t. Presented for the simulation over the years 2022 and 2023 for primary school De Binnentuin.*

Primary school De Binnentuin is not net-zero from an electricity perspective in either of the scenario's. Moreover, only around 23% of the electricity demand is generated on site in the 100% PV/t scenario. Only De Weide Vleuten has a lower percentage. The reason for this, is the large electricity demand. This is the case because De Binnentuin is built in 2012, resulting in a high electricity demand in kWh/m^2. Additionally, De Binnentuin has an above average floor area.

6.4.5 Technical scenario analysis Montessori Buiten Wittevrouwen

Primary school Montessori Buiten Wittevrouwen has 2 stories with a roof area of only 939 m^2. Even tough the roof is small, there are minimal installation or other obstacles, maximizing the area available for solar panels. A top view of Montessori Buiten Wittevrouwen is presented in Appendix K. The area's, orientation, tilt of the panels, row spacing and maximum panels are shown in Table20.

Roof Area [m^2]	**Tilt [°]**	**Azimuth [°]**	**Row Space [m]**	**Max panels**
133	12	220	0.8	39
111	12	220	0.8	33

Table 20. *Available space for solar panels with appropriate tilt and azimuth for primary school Montessori Buiten Wittevrouwen.*

Because of the flat roof a row spacing of 0.8 meters and tilt of 12 °is used. The scenario's for primary school Montessori Buiten Wittevrouwen corresponds to the maximum number of solar panels shown in Table20 are presented in Table21.

Array	**Tilt**	**Azimuth**	**100%**	**50%**	**25%**
1 PV/t	12	195	129	64	32
1 PV	12	195	0	64	96

Table 21. *Number of PV/t and PV panels installed in different scenario's for primary school Montessori Buiten Wittevrouwen.*

Only one array is used as the orientation and tilt of both area's are the same.

The results of the thermal energy generation, losses and demand are shown in Figure 27.

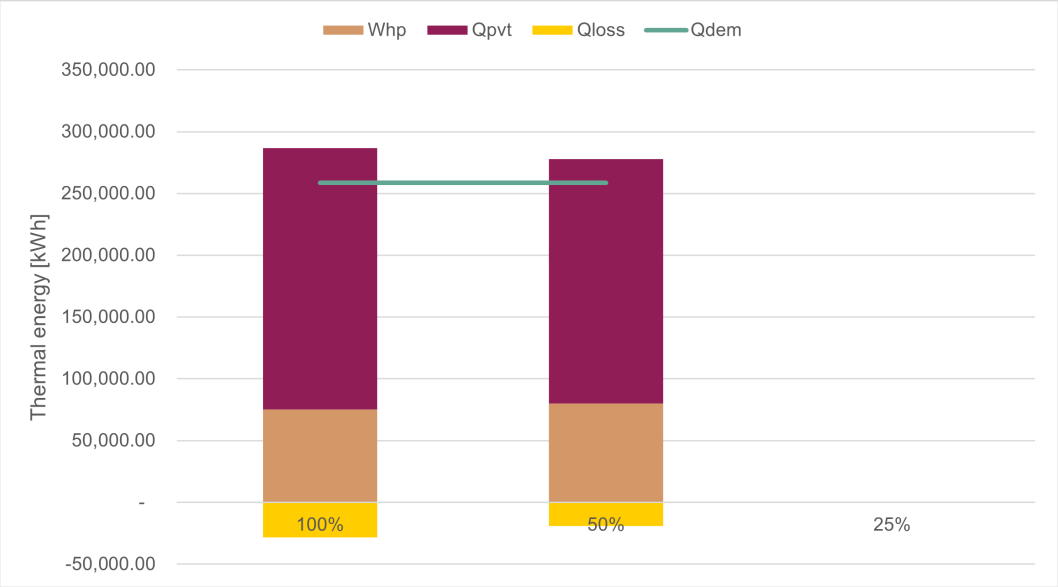

Figure 27. *Thermal energy demand (Qdem), production (Qpvt and Whp) and storage losses (Qloss) for the scenario's, 100%, 50% and 25% of available roof area filled in with PV/t. Presented for the simulation over the years 2022 and 2023 for primary school Montessori Buiten Wittevrouwen.*

Primary school Montessori Buiten Wittevrouwen is from a thermal perspective net-zero in 2 of the 3 scenario's. The last scenario, in which 25% of the available roof area is filled with PV/t and the other 75% with PV is not thermally net-zero. The thermal energy produced by the PV/t panels is lower compared to the previous schools. This is the case because only 72 PV/t panels are installed, as a maximum. This is 19 panels fewer than De Olijfboom, which has the lowest number of PV/t panels of the previously mentioned schools. The thermal energy demand of the Montessori Buiten Wittevrouwen is below average, as can be observed in Appendix H. Because of this, the Montessori Buiten Wittevrouwen is thermally net-zero in 2 of the 3 scenario's, despite the low amount of PV/t panels. The ratio between thermal energy from the PV/t panels and heat pump is similar to previous schools. This can be observed from the COP shown in Table22.

	100%	**50%**	**25%**	Unit
Storage Cap	1,085.38	1,485.80	-	m^3
AveCOP	3.96	3.50	-	

Table 22. *Storage capacity and average COP of the heat pump over years 2022 and 2023 in different scenario's for primary school Montessori Buiten Wittevrouwen.*

Even though the COP of the scenario's of the Montessori Buiten Wittevrouwen are similar to other schools. The COP of the 50% scenario is on the lower side. This is due to the low amount of PV/t panels installed in that scenario. The storage capacity is considerably smaller compared to other schools, especially De Weide Vleuten. The

reason for this, is the lower thermal energy demand of primary school Montessori Buiten Wittevrouwen.

The electricity generation and demand is shown in Figure 28.

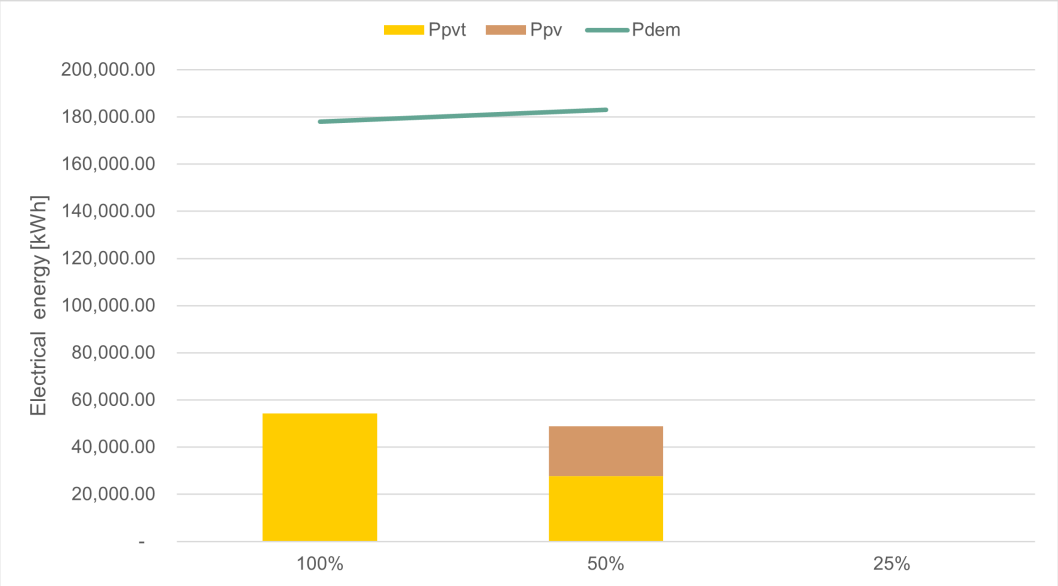

Figure 28. *Electrical energy demand (Pdem) and production (Ppvt and Ppv) for the scenario's, 100%, 50% and 25% of available roof area filled in with PV/t. Presented for the simulation over the years 2022 and 2023 for primary school Montessori Buiten Wittevrouwen.*

The Montessori Buiten Wittevrouwen couldn't reach fully net-zero form an electricity perspective in either of the scenario's. 31% of the electricity is generated on site in the 100% PV/tscenario and 28% in the 50% PV/t scenario. This is the case because of the limited roof area for solar panels. The small size of the school is not enough to offset this. If the primary school had only 1 story the Montessori Buiten Wittevrouwen would have been much closer to fully net-zero from a thermal and electrical perspective.

6.4.6 Technical scenario analysis Luc Stevenschool

The Luc Stevenschool is a one story high primary school with a roof area of 1.572 m^2. A large part of the roof is already filled with an PV array. Despite this, a large part of the roof is still empty. These empty area's are shown in the top view of The Luc Stevenschool in Appendix K. The maximum number of panels for these area's are shown in Table23.

Roof Area [m^2]	**Tilt [°]**	**Azimuth [°]**	**Row Space [m]**	**Max panels**
256	12	145	0.8	75
45	12	145	0.8	13

Table 23. *Available space for solar panels with appropriate tilt and azimuth for primary school Luc Stevenschool.*

The tilt and orientation of the available area's for solar panels is similar to the already installed PV array. These maximum panels lead to the following scenario's, shown in Table 24.

Array	**Tilt**	**Azimuth**	**100%**	**50%**	**25%**
1 PV/t	12	145	89	44	22
1 PV	12	145	0	44	66

Table 24. *Number of PV/t and PV panels installed in different scenario's for primary school Luc Stevenschool.*

One array is considered, as both area's have the same orientation and tilt.

The thermal results of the 3 scenario's are presented in Figure 29.

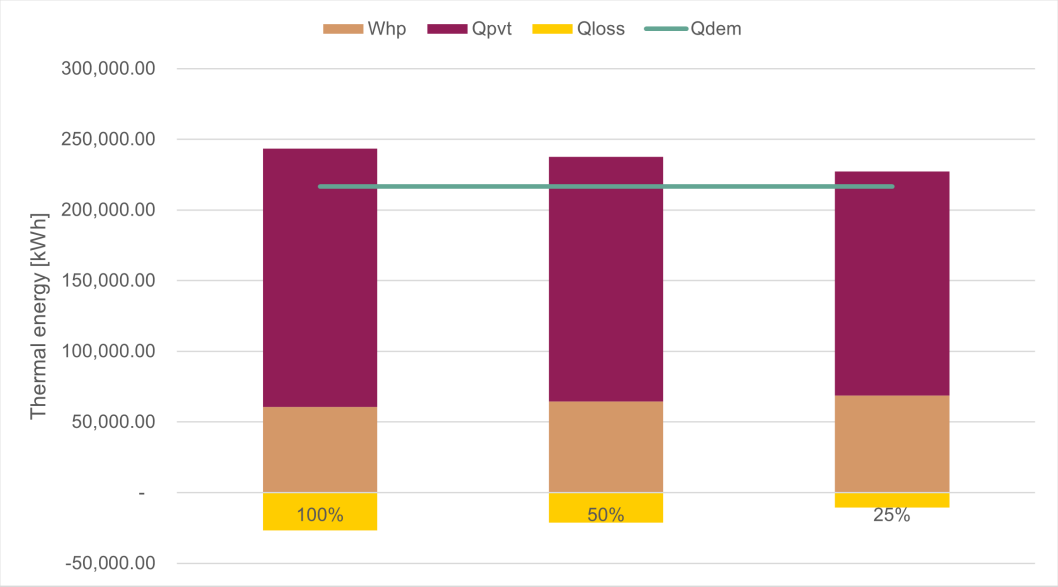

Figure 29. *Thermal energy demand (Qdem), production (Qpvt and Whp) and storage losses (Qloss) for the scenario's, 100%, 50% and 25% of available roof area filled in with PV/t. Presented for the simulation over the years 2022 and 2023 for primary school Luc Stevenvschool.*

All 3 scenario's result in a thermally net-zero energy primary school. This is even the case with 25% of the available roof area filled with PV/t panels. The reason for this, is the low thermal energy demand. Most schools have twice, or three times the thermal energy demand of the Luc Stevenschool. Only primary school, Montessori Buiten Wittevrouwen has a energy demand close to that of the Luc Stevenschool. The low thermal energy demand is a result of the small floor area, only 1.572 m^2. Because the Luc Stevenschool has only one story, the ratio between energy demand and roof area available for PV/t panels is favourable. This favourable ratio effects the storage capacity, shown in Table25.

	100%	**50%**	**25%**	Unit
Storage Cap	809.71	1,014.93	1,712.88	m^3
AveCOP	4.24	3.76	3.30	

Table 25. *Storage capacity and average COP of the heat pump over years 2022 and 2023 in different scenario's for primary school Luc Stevenschool.*

Because of the low thermal energy demand, relative to the number of PV/t panels installed in the scenario's, the storage capacity of the Luc Stevenschool is about twice as small as other schools, except the Montessori Buiten Wittevrouwen. The COP of the 100% scenario is the second highest of the 7 primary school. The reason for this, is the same as for the low required storage capacity. On the other hand, the COP of the 25% scenario is the lowest of the 7 primary schools. This is due to the low average storage temperature, related to the low number of PV/t panels in this scenario.

The results of the electricity generation and demand for the Luc Stevenschool are shown in Figure 30.

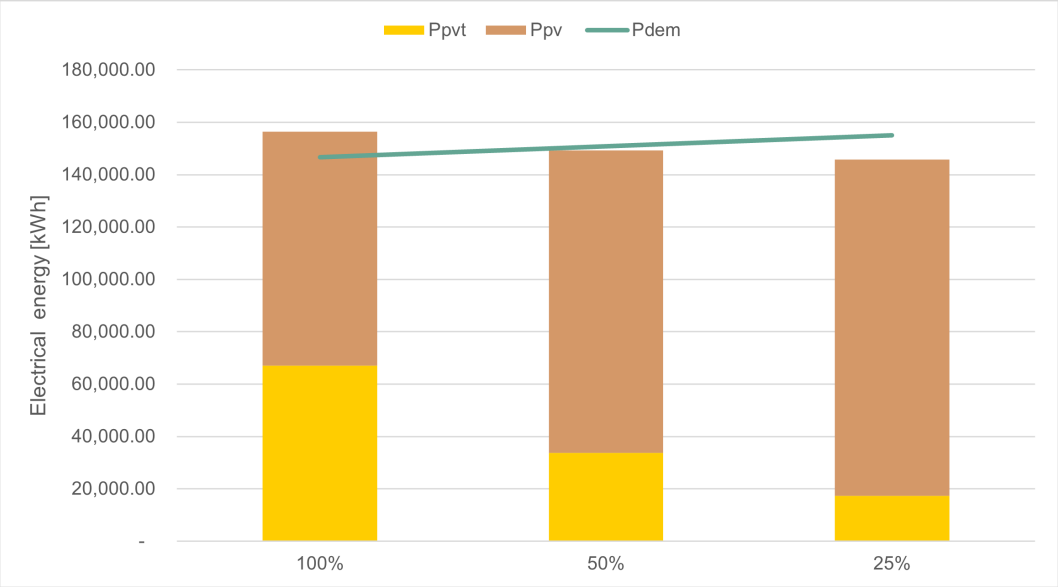

Figure 30. *Electrical energy demand (Pdem) and production (Ppvt and Ppv) for the scenario's, 100%, 50% and 25% of available roof area filled in with PV/t. Presented for the simulation over the years 2022 and 2023 for primary school Luc Stevenschool.*

The Luc Stevenschool is in the 100% scenario net-zero from an electrical perspective. This is for a large part due to the already installed PV array and the favourable ratio between electricity demand and available roof area. The primary school is not net-zero form an electricity perspective in the scenario's in which 50% and 25% of the available roof area is filled with PV/t. Although, in the 50% scenario 99% of the electricity is generated on site. The scneario's are not net-zero from an electrical perspective because of the increase in electricity demand, due to the heat pump. Additionally, less electricity is generated due to the switch from monocrystalline PV/t panels to polycrystalline PV panels. Despite the Luc Stevenschool being net-zero from an electrical perspective, a grid connection is still needed. The reason for this, is the mismatch between the generation and demand of electricity.

6.4.7 Technical scenario analysis Prof. Kohnstammschool

The Prof. Kohnstammschool is built in 1955. The building is made up of 2 stories and has a roof area 2.411 m^2. The primary school is divided into two blocks. The roof of one block is already full of PV panels. While the roof of the other block is empty, except from some installations. A top view with the available area's for solar panels is shown in Appendix K. The corresponding azimuth, tilt, row spacing and maximum panels are shown in table 26.

Roof Area [m^2]	**Tilt [°]**	**Azimuth [°]**	**Row Space [m]**	**Max panels**
37	12	80	0	20
27.5	12	80	0	15
70.5	12	80	0	37
37	12	260	0	20
27.5	12	260	0	15
70.5	12	260	0	37

Table 26. *Available space for solar panels with appropriate tilt and azimuth for primary school Prof. Kohnstammschool.*

The 3 area's shown in the top view in Appendix K, are divided into 6 area's (3 East and 3 West area's) to represent and East-West setup. This setup is selected, because this is similar to the already installed PV array. For the same reason a row space of 0 is selected. The scenario's of the Prof. Kohnstammschool are shown in Table 27.

Array	**Tilt**	**Azimuth**	**100%**	**50%**	**25%**
1 PV/t	12	80	71	36	18
1 PV	12	80	0	36	54
2 PV/t	12	260	71	36	18
2 PV	12	260	0	36	54

Table 27. *Number of PV/t and PV panels installed in different scenario's for primary school Prof. Kohnstammschool.*

The East facing panels are combined into array 1 and the West facing panels are combined into array 2.

The generated, lost and demanded thermal energy for the 3 scenario's is shown in Figure 31

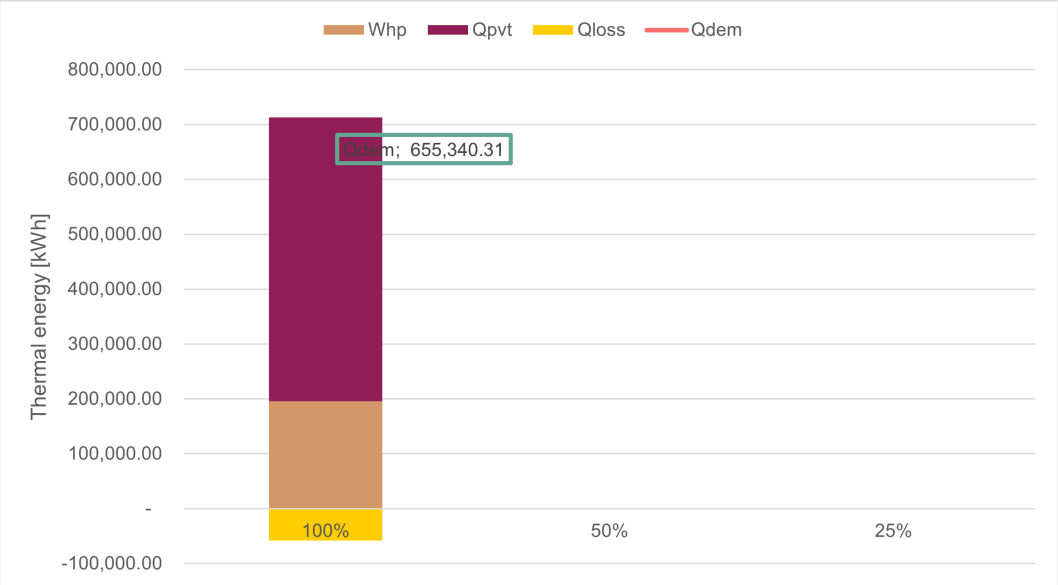

Figure 31. *Thermal energy demand (Qdem), production (Qpvt and Whp) and storage losses (Qloss) for the scenario's, 100%, 50% and 25% of available roof area filled in with PV/t. Presented for the simulation over the years 2022 and 2023 for primary school Prof. Kohnstammschool.*

The Prof. Kohnstammschool is only net-zero from a thermal perspective in the scenario in which 100% of the available roof area is filled with PV/t panels. In the other two scenario's a net-zero system wasn't possible. The 100% scenario generates the most thermal energy of all 7 primary schools. The same is true for the thermal energy provided by the heat pump. The system is modelled to generate that much energy because the thermal energy demand of the Prof. Kohnstammschool is twice or tree times as high as the other schools. The high thermal energy demand is also the reason why the Prof. Kohnstammschool isn't net-zero from a thermal perspective in the 50% and 25% scenario's. The storage capacity and COP are shown in Table 28.

	100%	**50%**	**25%**	Unit
Storage Cap	3,039.02	-	-	m^3
AveCOP	3.76	-	-	

Table 28. *Storage capacity and average COP of the heat pump over years 2022 and 2023 in different scenario's for primary school Prof. Kohnstammschool.*

The storage capacity needed in the 100% PV/t scenario is large compared to previous schools. Only the storage capacity for primary school De Weide Vleuten in the same scenario was larger. The storage is this large due to the low thermal energy production relative to the thermal energy demand. Therefore, the 100% scenario relies on the energy from the ground in the winter. The thermal energy yield from the ground increases as the storage capacity increase.

The electricity generation and demand for the Prof. Kohnstammschool is shown in Figure 32.

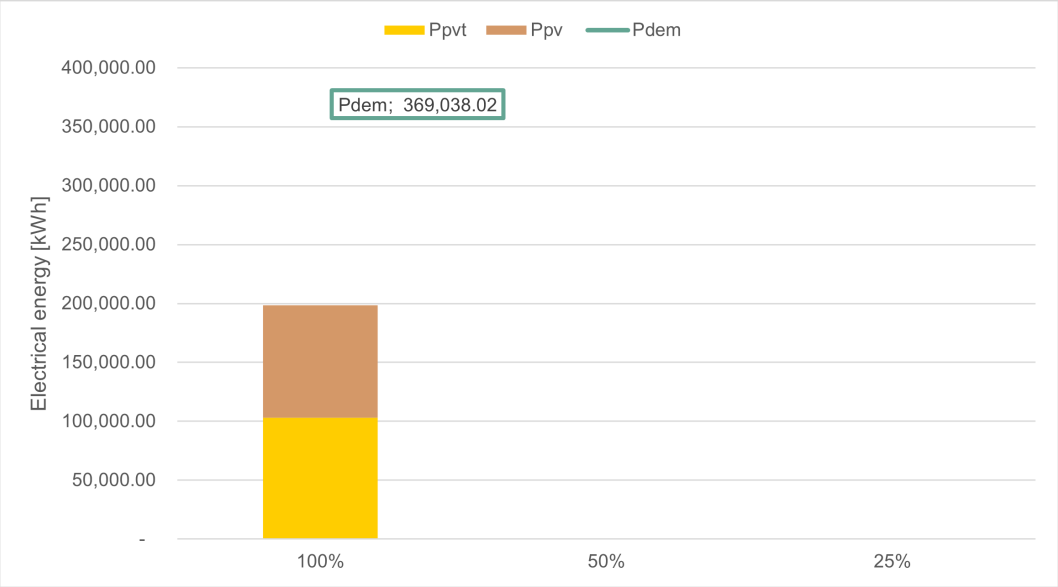

Figure 32. *Electrical energy demand (Pdem) and production (Ppvt and Ppv) for the scenario's, 100%, 50% and 25% of available roof area filled in with PV/t. Presented for the simulation over the years 2022 and 2023 for primary school Prof. Kohnstammschool.*

The Prof. Kohnstammschool is in no scenario net-zero from an electrical perspective. The electricity demand is too high to be fulfilled by only PV/t panels and the already installed PV array. Therefore, imported electricity form the grid is needed to provide the required electricity. Despite this, over 50% of the electricity is generated on site, which is average compared to the other 7 primary schools.

As mentioned at be beginning of this chapter, the net-zero capabilties of all 115 primary schools are shown in Appendix M.

6.4.8 Storage temperature

The technical analysis shows how PV/t panels in combination with STES and a heat pump, placed in the setup as described in Section 6.3, can contribute to the transition towards near net-zero energy for primary schools. Figure 33 shows the storage temperature during 2022 and 2023 for the 7 previously mentioned primary schools. This Figure gives an insight in how the PV/t system performs in different schools.

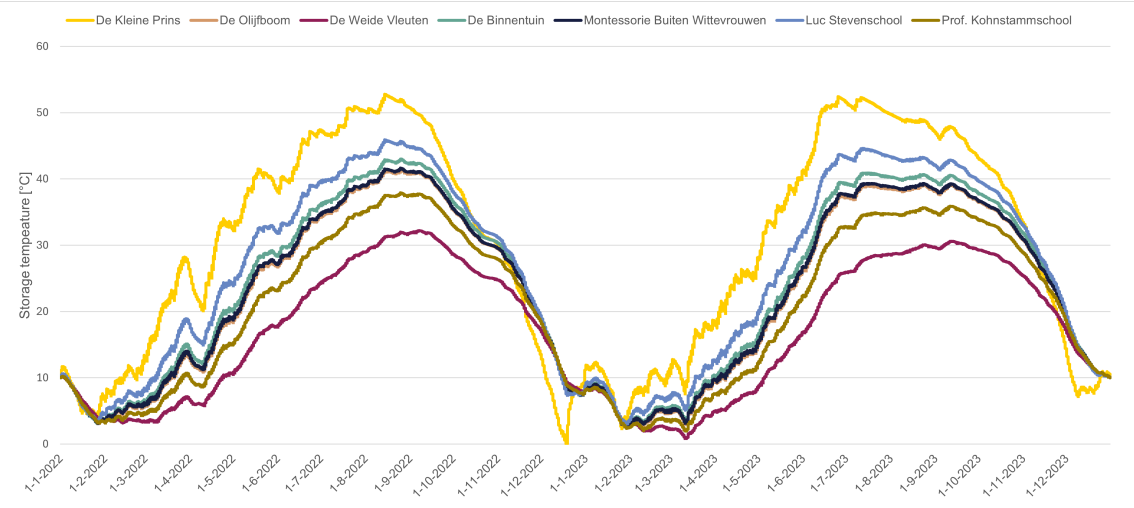

Figure 33. *Storage temperature of primary schools: De Kleine Prins, De Olijfboom, De Weide Vleuten, De Binnentuin, Montessori Buiten Wittevrouwen, Luc Stevenschool and Prof. Kohnstammschool during the years 2022 and 2023. Only the scenario's with 100% PV/t panels on the available roof area are included. This is the only scenario in which all 7 primary schools are thermally net-zero energy.*

The storage temperature in figure 33 gives an indication on the year-round performance of the system. Primary schools De Kleine Prins and the Luc Stevenschool are the two highest lines in Figure 33. The reason for this, is their favourable ratio between installed PV/t panels and thermal energy demand. This ratio is more favourable compared too other schools, because these primary schools are only 1 story high and energy demand is highly correlated to the size of the school. The storage temperature of these schools increases and decreases the fastest. This is due to their small storage capacities.

The middle lines in Figure 33 are De Olijfboom, De Binnentuin and Montessori Buiten Wittevrouwen. All these storage temperatures are close to each other. This is the case because their maximum panels, storage sizes and thermal energy demand are similar.

Lastly, De Weide Vleuten and Prof. Kohnstammschool have the lowest peek temperature. However, in the winter the temperature of the storage of De Weide Vleuten and Prof. Kohnstammschool is equal to the other schools. The reason for this, is the larger storage capacities in the scenario's for these schools. Additionally, this results in a slow increase and decrease in storage temperature.

7 Discussion

In this Section the key findings of the results are discussed. In addition to this, the limitations and further recommendations are elaborated upon.

7.1 Interpretation

In this research the technical capabilities of a PV/t based electricity and heating system, in combination with STES and a heat pump, with the aim of near net-zero, are analyzed.

The results in Section 6.1 show that reducing energy demand is a measure with high potential when it comes to the transition towards net-zero energy for utility buildings. After all, the energy not used, does not have to be generated. Reduction is also the first step in the Trias Energetica. The second step are more efficient installations e.g., heat generation, HVAC, HRV, DHW production, etc. Therefore, it is important to note that this research didn't focus on the first step, as energy reduction isn't directly included. The reason for this, is the constructional changes that come with the installation of insulation. This is especially true for older building as mentioned by Jones et al. [10]. However, energy reduction has a large impact on the technical capabilities of the heating and electricity systems, based on PV/t panels, STES and heat pump and can therefore not be overlooked.

Furthermore, the results in Section 6.2 indicate that the current energy demand of the primary school is highly correlated to the floor space of the school. This seems logical, as larger schools have more rooms that need to be heated and more appliances that use electricity. The size of the heat transmission area i.e., facade, roof and floor and construction year impact the energy demand as well. However, not as significantly as the floor area. The thermal energy demand, decreases for newer buildings, accounting for better insulation. The contrary is true for the electricity demand. This is the case because newer buildings have more appliances. It can be expected that these newer appliances are more efficient. However, according to the CBS dataset, this doesn't outweigh the increase in appliances [95].

There were some unexpected results, when it came to the electricity demand. The electricity demand for the larger schools was higher then expected. In some cases more than 250,000 kWh per year was required. The reason for these high values can be related to the energy demand per m^2, obtained from the CBS dataset [50]. There are some limitations to the CBS dataset that are further elaborated upon in the next section. Despite this, the impact from the limitations of the dataset on the results is small, as there are few schools that show exceptionally high energy demands. Additionally, the values for natural gas demand per m^2 were validated with other sources. This is also mentioned in Section 5.3.2. Therefore, these limitations only extent to the electricity demand.

The results in Section 6.2 show that the distribution of the thermal energy demand is correlated with the ambient temperature. This was expected, because the distribution is made according to HDD's. As a results of this, more energy is needed for heating when it is colder outside. There is also a link between the thermal energy distribution and moments when the primary school is in use. This results in a higher thermal energy demand when the school is open, typically on schooldays between 8 and 17 o'clock. When it comes to the electricity distribution, the results show a peek at 8 o'clock, which slowly decrease to base load at 21 o'clock. This is also in line with the opening of the school.

The results in Section 6.4 indicate that the technical capabilities of the PV/t based electricity and heating system, in combination with STES and a heat pump vary highly from school to school. The system is more potent for primary schools with low energy demand and a large available roof area for PV/t and PV panels. To this end, it is obvious that one story primary schools have high technical potential for a near net-zero PV/t based systems. The low potential of the De Weide Vleuten, a 3 story building and the Prof. Kohnstammschool, an old school with a high energy demand strengthen this. These schools are only thermally net-zero with 100% of the available roof space used for PV/t and a larger energy storage, compared to the other schools. Additionally, they are far from net-zero from an electrical perspective.

When it comes to the year round performance, the results in Section 6.4 show that the heat pump in primary schools with a more favourable ratio between available roof area and energy demand, have a average COP round 4.5. Primary schools with an unfavourable ratio have a heat pump COP of 3.5. The reason for this decrease is the lower storage temperature in combination with the higher thermal energy demand. The maximum storage temperature for a primary school with an unfavourable ratio can be between 20 to 30 °C lower, compared to primary schools with a favourable ratio. To counter this, more energy is required from the heat pump, resulting in a lower COP.

From there, it seems obvious that more PV/t panels and a lower energy demand result in a system with more technical potential to transition towards net-zero energy. However, this is not the case for primary school De Kleine Prins. In this instance, the scenario with 50% PV/t panels generated more thermal energy than the scenario with 100% PV/t panels. The reason for this, is the stagnation of the temperature in the system, in combination with the unstable storage temperature, due to the small storage capacity. These results of De Kleine Prins show that more PV/t panels are not always better. There is a certain cross over point where adding more PV/t yields no technical potential anymore. In this case, scaling down the PV/t, while increasing the storage capacity slightly results in the same outcome with less components.

The results in Section 6.4 focused on 7 primary schools. These 7 primary schools were selected due to their estimated potential or building characteristics. To determine whether the net-zero energy capabilities of these 7 primary schools can reliably apply to other schools. The net-zero energy results of the 7 primary schools are put into the perspective of the results of the 115 primary schools in the region of Utrecht. Figure 34 provides an concise overview of Appendix M, where the results can be found.

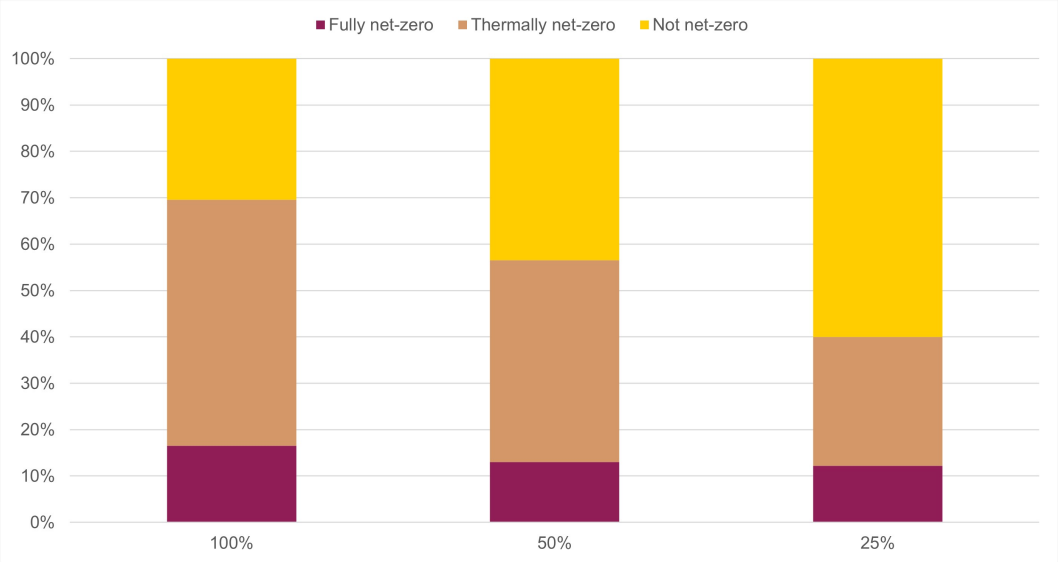

Figure 34. *Percentages of the 115 primary schools in the region of Utrecht that are Fully net-zero, Thermally net-zero or Not net-zero in the 100%, 50% and 25% scenario's.*

Figure 34 shows that in the 100% scenario 70% of the primary schools are either thermally net-zero or fully net-zero. This percentage decreases per scenario due to the decrease in installed PV/t panels. Ultimately, in the 25% scenario only 40% of the 115 primary schools are thermally net-zero or fully net-zero. This decrease is mostly due to the decrease of schools that reach thermally net-zero. The results of the 7 primary schools focused on in Sections 6.2 and 6.4 are in line with the trend and proportions presented in Figure 34. The only exception to this, is the relatively high percentage of fully net-zero primary schools in the 25% PV/t scenario. None of the 7 primary schools elaborated upon in Sections 6.2 and 6.4 were fully net-zero in the 25% scenario. However, of the 115 primary schools it is 12%. These 12% often have a large (>3000 m^2) or a small (<500 m^2) floor area, in combination with a relatively large available roof area for solar panels.

In the 100% PV/t scenario, 70% of the primary schools were either thermally net-zero or fully net-zero. Therefore, a PV/t based system looks to be an reasonable alternative to the natural gas boiler. This not only extents to a Mediterranean climate, however this research shows this is also the case in a Central European climate.

7.2 Limitations

In the results the possibility of energy saving measures is not taken into account. This was beyond the scope of this research because the installation of insulation leads to constructional changes that are not possible in every building. Even if accurate data on this was available, it would be too time consuming to model accurately. However, as shown by the literature review in Section 6.1, energy saving measure yield high potential for primary schools when transitioning towards net-zero energy. Therefore, energy saving measures could make primary schools with a low net-zero energy potential due, to the high energy demand more viable.

As mentioned in the previous section, the CBS dataset is not without its flaws. To determine this energy use per m^2, the CBS analyzed the natural gas and electricity use of all primary school in the Netherlands. However, the research population for primary schools with rare sizes or construction years were small. Therefore, the energy use per m^2 is more susceptible to deviation in energy use. These deviation can occur because of economical or uneconomical energy use. Nevertheless, the CBS dataset produced accurate results in most cases. However, a more accurate determination on the energy demand per m^2 for rare building sizes and construction years would increase the reliability of the results. Especially, because reaching net-zero is highly dependent on the energy demand of the primary school.

When determining the energy demand of the primary schools. The assumption is made that all primary schools use natural gas for heating and electricity for appliances. However, the municipality of Utrecht features an extensive district heating network and all-electric heating systems not uncommon. Therefore, this assumption might be untrue for some primary schools. It was not possible to determine the energy carriers for each primary school in the region of Utrecht. However, it can be assumed that some of the primary schools included in this research are already disconnected from the natural gas grid. In their case, there is no need for an PV/t based electricity and heating system. Despite this, the results as they are presented remain accurate. Whether the primary school is heated by a natural gas boiler, district heating net work or PV/t based energy system. The same amount of heat has to be generated to keep the primary school warm.

The output temperature of the heat pump in this research is set at 75 °C. This is in line with the output temperature of a natural gas boiler. However, the output temperature fluctuates a bit depending on the ambient temperature. Whenever the ambient temperature is low the output temperature increases to provide enough heat and vice versa. It was not possible to model this for the heat pump in Excel. The COP of the heat pump is therefore in reality slightly worse than portrait in this research. The impact on the results is estimated to be minimal, as the COP increases and decreases only slightly. Additionally, because the change in COP is negative in the winter and positive in the summer, it balances out when determined the average over 2 years.

In the model certain energy losses are neglected because their impact on the results was expected to be small. An example of this is the energy loss between the PV/t panels and the storage. The impact on the results, due to the neglect of small energy losses, would be a slightly larger required storage capacity.

While the electricity used by the heat pump is accounted for in the results. In both the PV/t panels and heat pump, fluid has to be pumped around. The electricity demand related to the pumps is not taken into account in this research. This probably didn't significantly impact the results as the pumps would be responsible for only a small portion of the total energy demand. Additionally, installing a PV/t system would replace certain excising equipment. The electricity previously used for this equipment would now be used for the PV/t electricity and heating system.

In this research only the standard indirect PV/t system is modelled. Despite the similarities between the different indirect PV/t systems, the results are only representative for the standard indirect PV/t setup. Applying an other type of PV/t system would not necessary result in the same outcome as presented in this research. Other setups are not modelled due to time limitations and complexity when modelling.

7.3 Recommendations

Further research on the PV/t system is needed to establish the technical potential further. This research shows that the system is in general technically feasible. However, a case study where this system is installed in a utility building would be a valuable addition to this research topic. With this case study, it is possible to make accurate measurements to understand the limitations and potential of this system further.

Further researches should take other types of utility buildings into account. The model in this research shows the technical capabilities of the PV/t system in a primary school. However, the energy demand and distribution might be different for other types of utility buildings, leading to different results than the ones portrait in this research.

The scenario's modelled for primary school De Kleine Prins showed that at a certain point, adding more PV/t panels didn't improve the technical capabilities. This implies there is a crossover point for the installed PV/t panels, in relation to the energy demand. Further research is needed to determine this crossover point more accurate. Knowing where this crossover point is prevents over-sizing when design choices have to be made.

It is recommended to further research the economic feasibility of the energy system based on PV/t panels, STES and a heat pump. While this research shows it technical capabilities, it remains unclear whether a business case for such a system exists. A research on the business case should take the Central European climate into account.

8 Conclusion

This research answers the question: What are the optimal design and operational parameters for a Photovoltaic Thermal system combined with energy storage and heat pump to effectively meet the heating and electricity demands of a near net-zero energy primary school in the Netherlands and what is the year-round technical performance of such a system?

The nuanced answer to this question is: It depends. This research showed that a thermally net-zero primary school is possible with energy generated by PV/t panels, stored in a STES and reheated by a heat pump. When including electricity, the systems is in most cases not fully net-zero. The required heat demand is provided, while a part of the electricity demand is generated on site and the other part is supplied by the grid. However, this is not always the case. There are primary schools where fully net-zero, electrical and thermal, is possible. These primary school typically have a favourable ratio between roof area available for solar panels and energy demand.

PV/t systems on primary schools with a favourable ratio have a higher year-round technical performance compared to schools with a small available roof area and high energy demand. The maximum storage temperature is an indicator of the year-round technical performance. Primary schools with an unfavourable ratio have a lower maximum storage temperature, compared to primary schools with a more favourable ratio. This difference can be between 20 and 30 °C. Additionally, a high the average COP indicates better year-round technical performance. Therefore, primary schools with a favourable ratio between available roof area and energy demand have a COP around 4.5. While, primary schools with a more unfavourable ratio have COP's in the range of 3.5, in the 100% scenario.

The same trend can be seen from the storage capacity. To meet the heating demand, primary schools with an unfavourable ratio between the maximum panels and energy demand generally require a larger storage compared to primary school with an favourable ratio. The reason for this, is the increased thermal energy from the ground when the storage capacity increases. Typically, primary schools with an unfavourable ratio require a storage capacity around 3,000 m^3. While, primary schools with a more favourable ratio require 800 m^3 of storage. Therefore, the optimal design parameters depend on the primary school.

These results show whether a near net-zero energy system based on PV/t panels is technically feasible for primary schools. This is relevant because primary schools need to transition towards net-zero in the coming years. Currently, in the built environment about 30% of the energy demand is electricity and the other 70% is heat [4]. And, 82% of this heat is provided by natural gas boiler [5]. This natural gas is used for residential and utility buildings, split 60% to 40%, respectively [6]. Because natural gas boilers emit CO_2, the continued use of natural gas boilers for heating is not in line with the national climate goals. Therefore, there are a lot of utility building that have to transition away from natural gas and towards a net-zero alternative.

The PV/t panels based energy system could full fill a role in this transition towards net-zero utility buildings. Because the system has some benefits compared to other near net-zero alternatives of the natural gas boiler, such as an air-water heat pump. The main benefit of the PV/t based energy system, is the high output temperature. The output temperature of the PV/t based system is similar to the output temperature of the natural gas boiler. Therefore, the current insulation is enough to make the PV/t based system work properly. With an air-water heat pump this is not always the case. Because of the low output temperature often additional insulation is required to provide enough heat on colder days. This makes a system based on PV/t panels, STES and a heat pump relevant in the Dutch energy transition.

The capabilities of a PV/t energy system were already studied by Del Amo et al., Pintanel et al., Martínez-Gracia et al. and Wang et al. However, these studies are all conducted in countries with Mediterranean climates such as: Italy and Spain. This research focused on the technical capabilities of a PV/t energy system in a Central European climate. The difference in climate changes the solar radiation and ambient temperature during the year, impacting the technical potential of the system. Because this research focuses on an colder climate in contrast to the previously conducted studies, this research is an addition to the knowledge base on this topic.

For these reasons this research is relevant from a societal and scientific point of view. It should be clear that this research doesn't present PV/t panels as a solution to every problem in the energy transition. However, it is important not to overlook a technology like PV/t panels, as this research showed that energy generated by PV/t panels, stored in a STES and reheated by a heat pump is a potent technology. Therefore, when deciding what (near) net-zero energy system to install for the next 20, 30 or 40 years, the system elaborated upon in this research shouldn't be overlooked. After all, with the understanding that this world is one in which we all share, comes the responsibility of knowing that the decisions you make today will have a lasting impact on the generations of tomorrow.

9 Acknowledgement

I wish to thank the Copernicus Institute of Sustainable Development for the opportunity to write my thesis there. Additionally, the would like to express my gratitude to Dr. Sara Mirbagheri Golroodbari for the supervision and academic guidance while conducting the research. My gratitude extends to the Prof. dr. Wilfried van Sark in his roll as second reader. Lastly, I wish to thank SolarGIS. They made it possible to use their services for this thesis.

References

[1] "Paris agreement," 2015, uNTC XXVII 7.d. [Online]. Available: https://treaties.un.org/Pages/ViewDetails.aspx?src=TREATY&mtdsg_no=XXVII-7-

[2] "Klimaatakkoord," pp. 7–9, June 2019. [Online]. Available: https://open.overheid.nl/documenten/ronl-7f383713-bf88-451d-a652-fbd0b1254c06/pdf

[3] Energie Beheer Nederland, "Infographic - ebn," January 2022. [Online]. Available: https://www.ebn.nl/feiten-en-cijfers/kennisbank/infographic-2022/

[4] ——, "Infographic - ebn," January 2021. [Online]. Available: https://www.ebn.nl/feiten-en-cijfers/kennisbank/infographic-2021/

[5] ——, "Infographic - ebn," January 2023. [Online]. Available: https://www.ebn.nl/feiten-en-cijfers/kennisbank/infographic-2023/

[6] Centraal Bureau voor de Statistiek, "Aardgas verbruik per maand naar sector — cbs," 5 2024. [Online]. Available: https://www.cbs.nl/nl-nl/maatwerk/2024/18/aardgas-verbruik-per-maand-naar-sector

[7] ——, "Warmtepompen; aantallen, thermisch vermogen en energiestromen,1994-2021," April 2023. [Online]. Available: https://www.cbs.nl/nl-nl/cijfers/detail/82380NED

[8] S. Rastegarpour, R. Scattolini, and L. Ferrarini, "Performance improvement of an air-to-water heat pump through linear time-varying mpc with adaptive cop predictor," *Journal of Process Control*, vol. 99, pp. 69–78, 2021. [Online]. Available: https://www.sciencedirect.com/science/article/pii/S0959152421000068

[9] R. Renaldi, A. Kiprakis, and D. Friedrich, "An optimisation framework for thermal energy storage integration in a residential heat pump heating system," *Applied Energy*, vol. 186, pp. 520–529, January 2017.

[10] P. Jones, S. Lannon, and J. Patterson, "Retrofitting existing housing: how far, how much?" *Building Research & Information*, vol. 41, pp. 532–550, October 2013. [Online]. Available: https://www.tandfonline.com/doi/abs/10.1080/09613218.2013.807064

[11] Centraal Bureau voor de Statistiek, "Hernieuwbare energie in nederland 2022," October 2023. [Online]. Available: https://www.cbs.nl/nl-nl/longread/rapportages/2023/hernieuwbare-energie-in-nederland-2022/5-zonne-energie#:~:text=5.1%20Zonnestroom&text=Het%20opgesteld%20vermogen%20voor%20en,MW%20opzichte%20van%20eind%202021.

[12] SolarPower Europe, "Top 10 eu countries solar capacity per capita - solarpower europe," 2023. [Online]. Available: https://www.solarpowereurope.org/advocacy/solar-saves/fact-figures/top-10-eu-countries-solar-capacity

[13] Netbeheer Nederland, "Netbeheerders zien aantal huishoudens met zonnepanelen verder groeien in 2023 — netbeheer nederland," 1 2024. [Online]. Available: https://www.netbeheernederland.nl/artikelen/nieuws/netbeheerders-zien-aantal-huishoudens-met-zonnepanelen-verder-groeien-2023

[14] Centraal Bureau voor de Statistiek, "Hernieuwbare energie in nederland 2020," September 2021. [Online]. Available: https://www.cbs.nl/nl-nl/longread/aanvullende-statistische-diensten/2021/hernieuwbare-energie-in-nederland-2020/5-zonne-energie

[15] S. S. Joshi and A. S. Dhoble, "Photovoltaic -thermal systems (pvt): Technology review and future trends," *Renewable and Sustainable Energy Reviews*, vol. 92, pp. 848–882, September 2018.

[16] Y. Tian and C. Y. Zhao, "A review of solar collectors and thermal energy storage in solar thermal applications," *Applied Energy*, vol. 104, pp. 538–553, April 2013.

[17] S. Abdul-Ganiyu, D. A. Quansah, E. W. Ramde, R. Seidu, and M. S. Adaramola, "Techno-economic analysis of solar photovoltaic (pv) and solar photovoltaic thermal (pvt) systems using exergy analysis," *Sustainable Energy Technologies and Assessments*, vol. 47, p. 101520, 2021. [Online]. Available: https://www.sciencedirect.com/science/article/pii/S2213138821005312

[18] A. Del Amo, A. Martínez-Gracia, T. Pintanel, A. Bayod-Rújula, and S. Torné, "Analysis and optimization of a heat pump system coupled to an installation of pvt panels and a seasonal storage tank on an educational building," *Energy and Buildings*, vol. 226, p. 110373, 2020.

[19] M. Teresa Pintanel, A. Martínez-Gracia, J. Uche, A. del Amo, Ángel A. Bayod-Rújula, S. Usón, and I. Arauzo, "Energy and environmental benefits of an integrated solar photovoltaic and thermal hybrid, seasonal storage and heat pump system for social housing," *Applied Thermal Engineering*, vol. 213, p. 118662, 2022. [Online]. Available: https://www.sciencedirect.com/science/article/pii/S1359431122006093

[20] A. Martínez-Gracia, S. Usón, M. T. Pintanel, J. Uche, Á. A. Bayod-Rújula, and A. Amo, "Exergy assessment and thermo-economic analysis of hybrid solar systems with seasonal storage and heat pump coupling in the social housing sector in zaragoza," *Energies*, 2021. [Online]. Available: https://api.semanticscholar.org/CorpusID:233973458

[21] K. Wang, M. Herrando, A. M. Pantaleo, and C. N. Markides, "Technoeconomic assessments of hybrid photovoltaic-thermal vs. conventional solar-energy systems: Case studies in heat and power provision to sports centres," *Applied Energy*, vol. 254, p. 113657, 2019. [Online]. Available: https://www.sciencedirect.com/science/article/pii/S0306261919313443

[22] Solargis, "Solar resource maps and gis data for 200+ countries — solargis," 2019. [Online]. Available: https://solargis.com/maps-and-gis-data/download/netherlands

[23] J. Akker, van den, H. Blok, C. Budd, R. Eggermont, A. Guterman, D. Lahaye, J. Lansink Rotgerink, K. Myerscough, C. Prins, T. Tromper, and W. Wadman, "A case study in the future challenges in electricity grid infrastructure," in *Proceedings of the 84th European Study Group Mathematics with Industry (SWI 2012)*, M. Boon, Ed., 2013, pp. 5–21, 84th European Study Group Mathematics with Industry (SWI 2012), SWI 2012 ; Conference date: 30-01-2012 Through 03-02-2012. [Online]. Available: http://www.maths-in-industry.org/past/ESGI/84/

[24] M. Ouf, M. Issa, and P. Merkel, "Analysis of real-time electricity consumption in canadian school buildings," *Energy and Buildings*, vol. 128, pp. 530–539, 9 2016.

[25] S. Utrecht, "Alle basisscholen in utrecht aardgasvrij," pp. 12–14, November 2019.

[26] A. A. Bayod-Rújula, A. Ortego-Bielsa, and A. Martínez-Gracia, "Photovoltaics on flat roofs: Energy considerations," *Energy*, vol. 36, pp. 1996–2010, April 2011.

[27] International Energy Agency, "Pvt systems: One on one with jean-christophe hadorn," *IEA SHC —— Task 60*, pp. 15–15, July 2021.

[28] Centraal Bureau voor de Statistiek, "Rendementen, co2-emissie elektriciteitsproductie, 2022 — cbs," December 2023. [Online]. Available: https://www.cbs.nl/nl-nl/maatwerk/2023/51/rendementen-co2-emissie-elektriciteitsproductie-2022

[29] A. Elmouatamid, R. Ouladsine, M. Bakhouya, N. E. Kamoun, M. Khaidar, and K. Zine-Dine, "Review of control and energy management approaches in micro-grid systems," *Energies 2021, Vol. 14, Page 168*, vol. 14, p. 168, December 2020. [Online]. Available: https://www.mdpi.com/1996-1073/14/1/168/htmhttps://www.mdpi.com/1996-1073/14/1/168

[30] S. Furbo, B. Perers, J. Dragsted, J. Gomes, M. Gomes, P. Coelho, H. Yildizhan, I. H. Yilmaz, B. Aksay, A. Bozkurt, D. Cabral, S. Hosouli, A. Hayati, J. Kaziukonytė, E. Sapeliauskas, and R. Kaliasas, "Best practices for pvt technology," *Citation*, pp. 420–429, 2021. [Online]. Available: https://doi.org/10.18086/swc.2021.22.04

[31] M. Koehl, M. Heck, S. Wiesmeier, and J. Wirth, "Modeling of the nominal operating cell temperature based on outdoor weathering," *Solar Energy Materials and Solar Cells*, vol. 95, no. 7, pp. 1638–1646, 2011. [Online]. Available: https://www.sciencedirect.com/science/article/pii/S0927024811000304

[32] D. Faiman, "Assessing the outdoor operating temperature of photovoltaic modules," *Progress in Photovoltaics: Research and Applications*, vol. 16, no. 4, pp. 307–315, 2008.

[33] M. Lämmle, M. Herrando, and G. Ryan, "Basic concepts of pvt collector technologies, applications and markets iea shc task 60/report d5," International Energy Agency, Tech. Rep., May 2021.

[34] International Energy Agency, "Pvt systems: Heat or electricity from solar why only one when you can have both?" International Energy Agency, Tech. Rep., 2021.

[35] F. A. Sachit, M. A. M. Rosli, N. Tamaldin, S. Misha, and A. L. Abdullah, "Numerical investigation and performance analysis of photovoltaic thermal pv/t absorber designs: a comparative study," *Journal of Advanced Research in Fluid Mechanics and Thermal Sciences*, vol. 58, no. 1, pp. 62–77, 2019.

[36] M. Timmerman, "Design of a pv-thermal panel integrated design with solar energy technologies," Rijksdienst voor Ondernemend Nederland, Tech. Rep., 2009.

[37] K. Terashima, H. Sato, and T. Ikaga, "Pv/t solar panel for supplying residential demands of heating/cooling and hot water with a lower environmental thermal load," *Energy and Buildings*, vol. 297, p. 113408, 2023. [Online]. Available: https://www.sciencedirect.com/science/article/pii/S0378778823006382

[38] K. Blok and E. Nieuwlaar, *Introduction to energy analysis*. Routledge, 2016.

[39] R. T. Balmer, "The first law of thermodynamics and energy transport mechanisms," *Modern Engineering Thermodynamics*, pp. 99–146, January 2011.

[40] DualSun, "Pv/t thermal performance explained! - dualsun," October 2023. [Online]. Available: https://dualsun.com/en/blog/solar-technology/pv-t-thermal-performance-explained/

[41] J. Xu, R. Wang, and Y. Li, "A review of available technologies for seasonal thermal energy storage," *Solar Energy*, vol. 103, pp. 610–638, 2014. [Online]. Available: https://www.sciencedirect.com/science/article/pii/S0038092X13002272

[42] T. Yang, W. Liu, G. J. Kramer, and Q. Sun, "Seasonal thermal energy storage: A techno-economic literature review," *Renewable and Sustainable Energy Reviews*, vol. 139, p. 110732, 2021. [Online]. Available: https://www.sciencedirect.com/science/article/pii/S1364032121000290

[43] H. Endou, "Improvement of compression heat pump performance," *Heat Pumps*, pp. 797–806, January 1990.

[44] K.-M. Adamson, T. G. Walmsley, J. K. Carson, Q. Chen, F. Schlosser, L. Kong, and D. J. Cleland, "High-temperature and transcritical heat pump cycles and advancements: A review," *Renewable and Sustainable Energy Reviews*, vol. 167, p. 112798, 2022. [Online]. Available: https://www.sciencedirect.com/science/article/pii/S1364032122006827

[45] Y. A. Cengel, M. A. Boles, and M. Kanoğlu, *Thermodynamics: an engineering approach*. McGraw-hill New York, 2011, vol. 5.

[46] N. Koruga, M. Dobrnjac, D. Golubović, and N. Dobrnjac, "Analysis of the influence of condensation temperature and compressor efficiency on heat pump system efficiency," *IOP Conference Series: Materials Science and Engineering*, vol. 1208, p. 012015, November 2021.

[47] A. Razak, "Thermodynamics of gas turbine cycles," *Industrial Gas Turbines*, pp. 13–59, January 2007.

[48] S. Dixon and C. Hall, "Chapter 1 - introduction: Basic principles," in *Fluid Mechanics and Thermodynamics of Turbomachinery (Sixth Edition)*, S. Dixon and C. Hall, Eds. Boston: Butterworth-Heinemann, 2010, pp. 1–27. [Online]. Available: https://www.sciencedirect.com/science/article/pii/B9781856177931000018

[49] B. van Aken, A. Binani, and K. Cesar, "Towards nature inclusive east-west orientated solar parks," November 2021.

[50] Centraal Bureau voor de Statistiek, "Energieverbruik vastgoed funderend onderwijs," 2018. [Online]. Available: https://dashboards.cbs.nl/v2/energieverbruik_vastgoed_funderend_onderwijs/

[51] S. J. M. Niessink, "Energielabels en het daadwerkelijk energieverbruik van scholen en tehuizen in de zorg," *Energieonderzoeks Centrum Nederland*, 2018.

[52] Gasunie, "Calorific values gasunie transport services," 2024. [Online]. Available: https://www.gasunietransportservices.nl/en/connected-parties/gas-quality-and-metering/calorific-values

[53] A. D'Amico, G. Ciulla, D. Panno, and S. Ferrari, "Building energy demand assessment through heating degree days: The importance of a climatic dataset," *Applied Energy*, vol. 242, pp. 1285–1306, 2019. [Online]. Available: https://www.sciencedirect.com/science/article/pii/S0306261919305744

[54] Koninklijk Nederlands Meteorologisch Instituut, "Uurwaarden van weerstations," 2022. [Online]. Available: https://daggegevens.knmi.nl/klimatologie/uurgegevens

[55] ——, personal communication, April 2024.

[56] G. A. H. van Amerongen, "bouwkundige- en installatietechnische richtlijnen voor zonne-energiesystemen," 2016.

[57] L. Jiang, S. Cui, P. Sun, Y. Wang, and C. Yang, "Comparison of monocrystalline and polycrystalline solar modules," in *2020 IEEE 5th Information Technology and Mechatronics Engineering Conference (ITOEC)*, 2020, pp. 341–344.

[58] A. Solar, "Abora solar — the most cost-effective solar panel," November 2022. [Online]. Available: https://abora-solar.com/en/

[59] C. Höges, L. Wissing, C. Vering, and D. Mueller, "How to choose the best refrigerant in heat pumps from an ecologic perspective? analyzing the influence of the evaluation method," June 2023.

[60] HoCoSto, personal communication, November 2023.

[61] Koninklijk Nederlands Meteorologisch Instituut, "Knmi - bodemtemperaturen," 2022. [Online]. Available: https://www.knmi.nl/nederland-nu/klimatologie/bodemtemperaturen

[62] E. Bellos and C. Tzivanidis, "Multi-objective optimization of a solar assisted heat pump-driven by hybrid pv," *Applied Thermal Engineering*, vol. 149, pp. 528–535, February 2019.

[63] A. Marszal, P. Heiselberg, J. Bourrelle, E. Musall, K. Voss, I. Sartori, and A. Napolitano, "Zero energy building – a review of definitions and calculation methodologies," *Energy and Buildings*, vol. 43, no. 4, pp. 971–979, 2011. [Online]. Available: https://www.sciencedirect.com/science/article/pii/S0378778810004639

[64] E. Parliament and E. Council, "On the energy performance of buildings," *Official Journal of the European Union*, vol. 153, pp. 13–35, 2010.

[65] I. Sartori, I. Graabak, and T. Dokka, "Proposal of a norwegian zeb definition: Storylines and criteria," *Proceedings of Renewable Energy Beyond 2020*, pp. 179–190, 2010.

[66] W. Zeiler, K. Gvozdenović, K. de Bont, and W. Maassen, "Toward cost-effective nearly zero energy buildings: The dutch situation," *Science and Technology for the Built Environment*, vol. 22, pp. 911–927, October 2016. [Online]. Available: https://www.tandfonline.com/doi/abs/10.1080/23744731.2016.1187552

[67] E. Musall, T. Weiss, A. Lenoir, K. Voss, F. Garde, and M. Donn, "Net zero energy solar buildings: an overview and analysis on worldwide building projects," in *EuroSun conference*, 2010, pp. 7–8.

[68] S. Pless and P. Torcellini, "Net-zero energy buildings: A classification system based on renewable energy supply options," National Renewable Energy Lab.(NREL), Golden, CO (United States), Tech. Rep., 2010.

[69] W. Wei and H. M. Skye, "Residential net-zero energy buildings: Review and perspective," *Renewable and Sustainable Energy Reviews*, vol. 142, p. 110859, 5 2021.

[70] J. Kneifel, E. O'Rear, D. Webb, and C. O'Fallon, "An exploration of the relationship between improvements in energy efficiency and life-cycle energy and carbon emissions using the birds low-energy residential database," *Energy and Buildings*, vol. 160, pp. 19–33, 2018. [Online]. Available: https://www.sciencedirect.com/science/article/pii/S0378778817315086

[71] D. Aelenei, L. E. Aelenei, E. Musall, E. Cubi, J. Ayoub, and A. Belleri, "Design strategies for non-residential zero-energy buildings: lessons learned from task40/annex 52: towards net zero-energy solar buildings," in *CLIMA 2013-11th REHVA World Congress & 8th International Conference on IAQVEC*, 2013.

[72] J. Kneifel, P. Lavappa, G. Eric, A. L. Greig, and S. Suh, *BIRDS v3. 1 Low-Energy Residential Database Technical Manual*. US Department of Commerce, National Institute of Standards and Technology, 2017.

[73] C. Good, I. Andresen, and A. G. Hestnes, "Solar energy for net zero energy buildings – a comparison between solar thermal, pv and photovoltaic–thermal (pv/t) systems," *Solar Energy*, vol. 122, pp. 986–996, 2015. [Online]. Available: https://www.sciencedirect.com/science/article/pii/S0038092X15005460

[74] O. B. Kazanci, M. Skrupskelis, B. W. Olesen, and G. K. Pavlov, "Solar sustainable heating, cooling and ventilation of a net zero energy house," in *CLIMA 2013-11th REHVA World Congress and the 8th International Conference on Indoor Air Quality, Ventilation and Energy Conservation in Buildings*, 2013, pp. 5513–5522.

[75] L. Aelenei and H. Gonçalves, "Sciencedirect shc 2013, international conference on solar heating and cooling for buildings and industry from solar building design to net zero energy buildings: performance insights of an office building," *Energy Procedia*, vol. 48, pp. 1236–1243, 2014. [Online]. Available: www.sciencedirect.com

[76] A. G. Entrop and H. J. Brouwers, "Assessing the sustainability of buildings using a framework of triad approaches," *Journal of Building Appraisal*, vol. 5, pp. 293–310, March 2010. [Online]. Available: https://link.springer.com/article/10.1057/jba.2009.36

[77] S. Attia, N. Shadmanfar, and F. Ricci, "Developing two benchmark models for nearly zero energy schools," *Applied Energy*, vol. 263, p. 114614, 2020. [Online]. Available: https://www.sciencedirect.com/science/article/pii/S0306261920301264

[78] M. Mohanraj, Y. Belyayev, S. Jayaraj, and A. Kaltayev, "Research and developments on solar assisted compression heat pump systems – a comprehensive review (part a: Modeling and modifications)," *Renewable and Sustainable Energy Reviews*, vol. 83, pp. 90–123, 2018. [Online]. Available: https://www.sciencedirect.com/science/article/pii/S1364032117311668

[79] J. Chu and C. A. Cruickshank, "Solar-assisted heat pump systems: A review of existing studies and their applicability to the canadian residential sector," *Journal of Solar Energy Engineering, Transactions of the ASME*, vol. 136, 11 2014. [Online]. Available: https://dx.doi.org/10.1115/1.4027735

[80] C. de Keizer, J. Bottse, M. De Jong, and W. Folkerts, "An overview of pvt modules on the european market and the barriers and opportunities for the dutch market," in *Proceedings of the ISES EuroSun 2018 Conference, Rapperswil, Switzerland*, 2018, pp. 10–13.

[81] G. Xu, S. Deng, X. Zhang, L. Yang, and Y. Zhang, "Simulation of a photovoltaic/thermal heat pump system having a modified collector/evaporator," *Solar Energy*, vol. 83, no. 11, pp. 1967–1976, 2009. [Online]. Available: https://www.sciencedirect.com/science/article/pii/S0038092X09001765

[82] E. Bellos, C. Tzivanidis, K. Moschos, and K. A. Antonopoulos, "Energetic and financial evaluation of solar assisted heat pump space heating systems," *Energy Conversion and Management*, vol. 120, pp. 306–319, 2016. [Online]. Available: https://www.sciencedirect.com/science/article/pii/S0196890416303703

[83] R. S. Kamel, A. S. Fung, and P. R. Dash, "Solar systems and their integration with heat pumps: A review," *Energy and buildings*, vol. 87, pp. 395–412, 2015.

[84] M. Herrando, A. Coca-Ortegón, I. Guedea, and N. Fueyo, "Solar assisted heat pump systems based on hybrid pvt collectors for the provision of hot water, cooling and electricity in buildings," in *Proceedings of the 13th International Conference on Solar Energy for Buildings and Industry, Virtual Conference*, 2020, pp. 1–3.

[85] M. Herrando, A. Coca-ortegón, I. Guedea, and N. Fueyo, "Experimental study of a solar system based on hybrid pvt collectors for the provision of heating, cooling and electricity in non-residential buildings," in *Proceedings of the 16th Conference on Sustainable Development of Energy, Water and Environment Systems, Dubrovnik, Croatia*, 2021, pp. 10–15.

[86] F. Calise, M. Dentice d'Accadia, R. D. Figaj, and L. Vanoli, "Thermoeconomic optimization of a solar-assisted heat pump based on transient simulations and computer design of experiments," *Energy Conversion and Management*, vol. 125, pp. 166–184, 2016, sustainable development of energy, water and environment systems for future energy technologies and concepts. [Online]. Available: https://www.sciencedirect.com/science/article/pii/S019689041630200X

[87] Y. Cui, J. Zhu, S. Zoras, Y. Qiao, and X. Zhang, "Energy performance and life cycle cost assessments of a photovoltaic/thermal assisted heat pump system," *Energy*, vol. 206, p. 118108, 2020. [Online]. Available: https://www.sciencedirect.com/science/article/pii/S0360544220312159

[88] A. Ramos, M. A. Chatzopoulou, I. Guarracino, J. Freeman, and C. N. Markides, "Hybrid photovoltaic-thermal solar systems for combined heating, cooling and power provision in the urban environment," *Energy Conversion and Management*, vol. 150, pp. 838–850, 2017. [Online]. Available: https://www.sciencedirect.com/science/article/pii/S0196890417302273

[89] G. Wang, Y. Zhao, Z. Quan, and J. Tong, "Application of a multi-function solar-heat pump system in residential buildings," *Applied Thermal Engineering*, vol. 130, pp. 922–937, 2018. [Online]. Available: https://www.sciencedirect.com/science/article/pii/S135943111734111X

[90] J. Zhou, X. Zhao, X. Ma, Z. Du, Y. Fan, Y. Cheng, and X. Zhang, "Clear-days operational performance of a hybrid experimental space heating system employing the novel mini-channel solar thermal & pv/t panels and a heat pump," *Solar Energy*, vol. 155, pp. 464–477, 2017.

[91] M. A. Obalanlege, Y. Mahmoudi, R. Douglas, E. Ebrahimnia-Bajestan, J. Davidson, and D. Bailie, "Performance assessment of a hybrid photovoltaic-thermal and heat pump system for solar heating and electricity," *Renewable Energy*, vol. 148, pp. 558–572, 2020. [Online]. Available: https://www.sciencedirect.com/science/article/pii/S0960148119315526

[92] L. Croci, L. Molinaroli, and P. Quaglia, "Dual source solar assisted heat pump model development, validation and comparison to conventional systems,"

Energy Procedia, vol. 140, pp. 408–422, 2017, beyond NZEB Buildings (AiCARR 50th International Congress, Matera (I), 10-11 May 2017). [Online]. Available: https://www.sciencedirect.com/science/article/pii/S1876610217355649

[93] F. Calise, R. D. Figaj, and L. Vanoli, "A novel polygeneration system integrating photovoltaic/thermal collectors, solar assisted heat pump, adsorption chiller and electrical energy storage: Dynamic and energy-economic analysis," *Energy Conversion and Management*, vol. 149, pp. 798–814, 2017. [Online]. Available: https://www.sciencedirect.com/science/article/pii/S0196890417302388

[94] F. Calise, M. Dentice d'Accadia, R. D. Figaj, and L. Vanoli, "A novel solar-assisted heat pump driven by photovoltaic/thermal collectors: Dynamic simulation and thermoeconomic optimization," *Energy*, vol. 95, pp. 346–366, 2016. [Online]. Available: https://www.sciencedirect.com/science/article/pii/S0360544215016345

[95] Centraal Bureau voor de Statistiek, "Statline - energiekentallen utiliteitsbouw dienstensector; bouwjaarklasse," January 2019. [Online]. Available: https://opendata.cbs.nl/statline/#/CBS/nl/dataset/83376NED/table?ts=1704893877627

Appendix A

Table A1. *General information primary schools in the region of Utrecht.*

Name	Location	Zipcode	Number
2e Marnixschool	Utrecht	3533VD	2a
Aboe Da'oed	Utrecht	3552HM	362
Agatha Snellenschool	Utrecht	3512XG	3
Agora HUB030	Utrecht	3532HK	515
Al Amana Leidsche Rijn	Utrecht	3544AK	88
Al Amana Utrecht	Utrecht	3561HX	10
Al Hambra	Utrecht	3526SG	157
Anne Frank Utrecht	Utrecht	3527XL	280
Apollo 11	De Meern	3454EN	98
Arcade Utrecht	Utrecht	3544DB	12
Ariane de Ranitz	Utrecht	3585LK	11
Ariëns	Utrecht	3525AR	18
Auris Fortaal	Utrecht	3563EN	92
Auris Fortaal	Utrecht	3563VJ	30
Auris Rotsoord	Utrecht	3523CL	36
Belle van Zuylen	Utrecht	3555GS	3
Blauwe Aventurijn	Utrecht	3523HT	4
Cleophas Jenaplan-School	Utrecht	3561JK	1c
Da Costa Hoograven	Utrecht	3525AR	16
De Achtbaan Utrecht	Utrecht	3544TT	121
De Beiaard Utrecht	Utrecht	3571XV	46
De Binnentuin	Vleuten	3452RN	6
De Boemerang Utrecht	Utrecht	3552CC	12
De Boomgaard Utrecht	Utrecht	3544TT	101
De Brug Utrecht	Utrecht	3531JJ	20
De Catharijnepoort	Utrecht	3532VM	1
De Cirkel Utrecht	Utrecht	3554GJ	124
De Fakkel Utrecht	Utrecht	3515VB	33/a
De Hoge Raven	Utrecht	3525AL	6
De Kaleidoskoop	Utrecht	3526EP	40
De Kleine Dichter	Utrecht	3521EX	1
De Kleine Prins	Utrecht	3563ST	15
De Kleine Vliegenier	Utrecht	3555VM	33
De Klim	Utrecht	3524HH	26
De Klimroos Utrecht	Utrecht	3544RK	231
De Koekoek	Utrecht	3514TT	1a
De Krullevaar De Meern	De Meern	3453RD	27
De Meander De Meern	De Meern	3454CX	1

Table A1. *General information primary schools in the region of Utrecht.*

Name	Location	Zipcode	Number
De Oase Utrecht	Utrecht	3544NE	9
De Odyssee Utrecht	Utrecht	3581MJ	40
De Olijfboom Utrecht	Utrecht	3526VN	28a
De Panda	Utrecht	3527BR	60a
De Pijlstaart Utrecht	Utrecht	3513AA	1
De Regenboog Utrecht	Utrecht	3571CG	70
De Ridderhof	Utrecht	3543BZ	66
De Schakel Utrecht	Utrecht	3564SC	4
De Spits	Utrecht	3524HH	8
De Twaalfruiter	Vleuten	3452SR	11
De Weide Vleuten	Vleuten	3452EC	1
De Wereldwijzer Utrecht	Utrecht	3522TM	2a
De Wissel Utrecht	Utrecht	3572ZM	1
De Zeven Gaven	Utrecht	3527BR	60b
Dr. Bosschool	Utrecht	3515VB	33
Drie Koningenschool	De Meern	3454AB	10
Eben-Haëzerschool Utrecht	Utrecht	3541DZ	3
Fier	Utrecht	3571KL	79
Gertrudis	Utrecht	3522AR	2
Het Schateiland Utrecht	Utrecht	3526GW	100
Het Veldhuis	De Meern	3453RD	23
Het Zand	Utrecht	3544DB	18
Hof ter Weide	Utrecht	3543BT	108
Joannes XXIII	Utrecht	3562CM	115
Johan de Witt	Utrecht	3533EW	2
Johannes Utrecht	Utrecht	3564XZ	3
Jules Verne Utrecht	Utrecht	3551XH	21
Kathedrale Koorschool	Utrecht	3512CA	5
Kees Valkensteinschool	Vleuten	3451VD	23
Kentalis College Utrecht	Utrecht	3523HB	37
Koningin Beatrixschool	De Meern	3454CR	6
Leeuwesteyn	Utrecht	3541GV	2
Leidsche Rijn	Vleuten	3451SX	8
Luc Stevensschool	Utrecht	3526GH	485
Ludger	Utrecht	3553SR	8
Lukasschool Utrecht	Utrecht	3527BR	60d
LUX SO	Utrecht	3563EP	2
Maaspleinschool	Utrecht	3522BV	1
Marcus	Utrecht	3563XC	1
Molenpark	Utrecht	3531EJ	40
Montessori Buiten	Utrecht	3581RP	3
Nieuwe Regentesseschool	Utrecht	3581GL	6

Table A1. *General information primary schools in the region of Utrecht.*

Name	Location	Zipcode	Number
Onder De Bogen	Utrecht	3541DZ	1
Oog in Al	Utrecht	3533CJ	34
Op Avontuur Utrecht	Utrecht	3524HH	20
Op De Groene Alm	Utrecht	3541SC	71
Op Dreef Utrecht	Utrecht	3561AA	27
Overvecht	Utrecht	3564XZ	1
Pantarijn De Meern	De Meern	3453RA	1
Paulus Utrecht	Utrecht	3571EL	51b
Pieterskerkhof	Utrecht	3512JR	10
Prinses Margrietschool	Utrecht	3554GE	20
Prof. Fritz Redlschool	Utrecht	3584CW	23D
Prof. Kohnstammschool	Utrecht	3582HD	1
Puntenburg	Utrecht	3511ER	2a
Rafael	Utrecht	3526XH	10
Rietendakschool	Utrecht	3552EZ	160
Rijnsweerd	Utrecht	3584GV	24
Rijnvliet	Utrecht	3545CJ	50
Shri Krishna School3	De Meern	3453RA	3
Sint Bonifatiusschool	Haarzuilens	3455SK	4
St. Dominicus	Utrecht	3533GH	51
St. Maarten Utrecht	Utrecht	3562CP	20
Stepping Stones	Utrecht	3582CJ	137
Stichting HAPPY KIDS	Utrecht	3561HX	6
Torenpleinschool	Vleuten	3451AA	7
Tuindorp Utrecht	Utrecht	3571EN	34
Utrechtse Schoolvereniging	Utrecht	3583BP	22-a
Van Asch van Wijckschool	Utrecht	3532CX	85
Vleuterweide	Vleuten	3452CZ	5
Voordorp	Utrecht	3573BK	15
Vrije School Utrecht	Utrecht	3512KV	3
Waterrijk Utrecht	Utrecht	3543BT	102
Wijzer aan de Vecht	Utrecht	3554VZ	32
Willibrordschool Vleuten	Vleuten	3451CC	28
Wittevrouwen	Utrecht	3572HD	73
Zonnewereld	Vleuten	3452CB	54

Appendix B

Table B1. *Characteristics Monocrystalline and Polycrystalline PV panels [31].*

Technology	Monocrystalline silicon (m-Si)	Polycrystalline silicon (p-Si)
Type	glass-polymer	glass-polymer
NOCT (°C)	45	46
Module Efficiency (%)	18.4	14.1
Temp. Coefficient (%/K)	-0.38	-0.45
U_0	30.02	30.02
U_1	6.28	6.28

Appendix C

Table C1. *Amount of installed solar panels, azimuths of the solar arrays and estimated yearly yield in [kWh]. Data is collected from SolarGis.*

Name	Number of solar panels	Azimuth [°]	Estimated yearly yield [kWh]
Anne Frank Utrecht	620	145	152,902.20
Apollo 11	120	190	29,807.40
Ariëns	276	280/100	61,346.50
Belle van Zuylen	35	215	8,540.60
Blauwe Aventurijn	228	290/110	50,961.00
Cleophas Jenaplan-School	352	270/90	78,252.90
Da Costa Hoograven	276	280/100	61,346.50
De Achtbaan Utrecht	704	275/95	156,788.40
De Beiaard Utrecht	84	185	20,891.00
De Binnentuin	52	195	12,891.80
De Boemerang Utrecht	80	210	19,620.80
De Boomgaard Utrecht	704	275/95	156,788.40
De Catharijnepoort	182	185	45,263.90
De Cirkel Utrecht	312	305/125	69,287.90
De Hoge Raven	276	280/100	61,346.50
De Kaleidoskoop	60	145	14,645.30
De Kleine Dichter	155	150/230/50	36,452.30
De Klim	44	185	11,260.20
De Klimroos Utrecht	80	180	19,906.20
De Meander De Meern	160	290/110	35,762.10
De Oase Utrecht	420	270/90	93,369.90
De Odyssee Utrecht	284	300/120/210/30	63,033.10
De Olijfboom Utrecht	138	145	33,684.20
De Pijlstaart Utrecht	24	205	6,021.70
De Ridderhof	16	275/95	3,556.60
De Twaalfruiter	130	195	32,229.50
De Wereldwijzer Utrecht	52	280/100	11,626.30
De Wissel Utrecht	120	200	29,663.30
Dr. Bosschool	99	275/95	21,911.60
Fier	288	275/95	64,019.70
Het Schateiland Utrecht	191	145	46,620.80
Joannes XXIII	72	220	17,469.20
Johannes Utrecht	288	285/105	64,009.80
Jules Verne Utrecht	400	295/115	88,864.90
Luc Stevensschool	183	145	44,668.10
Maaspleinschool	117	180/210	29,587.10
Marcus	180	130	43,115.60
Molenpark	66	165	16,362.30
Oog in Al	180	170	44,714.40

Table C1. *Amount of installed solar panels, azimuths of the solar arrays and estimated yearly yield in [kWh]. Data is collected from SolarGis.*

Name	Number of solar panels	Azimuth [°]	Estimated yearly yield [kWh]
Op Avontuur Utrecht	18	185	4,606.50
Op De Groene Alm	62	160	15,326.90
Overvecht	288	285/105	64,009.80
Paulus Utrecht	288	205/25	63,892.80
Prinses Margrietschool	75	200/220	18,655.80
Prof. Kohnstammschool	214	260/80	47,563.00
Rijnsweerd	116	130	27,785.60
Rijnvliet	580	280/100	128,916.40
Tuindorp Utrecht	146	290/110	32,441.80
Voordorp	80	195/155	20,192.60

Appendix D

Table D1. *Building Information primary schools in the region of Utrecht. Data is collected from the Basisregistratie Adressen en Gebouwen and GoogleMaps.*

Name	Built Year	Roofsize [m^2]	Levels	Floorsize [m^2]
2e Marnixschool	1946	1570	2	3140
Aboe Da'oed	1928	1852	2	3704
Agatha Snellenschool	1883	1330	2	2660
Agora HUB030	1953	1706	2.4	4094.4
Al Amana Leidsche Rijn	2004	1136	1.8	2044.8
Al Amana Utrecht	2011	826	1	826
Al Hambra	1971	1785	1	1785
Anne Frank Utrecht	2008	2180	1.5	3270
Apollo 11	2012	1783	1	1783
Arcade Utrecht	2005	2116	2	4232
Ariane de Ranitz	1962	7200	1	7200
Ariëns	2013	976	2	1952
Auris Fortaal	1970	1445	1.6	2312
Auris Fortaal	1973	5139	1.1	5652.9
Auris Rotsoord	1961	2697	2	5394
Belle van Zuylen	1957	1463	1.6	2340.8
Blauwe Aventurijn	2012	1448	1	1448
Cleophas Jenaplan-School	2017	1595	2	3190
Da Costa Hoograven	2013	1093	2	2186
De Achtbaan Utrecht	2001	2559	2	5118
De Beiaard Utrecht	1981	996	1.9	1892.4
De Binnentuin	2012	3017	2	6034
De Boemerang Utrecht	2023	1505	2	3010
De Boomgaard Utrecht	2001	3210	2	6420
De Brug Utrecht	1930	1156	1.6	1849.6
De Catharijnepoort	1994	1430	2	2860
De Cirkel Utrecht	1999	2107	1.5	3160.5
De Fakkel Utrecht	1979	1780	2	3560
De Hoge Raven	2013	1474	2	2948
De Kaleidoskoop	1965	1194	2	2388
De Kleine Dichter	2004	2393	2	4786
De Kleine Prins	1979	1690	1	1690
De Kleine Vliegenier	1957	2449	2	4898
De Klim	1979	400	1	400
De Klimroos Utrecht	2000	1276	2	2552
De Koekoek	1903	2042	2.1	4288.2
De Krullevaar De Meern	2003	1401	2	2802
De Meander De Meern	1967	1700	2	3400

Table D1. *Building Information primary schools in the region of Utrecht. Data is collected from the Basisregistratie Adressen en Gebouwen and GoogleMaps.*

Name	Built Year	Roofsize [m^2]	Levels	Floorsize [m^2]
De Oase Utrecht	2015	4650	2	9300
De Odyssee Utrecht	1932	3907	2	7814
De Olijfboom Utrecht	2015	1552	2	3104
De Panda	2006	1925	2	3850
De Pijlstaart Utrecht	1988	1550	1	1550
De Regenboog Utrecht	1956	1074	3	3222
De Ridderhof	2008	1805	2	3610
De Schakel Utrecht	2010	1207	2	2414
De Spits	1979	1979	1	1979
De Twaalfruiter	2012	4203	2.1	8826.3
De Weide Vleuten	2004	2874	3	8622
De Wereldwijzer Utrecht	1982	1628	1	1628
De Wissel Utrecht	1973	1185	1.8	2133
De Zeven Gaven	2006	1945	2	3890
Dr. Bosschool	1950	2665	1.8	4797
Drie Koningenschool	1955	1590	1.2	1908
Eben-Haëzerschool Utrecht	2017	2834	2	5668
Fier	2020	1196	1.9	2272.4
Gertrudis	1923	1465	2	2930
Het Schateiland Utrecht	2013	2520	2	5040
Het Veldhuis	2003	1966	1	1966
Het Zand	2005	415	2	830
Hof ter Weide	2004	2653	2	5306
Joannes XXIII	2015	2248	2	4496
Johan de Witt	1932	1329	2.1	2790.9
Johannes Utrecht	2017	1625	1.8	2925
Jules Verne Utrecht	2021	1690	2	3380
Kathedrale Koorschool	1900	632	3	1896
Kees Valkensteinschool	1996	73	1	73
Kentalis College Utrecht	2015	3285	2	6570
Koningin Beatrixschool	2022	1492	1	1492
Leeuwesteyn	2022	3133	2	6266
Leidsche Rijn	2012	1258	2	2516
Luc Stevensschool	2015	1572	1	1572
Ludger	1983	1084	1	1084
Lukasschool Utrecht	2006	1775	2	3550
LUX SO	1973	2150	1.8	3870
Maaspleinschool	1984	1335	1	1335
Marcus	2014	2766	2	5532
Molenpark	1989	1286	1	1286
Montessori Buiten	1993	939	2	1878
Nieuwe Regentesseschool	1991	1209	2	2418

Table D1. *Building Information primary schools in the region of Utrecht. Data is collected from the Basisregistratie Adressen en Gebouwen and GoogleMaps*

Name	Built Year	Roofsize [m^2]	Levels	Floorsize [m^2]
Onder De Bogen	2017	945	2	1890
Oog in Al	2016	2474	2	4948
Op Avontuur Utrecht	1979	400	1	400
Op De Groene Alm	2014	2354	2	4708
Op Dreef Utrecht	2014	1814	1.5	2721
Overvecht	2017	1770	1.8	3186
Pantarijn De Meern	2022	1300	2	2600
Paulus Utrecht	2004	1770	2	3540
Pieterskerkhof	1896	1400	1.6	2240
Prinses Margrietschool	1991	1863	1.9	3539.7
Prof. Fritz Redlschool	2013	2165	2	4330
Prof. Kohnstammschool	1955	2411	2	4822
Puntenburg	1941	4172	1	4172
Rafael	2022	4129	2	8258
Rietendakschool	1998	1196	2	2392
Rijnsweerd	2000	1814	2	3628
Rijnvliet	2021	2954	3	8862
Shri Krishna School	2022	736	2	1472
Sint Bonifatiusschool	2000	676	1	676
St. Dominicus	1932	2822	2	5644
St. Maarten Utrecht	1995	2090	1.3	2717
Stepping Stones	1966	1622	1.6	2595.2
Stichting HAPPY KIDS	1965	1388	1.9	2637.2
Torenpleinschool	1930	1817	2	3634
Tuindorp Utrecht	1933	1945	2	3890
Utrechtse Schoolvereniging	1920	1046	2	2092
Van Asch van Wijckschool	1939	1998	2.9	5794.2
Vleuterweide	2023	2271	2	4542
Voordorp	1992	1497	1	1497
Vrije School Utrecht	1902	967	2.5	2417.5
Waterrijk Utrecht	2004	2798	2	5596
Wijzer aan de Vecht	1951	1216	2	2432
Willibrordschool Vleuten	2008	1833	1	1833
Wittevrouwen	1893	2102	2	4204
Zonnewereld	2005	1786	2	3572

Appendix E

Table E1. *Holiday schedule primary schools the Netherlands 2022 and 2023 based on the middle region.*

Year	Holiday	Start	End
2022	Christmas	1-1-2022	9-1-2022
2022	Easter	26-2-2022	6-3-2022
2022	Spring	30-4-2022	8-5-2022
2022	Summer	9-7-2022	21-8-2022
2022	Autumn	22-10-2022	30-10-2022
2022-2023	Christmas	24-12-2022	8-1-2023
2023	Easter	25-2-2023	5-3-2023
2023	Spring	29-4-2023	7-5-2023
2023	Summer	8-7-2023	20-8-2023
2023	Autumn	14-10-2023	22-10-2023
2023	Christmas	23-12-2023	31-12-2023

Appendix F

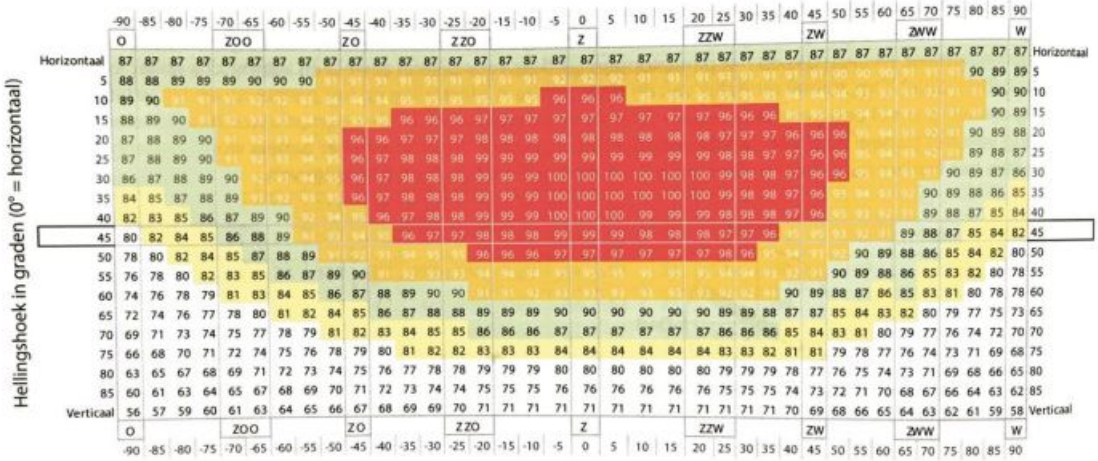

Figure F1. *Relatively, yearly mean solar insulation for different orientations and tilt angels for North/West Europe [56].*

Appendix G

Table G1. *Saturation table R134a, including temperature, saturated vapor enthalpy, saturated vapor entropy and enthalpy at entropy level and 2356.8 kPa of pressure [45].*

T [°C]	h_1 [kJ/kg]	s [kJ/kgK]	h_2 [kJ/kgK] (when $p_2 = 2365.8$ kPa)
0	250.45	0.93139	293.60
2	251.61	0.93031	293.20
4	252.77	0.92927	292.80
6	253.91	0.92828	292.50
8	255.04	0.92733	292.10
10	256.16	0.92641	291.80
12	257.27	0.92554	291.50
14	258.37	0.92470	291.20
16	259.46	0.92389	290.90
18	260.53	0.92310	290.60
20	261.59	0.92234	290.40
22	262.64	0.92160	290.10
24	263.67	0.92088	289.90
26	264.68	0.92018	289.60
28	265.68	0.91948	289.40
30	266.66	0.91879	289.10
32	267.62	0.91811	288.90
34	268.57	0.91743	288.60
36	269.49	0.91675	288.40
38	270.39	0.91606	288.20
40	271.27	0.91536	287.90
42	272.12	0.91464	287.70
44	272.95	0.91391	287.40
46	273.75	0.91315	287.10
48	274.53	0.91236	286.90
52	275.98	0.91067	286.30
56	277.30	0.90880	285.60
60	278.46	0.90669	284.90
65	279.64	0.90359	283.80
70	280.46	0.89982	282.50
75	280.82	0.89512	280.82

Appendix H

Table H1. *Yearly heat demand in [kWh] and electricity demand in [kWh] for all 115 primary schools in the region of Utrecht.*

School	Heat [kWh]	Electricity [kWh]
2e Marnixschool	222,023.19	60,288.00
Aboe Da'oed	261,902.51	71,116.80
Agatha Snellenschool	188,083.34	51,072.00
Agora HUB030	278,227.43	73,699.20
Al Amana Leidsche Rijn	140,828.34	56,027.52
Al Amana Utrecht	78,125.94	22,632.40
Al Hambra	170,470.61	37,485.00
Anne Frank Utrecht	180,167.71	104,313.00
Apollo 11	122,797.80	48,854.20
Arcade Utrecht	233,171.18	135,000.80
Ariane de Ranitz	257,854.71	60,480.00
Ariëns	134,437.07	53,484.80
Auris Fortaal	220,800.03	48,552.00
Auris Fortaal	202,448.18	47,484.36
Auris Rotsoord	193,176.15	45,309.60
Belle van Zuylen	223,550.48	49,156.80
Blauwe Aventurijn	99,725.86	39,675.20
Cleophas Jenaplan-School	131,819.96	136,532.00
Da Costa Hoograven	150,552.99	59,896.40
De Achtbaan Utrecht	183,291.72	174,012.00
De Beiaard Utrecht	173,776.44	42,011.28
De Binnentuin	216,096.57	205,156.00
De Boemerang Utrecht	124,381.84	128,828.00
De Boomgaard Utrecht	229,920.45	218,280.00
De Brug Utrecht	185,132.33	41,061.12
De Catharijnepoort	157,577.88	91,234.00
De Cirkel Utrecht	174,134.57	100,819.95
De Fakkel Utrecht	228,836.87	66,216.00
De Hoge Raven	162,426.43	94,041.20
De Kaleidoskoop	228,058.16	50,148.00
De Kleine Dichter	263,695.01	152,673.40
De Kleine Prins	155,190.33	37,518.00
De Kleine Vliegenier	332,834.60	88,164.00
De Klim	51,424.02	10,080.00
De Klimroos Utrecht	140,607.95	81,408.80
De Koekoek	303,210.14	82,333.44
De Krullevaar De Meern	154,382.24	89,383.80
De Meander De Meern	231,040.76	61,200.00

Table H1. *Yearly heat demand in [kWh] and electricity demand in [kWh] for all 115 primary schools in the region of Utrecht.*

School	Heat [kWh]	Electricity [kWh]
De Oase Utrecht	333,062.33	316,200.00
De Odyssee Utrecht	291,189.01	70,013.44
De Olijfboom Utrecht	171,021.58	99,017.60
De Panda	212,124.07	122,815.00
De Pijlstaart Utrecht	142,334.33	34,410.00
De Regenboog Utrecht	218,945.09	57,996.00
De Ridderhof	198,900.75	115,159.00
De Schakel Utrecht	166,255.68	66,143.60
De Spits	181,728.80	43,933.80
De Twaalfruiter	316,097.64	300,094.20
De Weide Vleuten	308,781.01	293,148.00
De Wereldwijzer Utrecht	149,496.96	36,141.60
De Wissel Utrecht	203,705.22	44,793.00
De Zeven Gaven	214,327.95	124,091.00
Dr. Bosschool	325,971.33	86,346.00
Drie Koningenschool	182,217.33	40,068.00
Eben-Haëzerschool Utrecht	152,241.72	258,560.30
Fier	106,422.37	84,760.52
Gertrudis	207,174.50	56,256.00
Het Schateiland Utrecht	180,498.30	171,360.00
Het Veldhuis	135,401.27	53,868.40
Het Zand	78,504.27	22,742.00
Hof ter Weide	190,024.60	180,404.00
Joannes XXIII	247,716.83	143,422.40
Johan de Witt	197,339.02	53,585.28
Johannes Utrecht	120,869.39	125,190.00
Jules Verne Utrecht	139,671.30	144,664.00
Kathedrale Koorschool	189,776.66	42,091.20
Kees Valkensteinschool	7,776.05	2,051.30
Kentalis College Utrecht	235,292.42	223,380.00
Koningin Beatrixschool	69,874.22	55,651.60
Leeuwesteyn	168,303.92	285,839.60
Leidsche Rijn	138,624.45	80,260.40
Luc Stevensschool	108,265.92	43,072.80
Ludger	99,542.20	24,064.80
Lukasschool Utrecht	195,594.92	113,245.00
LUX SO	262,978.74	69,660.00
Maaspleinschool	122,591.18	29,637.00
Marcus	198,118.37	188,088.00
Molenpark	118,091.58	28,549.20
Montessori Buiten	129,340.58	51,457.20
Nieuwe Regentesseschool	222,041.55	53,679.60

Table H1. *Yearly heat demand in [kWh] and electricity demand in [kWh] for all 115 primary schools in the region of Utrecht.*

School	Heat [kWh]	Electricity [kWh]
Onder De Bogen	88,513.59	70,497.00
Oog in Al	204,465.56	211,774.40
Op Avontuur Utrecht	51,424.02	10,080.00
Op De Groene Alm	259,397.43	150,185.20
Op Dreef Utrecht	149,919.37	86,799.90
Overvecht	131,654.66	136,360.80
Pantarijn De Meern	107,439.46	111,280.00
Paulus Utrecht	195,043.95	112,926.00
Pieterskerkhof	224,208.71	49,728.00
Prinses Margrietschool	227,531.99	65,838.42
Prof. Fritz Redlschool	238,570.70	138,127.00
Prof. Kohnstammschool	327,670.16	86,796.00
Puntenburg	294,993.87	80,102.40
Rafael	221,808.06	49,160.40
Rietendakschool	164,740.51	65,540.80
Rijnsweerd	199,892.50	115,733.20
Rijnvliet	238,032.13	404,262.77
Shri Krishna School	68,937.57	54,905.60
Sint Bonifatiusschool	63,938.42	18,522.40
St. Dominicus	210,323.88	50,570.24
St. Maarten Utrecht	149,698.98	86,672.30
Stepping Stones	176,352.05	46,713.60
Stichting HAPPY KIDS	179,206.08	47,469.60
Torenpleinschool	256,952.95	69,772.80
Tuindorp Utrecht	275,054.21	74,688.00
Utrechtse Schoolvereniging	209,394.92	46,442.40
Van Asch van Wijckschool	215,921.09	51,916.03
Vleuterweide	187,688.48	194,397.60
Voordorp	137,467.41	33,233.40
Vrije School Utrecht	241,975.25	53,668.50
Waterrijk Utrecht	200,410.41	190,264.00
Wijzer aan de Vecht	232,260.24	51,072.00
Willibrordschool Vleuten	126,241.37	50,224.20
Wittevrouwen	297,256.52	80,716.80
Zonnewereld	196,807.06	113,946.80

Appendix I

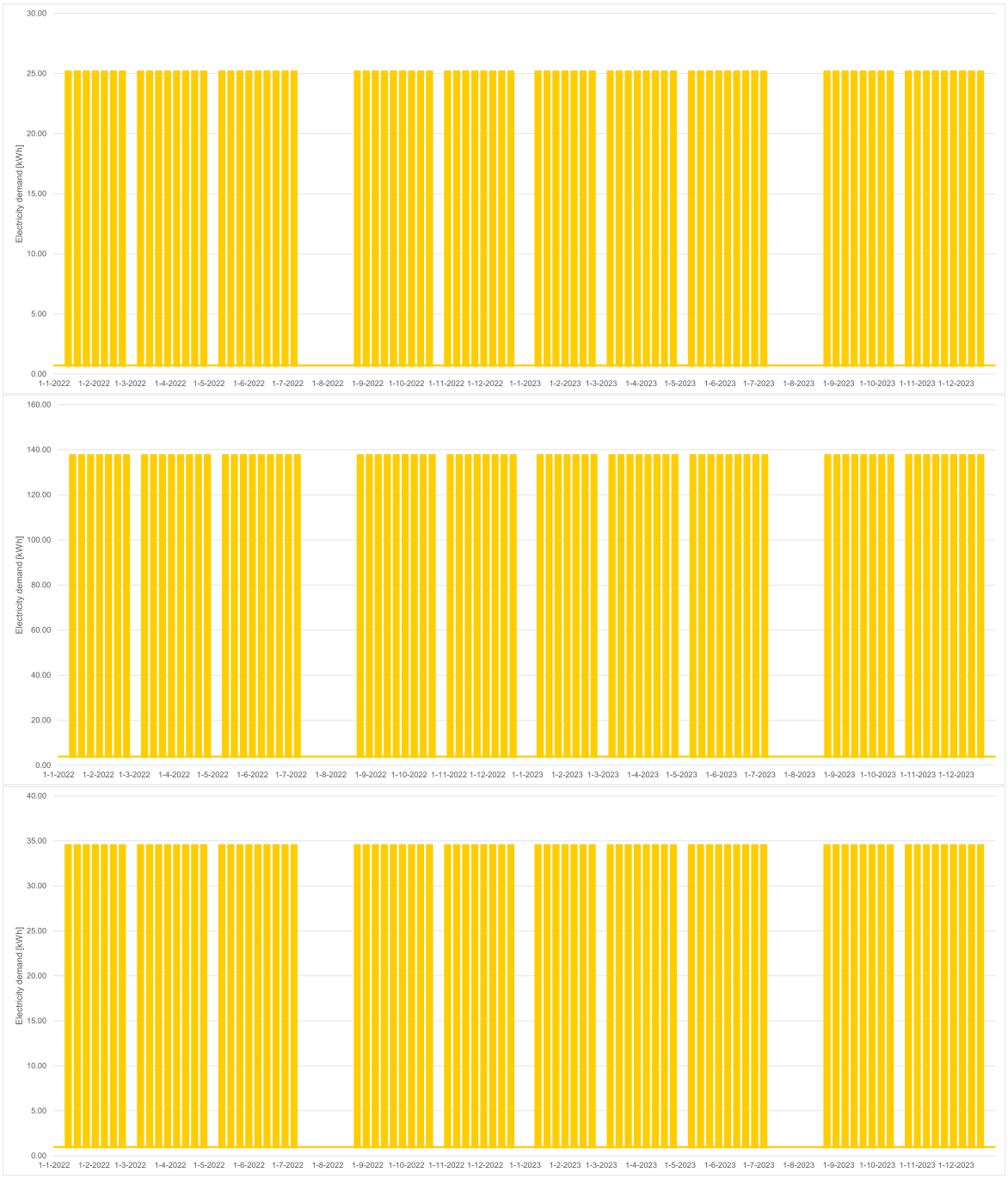

Figure I1. *Electricity demand distribution in kWh over the years 2022 and 2023. From top to bottem: De Kleine Prins, De Binnentuin, Montessori Buiten Wittevrouwen, De Olijfboom and Prof. Kohnstammschool.*

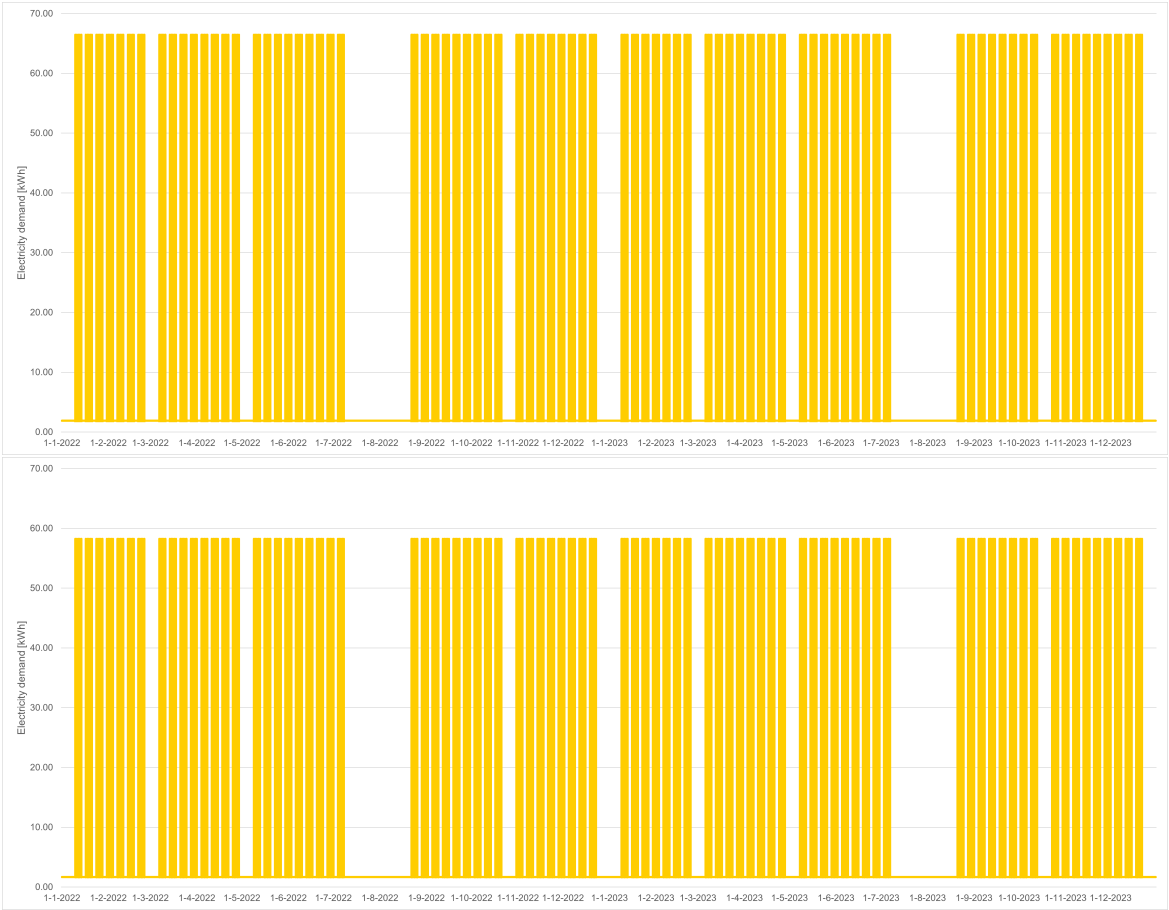

Figure I1. *Electricity demand distribution in kWh over the years 2022 and 2023. From top to bottem: De Kleine Prins, De Binnentuin, Montessori Buiten Wittevrouwen, De Olijfboom and Prof. Kohnstammschool.*

Appendix J

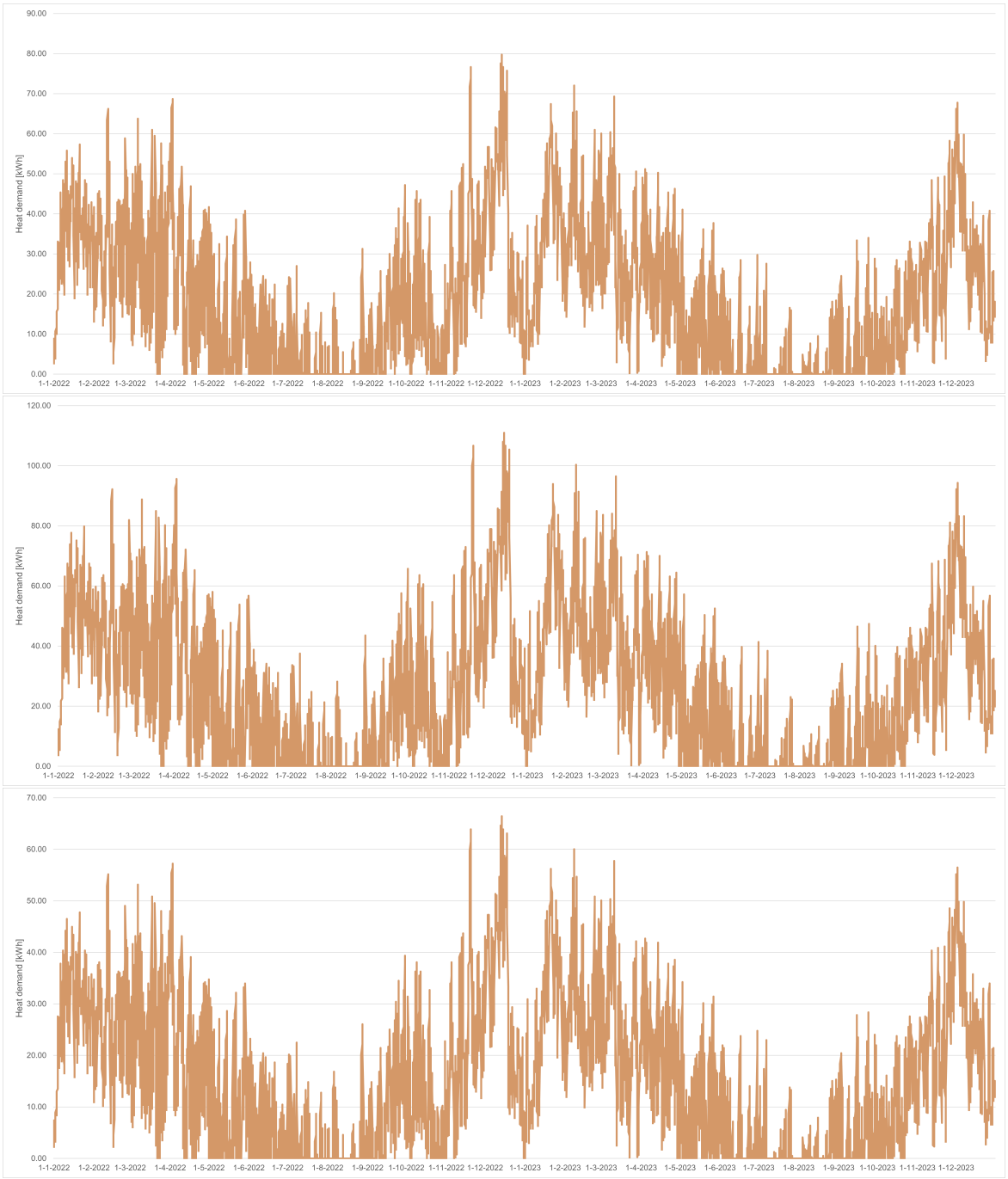

Figure J1. *Heat demand distribution in kWh over the years 2022 and 2023. From top to bottem: De Kleine Prins, De Binnentuin, Montessori Buiten Wittevrouwen, De Olijfboom and Prof. Kohnstammschool.*

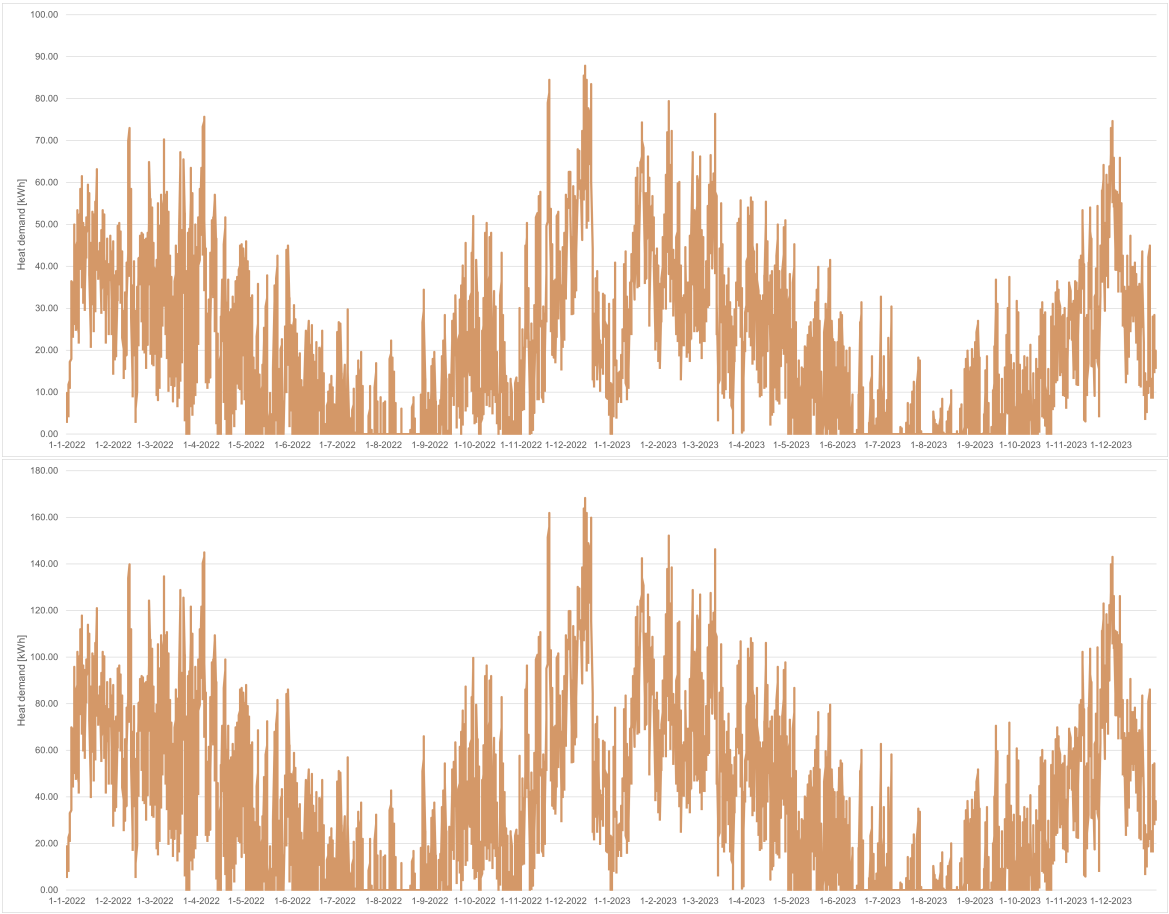

Figure J1. *Heat demand distribution in kWh over the years 2022 and 2023. From top to bottem: De Kleine Prins, De Binnentuin, Montessori Buiten Wittevrouwen, De Olijfboom and Prof. Kohnstammschool.*

Appendix K

Figure K1. *Top view of primary school De Kleine Prins, with available space for solar panels, obtained from Google Map.*

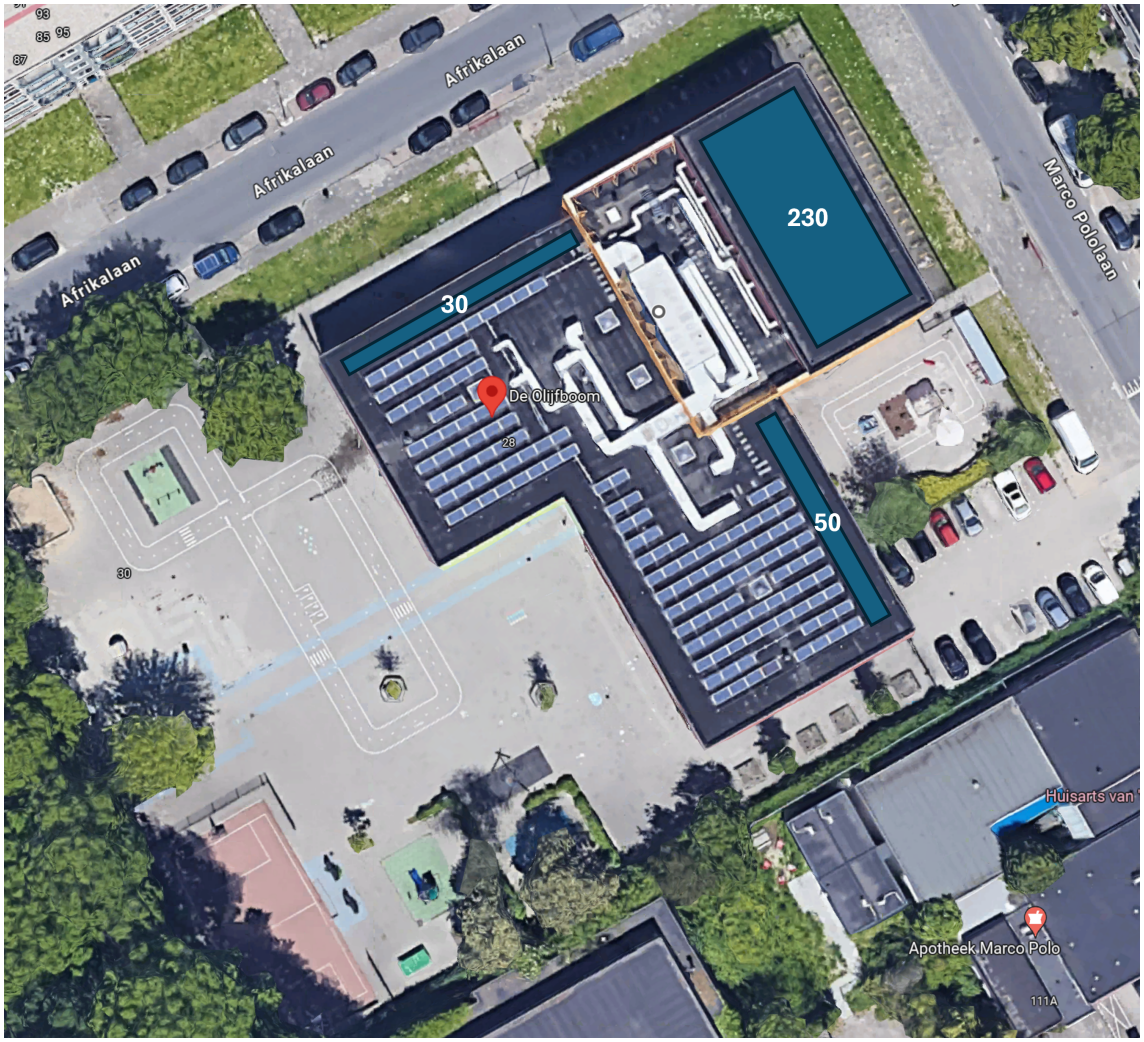

Figure K2. *Top view of primary school De Olijfboom, with available space for solar panels, obtained from Google Map.*

Figure K3. *Top view of primary school De Weide Vleuten, with available space for solar panels, obtained from Google Map.*

Figure K4. *Top view of primary school De Binnentuin, with available space for solar panels, obtained from Google Map.*

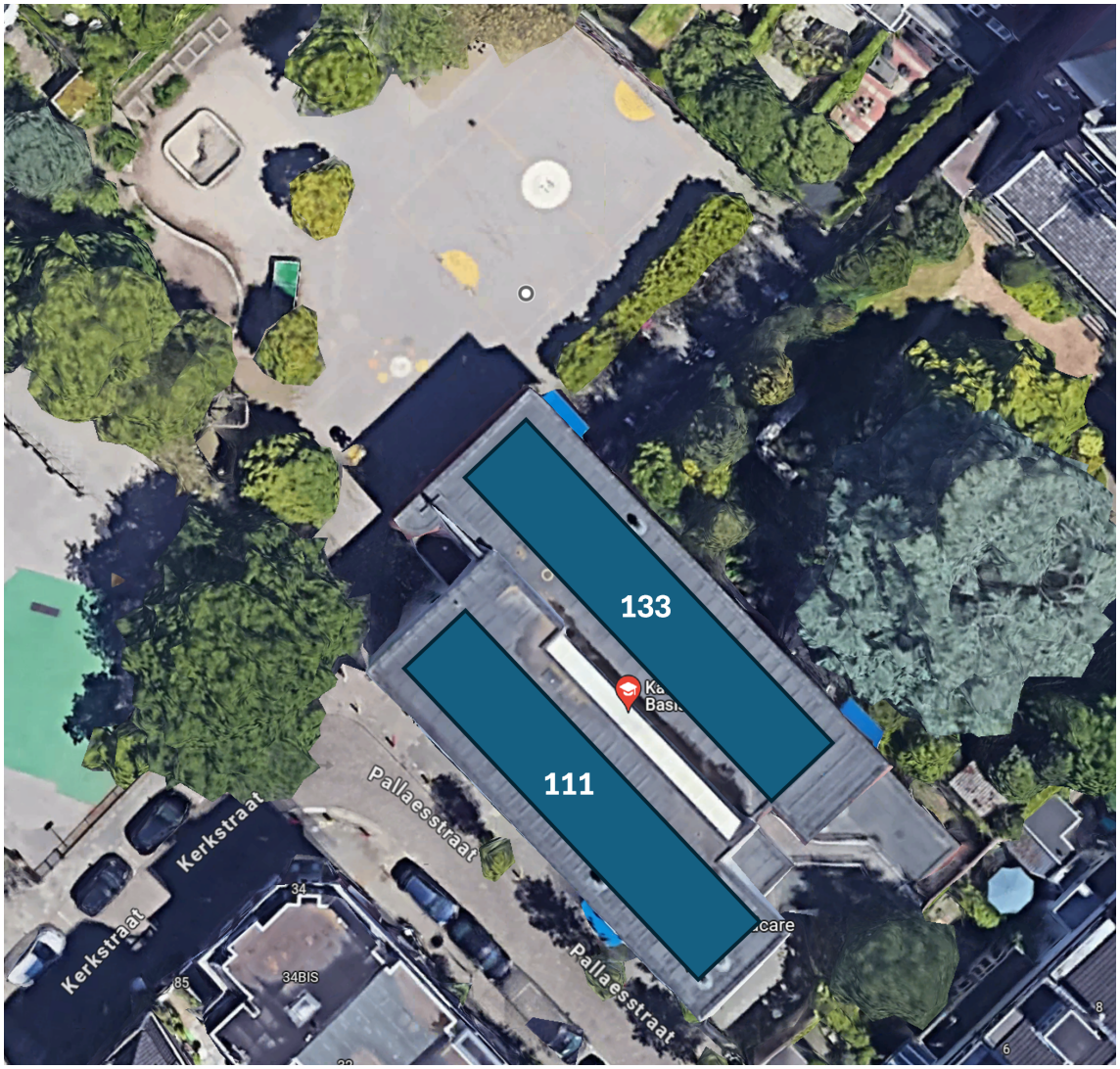

Figure K5. *Top view of primary school Montessori Buiten Wittevrouwen, with available space for solar panels, obtained from Google Map.*

Figure K6. *Top view of primary school Luc Stevenschool, with available space for solar panels, obtained from Google Map.*

Figure K7. *Top view of primary school Prof. Kohnstammschool, with available space for solar panels, obtained from Google Map.*

Appendix L

Table L1. *Number of array's, Available roof area [m^2], Row space [m^2], tilt [°] and Azimuth [°] for all 115 primary schools in the region of Utrecht.*

School	Array	Roof Area	Row Space	Tilt	Azimuth
2e Marnixschool	1	120	0	35	195
	2	0	0	0	0
Aboe Da'oed	1	144	0	45	145
	2	197	0.8	12	145
Agatha Snellenschool	1	30	0	45	135
	2	96	0.8	12	135
Agora HUB030	1	110	0	45	95
	2	70	0	45	185
Al Amana Leidsche Rijn	1	460	0	30	90
	2	460	0	30	270
Al Amana Utrecht	1	280	0.8	12	145
	2	0	0	0	0
Al Hambra	1	1427	0.8	12	195
	2	0	0	0	0
Anne Frank Utrecht	1	296	0	12	145
	2	0	0	0	0
Apollo 11	1	145	0.8	12	190
	2	0	0	0	0
Arcade Utrecht	1	785	0.8	12	185
	2	0	0	0	0
Ariane de Ranitz	1	3342	0.8	12	200
	2	0	0	0	0
Ariëns	1	0	0	0	0
	2	0	0	0	0
Auris Fortaal	1	764	0.8	12	135
	2	0	0	0	0
Auris Fortaal	1	1443	0.8	12	145
	2	0	0	0	0
Auris Rotsoord	1	632	0.8	12	180
	2	0	0	0	0
Belle van Zuylen	1	132	0.8	12	215
	2	0	0	0	0
Blauwe Aventurijn	1	150	0	12	290
	2	150	0	12	110
Cleophas Jenaplan-School	1	300	0.8	12	160
	2	142	0.8	12	225
Da Costa Hoograven	1	0	0	0	0
	2	0	0	0	0

Table L1. *Number of array's, Available roof area [m^2], Row space [m^2], tilt [°] and Azimuth [°] for all 115 primary schools in the region of Utrecht.*

School	Array	Roof Area	Row Space	Tilt	Azimuth
De Achtbaan Utrecht	1	0	0	0	0
	2	0	0	0	0
De Beiaard Utrecht	1	265	0.8	12	185
	2	0	0	0	0
De Binnentuin	1	437	0.8	12	195
	2	0	0	0	0
De Boemerang Utrecht	1	250	0.8	12	210
	2	0	0	0	0
De Boomgaard Utrecht	1	0	0	0	0
	2	0	0	0	0
De Brug Utrecht	1	131	0.8	12	145
	2	94	0.8	12	170
De Catharijnepoort	1	0	0	0	0
	2	0	0	0	0
De Cirkel Utrecht	1	122	0	12	300
	2	122	0	12	120
De Fakkel Utrecht	1	253	0.8	12	275
	2	121	0	45	95
De Hoge Raven	1	0	0	0	0
	2	0	0	0	0
De Kaleidoskoop	1	278	0.8	12	145
	2	0	0	0	0
De Kleine Dichter	1	155	0.8	12	150
	2	0	0	0	0
De Kleine Prins	1	196	0.8	12	120
	2	367	0	20	210
De Kleine Vliegenier	1	1423	0.8	12	145
	2	0	0	0	0
De Klim	1	99	0.8	45	275
	2	43	0.8	45	95
De Klimroos Utrecht	1	134	0.8	12	180
	2	0	0	0	0
De Koekoek	1	57	0	45	180
	2	96	0	45	90
De Krullevaar De Meern	1	291	0.8	12	185
	2	0	0	0	0
De Meander De Meern	1	0	0	0	0
	2	0	0	0	0
De Oase Utrecht	1	0	0	0	0
	2	0	0	0	0
De Odyssee Utrecht	1	161	0	12	120
	2	161	0	12	300

Table L1. *Number of array's, Available roof area [m^2], Row space [m^2], tilt [°] and Azimuth [°] for all 115 primary schools in the region of Utrecht.*

School	Array	Roof Area	Row Space	Tilt	Azimuth
De Olijfboom Utrecht	1	310	0.8	12	145
	2	0	0	0	0
De Panda	1	617	0	12	65
	2	617	0	12	245
De Pijlstaart Utrecht	1	145	0.8	12	205
	2	0	0	0	0
De Regenboog Utrecht	1	66	0.8	12	75
	2	43	0.8	12	255
De Ridderhof	1	294	0.8	12	180
	2	0	0	0	0
De Schakel Utrecht	1	116	0.8	12	145
	2	0	0	0	0
De Spits	1	87	0.8	12	175
	2	0	0	0	0
De Twaalfruiter	1	423	0.8	12	195
	2	485	0.8	12	165
De Weide Vleuten	1	109	0	45	120
	2	82	0	45	300
De Wereldwijzer Utrecht	1	142	0	35	110
	2	93	0	35	290
De Wissel Utrecht	1	0	0	0	0
	2	0	0	0	0
De Zeven Gaven	1	617	0	12	65
	2	617	0	12	245
Dr. Bosschool	1	87	0	12	275
	2	87	0	12	95
Drie Koningenschool	1	144	0	45	200
	2	261	0	45	285
Eben-Haëzerschool Utrecht	1	598	0.8	12	165
	2	0	0	0	0
Fier	1	126	0	12	95
	2	126	0	12	275
Gertrudis	1	300	0.8	12	175
	2	0	0	0	0
Het Schateiland Utrecht	1	0	0	0	0
	2	0	0	0	0
Het Veldhuis	1	64	0.8	12	180
	2	0	0	0	0
Het Zand	1	680	0.8	12	180
	2	0	0	0	0
Hof ter Weide	1	214	0.8	12	155
	2	0	0	0	0

Table L1. *Number of array's, Available roof area [m^2], Row space [m^2], tilt [°] and Azimuth [°] for all 115 primary schools in the region of Utrecht.*

School	Array	Roof Area	Row Space	Tilt	Azimuth
Joannes XXIII	1	0	0	0	0
	2	0	0	0	0
Johan de Witt	1	47	0	45	75
	2	42	0	45	165
Johannes Utrecht	1	198	0	12	285
	2	198	0	12	105
Jules Verne Utrecht	1	62	0	12	295
	2	62	0	12	115
Kathedrale Koorschool	1	50	0	12	95
	2	50	0	12	275
Kees Valkensteinschool	1	20	0	12	80
	2	20	0	12	260
Kentalis College Utrecht	1	482	0	12	105
	2	482	0	12	285
Koningin Beatrixschool	1	0	0	0	0
	2	0	0	0	0
Leeuwesteyn	1	0	0	0	0
	2	0	0	0	0
Leidsche Rijn	1	0	0	0	0
	2	0	0	0	0
Luc Stevensschool	1	301	0.8	12	145
	2	0	0	0	0
Ludger	1	152	0	45	145
	2	75	0	45	75
Lukasschool Utrecht	1	617	0	12	65
	2	617	0	12	245
LUX SO	1	552	0.8	12	140
	2	140	0	35	230
Maaspleinschool	1	248	0.8	12	210
	2	65	0.8	12	180
Marcus	1	0	0	0	0
	2	0	0	0	0
Molenpark	1	674	0.8	12	165
	2	0	0	0	0
Montessori Buiten	1	244	0.8	12	220
	2	0	0	0	0
Nieuwe Regentesseschool	1	90	0	25	120
	2	90	0	25	210
Onder De Bogen	1	598	0.8	12	165
	2	0	0	0	0
Oog in Al	1	0	0	0	0
	2	0	0	0	0

Table L1. *Number of array's, Available roof area [m^2], Row space [m^2], tilt [°] and Azimuth [°] for all 115 primary schools in the region of Utrecht.*

School	Array	Roof Area	Row Space	Tilt	Azimuth
Op Avontuur Utrecht	1	140	0	45	275
	2	60	0.8	12	185
Op De Groene Alm	1	0	0	0	0
	2	0	0	0	0
Op Dreef Utrecht	1	0	0	0	0
	2	0	0	0	0
Overvecht	1	198	0	12	285
	2	198	0	12	105
Pantarijn De Meern	1	0	0	0	0
	2	0	0	0	0
Paulus Utrecht	1	148	0	12	115
	2	148	0	12	295
Pieterskerkhof	1	244	0.8	12	120
	2	0	0	0	0
Prinses Margrietschool	1	104	0.8	12	220
	2	0	0	0	0
Prof. Fritz Redlschool	1	689	0.8	12	180
	2	0	0	0	0
Prof. Kohnstammschool	1	135	0	12	80
	2	135	0	12	260
Puntenburg	1	447	0	12	70
	2	447	0	12	250
Rafael	1	0	0	0	0
	2	0	0	0	0
Rietendakschool	1	0	0	0	0
	2	0	0	0	0
Rijnsweerd	1	0	0	0	0
	2	0	0	0	0
Rijnvliet	1	0	0	0	0
	2	0	0	0	0
Shri Krishna School	1	0	0	0	0
	2	0	0	0	0
Sint Bonifatiusschool	1	38	0	45	185
	2	0	0	0	0
St. Dominicus	1	424	0.8	12	180
	2	0	0	0	0
St. Maarten Utrecht	1	553	0.8	12	135
	2	0	0	0	0
Stepping Stones	1	235	0	12	80
	2	235	0	12	260
Stichting HAPPY KIDS	1	470	0.8	12	220
	2	0	0	0	0

Table L1. *Number of array's, Available roof area [m^2], Row space [m^2], tilt [°] and Azimuth [°] for all 115 primary schools in the region of Utrecht.*

School	Array	Roof Area	Row Space	Tilt	Azimuth
Torenpleinschool	1	213	0	12	90
	2	213	0	12	270
Tuindorp Utrecht	1	0	0	0	0
	2	0	0	0	0
Utrechtse Schoolvereniging	1	170	0	35	130
	2	0	0	0	0
Van Asch van Wijckschool	1	170	0	45	185
	2	138	0	45	95
Vleuterweide	1	0	0	0	0
	2	0	0	0	0
Voordorp	1	307	0.8	12	155
	2	427	0.8	12	195
Vrije School Utrecht	1	0	0	0	0
	2	0	0	0	0
Waterrijk Utrecht	1	637	0.8	12	180
	2	0	0	0	0
Wijzer aan de Vecht	1	147	0.8	45	135
	2	0	0	0	0
Willibrordschool Vleuten	1	307	0	20	130
	2	307	0	20	210
Wittevrouwen	1	54	0	45	110
	2	60	0	45	215
Zonnewereld	1	265	0	12	110
	2	265	0	12	290

Appendix M

Table M1. *Possibilities of reaching net-zero for all 115 primary schools based on the data presented in Appendix L. In the case of "No" net-zero wasn't possible, in the case of "Thermal only" enough heat was produced, however not enough electricity to be fully net-zero. In the case of "Yes" fully net-zero was reached in the scenario.*

School	100%	50%	25%
2e Marnixschool	Thermal only	No	No
Aboe Da'oed	Thermal only	Thermal only	No
Agatha Snellenschool	Thermal only	No	No
Agora HUB030	Thermal only	No	No
Al Amana Leidsche Rijn	Yes	Yes	Yes
Al Amana Utrecht	Thermal only	Thermal only	Thermal only
Al Hambra	Yes	Yes	Yes
Anne Frank Utrecht	Yes	Yes	Yes
Apollo 11	Thermal only	Thermal only	No
Arcade Utrecht	Thermal only	Thermal only	Thermal only
Ariane de Ranitz	Yes	Yes	Yes
Ariëns	No	No	No
Auris Fortaal	Thermal only	Thermal only	Thermal only
Auris Fortaal	Thermal only	Thermal only	Thermal only
Auris Rotsoord	Thermal only	Thermal only	Thermal only
Belle van Zuylen	No	No	No
Blauwe Aventurijn	Yes	Yes	Yes
Cleophas Jenaplan-School	Thermal only	Thermal only	Thermal only
Da Costa Hoograven	No	No	No
De Achtbaan Utrecht	No	No	No
De Beiaard Utrecht	Thermal only	Thermal only	No
De Binnentuin	Thermal only	Thermal only	No
De Boemerang Utrecht	Thermal only	Thermal only	No
De Boomgaard Utrecht	No	No	No
De Brug Utrecht	Thermal only	Thermal only	No
De Catharijnepoort	No	No	No
De Cirkel Utrecht	Thermal only	Thermal only	Thermal only
De Fakkel Utrecht	Thermal only	Thermal only	No
De Hoge Raven	No	No	No
De Kaleidoskoop	Thermal only	No	No
De Kleine Dichter	No	No	No
De Kleine Prins	Yes	Yes	Thermal only
De Kleine Vliegenier	Thermal only	Thermal only	Thermal only
De Klim	Yes	Thermal only	Thermal only
De Klimroos Utrecht	Thermal only	No	No
De Koekoek	Thermal only	No	No
De Krullevaar De Meern	Thermal only	Thermal only	No
De Meander De Meern	No	No	No

Table M1. *Possibilities of reaching net-zero for all 115 primary schools based on the data presented in Appendix L. In the case of "No" net-zero wasn't possible, in the case of "Thermal only" enough heat was produced, however not enough electricity to be fully net-zero. In the case of "Yes" fully net-zero was reached in the scenario.*

School	**100%**	**50%**	**25%**
De Oase Utrecht	No	No	No
De Odyssee Utrecht	Thermal only	Thermal only	No
De Olijfboom Utrecht	Thermal only	Thermal only	No
De Panda	Yes	Yes	Yes
De Pijlstaart Utrecht	Thermal only	No	No
De Regenboog Utrecht	No	No	No
De Ridderhof	Thermal only	Thermal only	No
De Schakel Utrecht	Thermal only	No	No
De Spits	No	No	No
De Twaalfruiter	Thermal only	Thermal only	No
De Weide Vleuten	Thermal only	No	No
De Wereldwijzer Utrecht	Thermal only	Thermal only	Thermal only
De Wissel Utrecht	No	No	No
De Zeven Gaven	Yes	Yes	Yes
Dr. Bosschool	Thermal only	No	No
Drie Koningenschool	Thermal only	Thermal only	Thermal only
Eben-Haëzerschool Utrecht	Thermal only	Thermal only	Thermal only
Fier	Thermal only	Thermal only	Thermal only
Gertrudis	Thermal only	Thermal only	No
Het Schateiland Utrecht	No	No	No
Het Veldhuis	No	No	No
Het Zand	Yes	Yes	Yes
Hof ter Weide	Thermal only	No	No
Joannes XXIII	No	No	No
Johan de Witt	Thermal only	No	No
Johannes Utrecht	Thermal only	Thermal only	Thermal only
Jules Verne Utrecht	Thermal only	Thermal only	No
Kathedrale Koorschool	Thermal only	No	No
Kees Valkensteinschool	Yes	Yes	Yes
Kentalis College Utrecht	Thermal only	Thermal only	Thermal only
Koningin Beatrixschool	No	No	No
Leeuwesteyn	No	No	No
Leidsche Rijn	No	No	No
Luc Stevensschool	Yes	Thermal only	Thermal only
Ludger	Thermal only	Thermal only	Thermal only
Lukasschool Utrecht	Yes	Yes	Yes
LUX SO	Thermal only	Thermal only	Thermal only
Maaspleinschool	Yes	Thermal only	Thermal only
Marcus	No	No	No
Molenpark	Yes	Yes	Yes
Montessori Buiten	Thermal only	Thermal only	No

Table M1. *Possibilities of reaching net-zero for all 115 primary schools based on the data presented in Appendix L. In the case of "No" net-zero wasn't possible, in the case of "Thermal only" enough heat was produced, however not enough electricity to be fully net-zero. In the case of "Yes" fully net-zero was reached in the scenario.*

School	**100%**	**50%**	**25%**
Nieuwe Regentesseschool	Thermal only	Thermal only	No
Onder De Bogen	Thermal only	Thermal only	Thermal only
Oog in Al	No	No	No
Op Avontuur Utrecht	Yes	Yes	Yes
Op De Groene Alm	No	No	No
Op Dreef Utrecht	No	No	No
Overvecht	Thermal only	Thermal only	Thermal only
Pantarijn De Meern	No	No	No
Paulus Utrecht	Thermal only	Thermal only	Thermal only
Pieterskerkhof	Thermal only	No	No
Prinses Margrietschool	No	No	No
Prof. Fritz Redlschool	Thermal only	Thermal only	Thermal only
Prof. Kohnstammschool	Thermal only	No	No
Puntenburg	Yes	Thermal only	Thermal only
Rafael	No	No	No
Rietendakschool	No	No	No
Rijnsweerd	No	No	No
Rijnvliet	No	No	No
Shri Krishna School	No	No	No
Sint Bonifatiusschool	Thermal only	Thermal only	No
St. Dominicus	Thermal only	Thermal only	No
St. Maarten Utrecht	Thermal only	Thermal only	Thermal only
Stepping Stones	Thermal only	Thermal only	Thermal only
Stichting HAPPY KIDS	Thermal only	Thermal only	Thermal only
Torenpleinschool	Thermal only	Thermal only	Thermal only
Tuindorp Utrecht	No	No	No
Utrechtse Schoolvereniging	Thermal only	Thermal only	No
Van Asch van Wijckschool	Thermal only	Thermal only	Thermal only
Vleuterweide	No	No	No
Voordorp	Yes	Yes	Yes
Vrije School Utrecht	No	No	No
Waterrijk Utrecht	Thermal only	Thermal only	Thermal only
Wijzer aan de Vecht	No	No	No
Willibrordschool Vleuten	Yes	Yes	Yes
Wittevrouwen	No	No	No
Zonnewereld	Thermal only	Thermal only	Thermal only